BUILDING SCIENCE MEASUREMENTS FOR THE HOSPITAL MICROBIOME PROJECT

BY

TIFFANIE RAMOS

DEPARTMENT OF
CIVIL, ARCHITECTURAL AND ENVIRONMENTAL ENGINEERING

Submitted in partial fulfillment of the
requirements for the degree of
Master of Science in Environmental Engineering
in the Graduate College of the
Illinois Institute of Technology

Approved _____
Adviser

Chicago, Illinois
May 2014

ACKNOWLEDGEMENT

I would like to thank my family and friends for all of their continued love and encouragement in all of my endeavors. I thank my primary advisor, Dr. Brent Stephens, for giving me the opportunity to work on this research and for his guidance, support and patience throughout the project. I would like to acknowledge the Alfred P. Sloan Foundation, Dr. Jeffrey Siegel, Dr. Jack Gilbert, Dr. Daniel Smith and Sandra Dedesko for being wonderful collaborators and for giving me the opportunity to be involved in this work. I also thank Stephen Weber, Elizabeth Lockwood, Marvin Kampenga and other hospital and facilities staff of the University of Chicago for accommodating our research and for providing indispensable assistance and data throughout the project.

I would like to thank Parham Azimi and Laurit Dide for their extensive help in data collection, and Zeineb El Orch and all members of IIT's Built Environment Research Group for their continued support and comic relief during all those long hours in the lab.

TABLE OF CONTENTS

Page

ACKNOWLEDGEMENT 1

LIST OF TABLES 4

LIST OF FIGURES 6

ABSTRACT 12

CHAPTER

1. INTRODUCTION 14

2. BACKGROUND & LITERATURE REVIEW 17
   - 2.1 Previous indoor microbial community research and the importance of hospital environments 17
   - 2.2 Building science measurements in recent DNA-based indoor literature 20
   - 2.3 Building environmental and operational factors influencing microbial survival and pathogen transmission 25
   - 2.4 Built environment metadata parameters and collection methods 28

3. METHODOLOGY 39
   - 3.1 Patient room and mechanical room characteristics 39
   - 3.2 Patient room and mechanical room coding for identification and confidentiality 42
   - 3.3 Sensor instrument selection and installation 43
   - 3.2 Data collection procedures 45
   - 3.3 Instrument Calibration and Initial Measurements 56
   - 3.3 Data Collection Procedures 64
   - 3.4 Analysis procedures 66

4. RESULTS 70
   - 4.1 Initial Visit and Further Calibration 70
   - 4.2 Example Time-series Data 82
   - 4.3 Summary of Results 101
   - 4.4 Variations *within* individual rooms and nurse stations 103
   - 4.5 Variations *between* individual rooms 109
   - 4.6 Variations between floors 136
   - 4.7 Within day differences (i.e. night and day) 138
   - 4.8 Monthly and seasonal variations within and between rooms 139

5. DISCUSSION 148
5.1 Interpretation of results 148
5.2 Meaning for other building science characterization studies.....150
5.3 Practical cost and reliability constraints 150
5.4 Data exclusions 151
5.5 What would we have done differently? 152

6. CONCLUSIONS.....154

BIBLIOGRAPHY 157

LIST OF TABLES

Table Page

1. Building science instruments.....45
2. Types of data loggers used.....46
3. Calibration factors for 17 SBA-5 CO_2 sensors.....58
4. Calibration factors for 10 differential pressure sensors.....60
5. Calibration factors for temperature and RH sensors.....61
6. Flow schedule and baseline measurements.....70
7. Correlation coefficients, R-squared, slope and y-intercept for daily total IR beam-break correlated with daily average CO_2, room source for all rooms.....98
8. Differential pressure measurements using a DG-700.....100
9. Summary statistics for all parameters measured within all 10 patient rooms.....101
10. Summary statistics for all parameters measured in mechanical rooms.....103
11. Correlation matrix for all rooms and nurse stations.....113
12. Fraction of measured temperature differences between rooms that were within the range of propagated uncertainty.....114
13. Correlation matrix for daily average RH (%) across all patient rooms and nurse stations.....117
14. Fraction of measured RH differences between rooms that were within the range of propagated uncertainty.....118
15. Correlation matrix for daily average absolute humidity across all patient room and nurse stations.....121
16. Fraction of measured absolute humidity differences between rooms that were within the range of propagated uncertainty.....122
17. Correlation matrix for daily average light intensity across all patient rooms and nurse stations.....125
18. Correlation matrix for daily total IR beam-break across all patient rooms and nurse stations.....128

19. Correlation matrix for daily average CO2 across all patient rooms and nurse stations. 131

20. Fraction of measured differences in daily mean CO2 concentrations between rooms that were within the range of propagated uncertainty 132

21. Correlation matrix for daily average CO_2 minus supply air CO_2 (limited to occupant-generated CO_2) across all patient rooms and nurse stations 135

22. Fraction of measured differences in daily mean CO2 concentrations (room source) between rooms that were within the range of propagated instrument uncertainty 136

LIST OF FIGURES

Figure Page

1. Diagram of sensors and locations in hospital patient rooms. 41
2. Air handling unit showing outdoor, recirculation, and supply air streams. 42
3. Typical patient room showing locations of building science sensors and microbial sampling 44
4. 3 types of Onset HOBO data loggers 46
5. HOBO data loggers located on a wall in patient room measure temperature, relative humidity and light intensity. 47
6. HOBO data logger located on a wall in patient room blended in with other room controls. 47
7. Differential pressure sensor; inside enclosure, attached to external data logger and two tubes for differential pressure measurement between inside and outside of room. 49
8. Differential pressure sensor located behind door, enclosed in box, external data logger, two tubes: short tube inside room, long tube extending outside room.....49
9. Beam-break people counter components and configuration 50
10. Location of beam-break people counters at patient room doorways.....50
11. SBA-5 CO_2 sensor with absorber column filled with self-indicating soda lime.....51
12. SBA-5 CO_2 sensor set-up and location in patient room. 52
13. Diagram showing how AHU's are connected to patient care floors 9 and 10. 53
14. Air-handling system schematic (A. Persily, 1997).....53
15. CO2 sensors installed at AHUs 54
16. Roll of filter media used for filter-based air sampling 55
17. Efficiency curve for filter media used in filter-based sampling. 55
18. Placement of magnetic filter frame for filter-based air sampling.....56
19. Magnetic frame design for filter-based air sampler 56

20. Co-location calibration of 17 SBA-5 CO2 sensors 58

21. Co-location calibration of pressure sensors.....59

22. Well-mixed test using 5 CO2 sensors 62

23. Time-series of 5 CO2 sensors used in well-mixed test 62

24. Regression analysis for 5 CO2 sensors used in well-mixed test. 63

25. Duct Blaster pressure matching flow meter for measuring airflow rates through supply diffusers and return grilles. 64

26. OA damper position from UCMC Facilities Department and measured OA fraction from AHU 6 72

27. Damper position (% open) of outside air to supply air in AHU 6 for 24-hour period starting 5/14/2013 10:30am from hospital facilities department. 73

28. Flow at outside air intake of AHU 6 for 24-hour period starting 5/14/2013 10:30am from hospital facilities department (units are CFM). 73

29. Temperature at outside air intake of AHU 6 for 24-hour period starting 5/14/2013 10:30am from hospital facilities department.....74

30. Temperature at outside air intake of AHU 6 for 24-hour period starting 5/14/2013 10:30am from project measurements 74

31. AHU 11-14 and AHU 6 correlated with outdoor air temperature.....76

32. AHU6 OA fraction averaged over each temperature, correlated with temperature. 76

33. AHU 11-14 OA fraction averaged over each temperature, correlated with temperature 77

34. AHU 6 and AHU 11-14 OA fraction averaged over enthalpy 78

35. AHU 6 and AHU 11-14 OA fractions averaged over 2°C bins, correlated with temperature 78

36. AHU 6 and AHU 11-14 OA fractions averaged over 2 units of enthalpy (kJ/kg), correlated with enthalpy.....79

37. Regression analysis for AHU 6 and AHU 11 OA fractions. 79

38. AHU 6 OA fractions before (raw) and after (scaled) applying slope factor. 80

39. AHU 11 OA fractions before (raw) and after (scaled) applying slope factor. 80

40. AHU 6 and AHU 11 OA fractions after applying slope factors. 81

41. Temperature measured at 5-minute intervals in one patient room during the 24-hour period of May 1, 2013. 83

42. Hourly average temperature in one patient room over the duration of the measurement period (Jan 2013 to Jan 2014) 83

43. Temperature measured at 5-minute intervals at one nurse station on May 1, 2013. 84

44. Hourly average temperature at one nurse station over the duration of the measurement period (Jan 2013 to Jan 2014) 85

45. Relative humidity measured at 5-minute intervals in one patient room during the 24-hour period of May 1, 2013. 85

46. Hourly average RH (%) in one patient room over the duration of the measurement period (Jan 2013 to Jan 2014) 86

47. Relative humidity at one nurse station, measured at 5-minute intervals during the 24-hour period of May 1, 2013. 87

48. Hourly average RH (%) at one nurse station over the duration of the measurement period (Jan 2013 to Jan 2014). 87

49. Absolute humidity measured at 5-minute intervals in one patient during the 24-hour period of May 1, 2013. 88

50. Hourly average absolute humidity in one patient room over the duration of the measurement period (Jan 2013 to Jan 2014) 89

51. Absolute humidity at a nurse station measured at 5-minute intervals during the 24-hour period of May 1, 2013. 90

52. Hourly average absolute humidity at a nurse station over the duration of the measurement period (Jan 2013 to Jan 2014). 90

53. Light intensity (lux) measured at 5-minute intervals in one patient room during the 24-hour period of May 1, 2013. 91

54. Hourly average light intensity (lux) over the duration of the measurement period (Jan 2013 to Jan 2014) 91

55. Light intensity (lux) at one nurse station measured at 5-minute intervals during the 24-hour period of May 1, 2013. 92

56. Hourly average light intensity (lux) at a nurse station over the duration of the measurement period (Jan 2013 to Jan 2014). 93

57. IR beam-breaks (count) measured at 5-minute intervals during the 24-hour period of May 1, 2013. 94

58. Hourly total IR beam-breaks (count) over the duration of the measurement period (Feb 2013 to Jan 2014) in one patient room. 95

59. CO_2 (ppm) measured at 5-minute intervals during the 24-hour period of May 1, 2013. 96

60. Hourly average CO_2 (ppm) over the duration of the measurement period (Feb 2013 to Jan 2014) in one patient room. 96

61. Daily IR beam-break data correlated with CO_2 in a patient room. 97

62. Daily total IR beam-break correlated with daily average CO_2, room source for all patient rooms 98

63. Differential pressure (Pa) measured at 5-minute intervals in one room during the 24-hour period of May 1, 2013.....99

64. Hourly average differential pressure (Pa) over the period (Sept 2013 to Jan 2014) in one patient room. 100

65. Variation in hourly average temperature (°C) in all patient rooms and nurse stations.....104

66. Variation in hourly average RH (%) in all patient rooms and nurse stations.....105

67. Variation in hourly average absolute humidity in all patient rooms and nurse stations.....106

68. Variation in daily average light intensity (lux) in all patient rooms and nurse stations.....107

69. Variation in daily total IR beam-breaks (count) in all patient rooms.....108

70. Variation in daily average CO2 (ppm) in all patient rooms. 109

71. Correlation matrix for temperature in lower floor nurse station and patient rooms. 110

72. Correlation matrix for temperature in upper floor nurse station and patient rooms. 111

73. Correlation matrix for temperature in all rooms and nurse stations. 112

74. Correlation matrix for daily average RH (%) across lower level nurse station and patient rooms. 115

75. Correlation matrix for daily average RH (%) across upper level nurse station and patient rooms. 115

76. Correlation matrix for daily average RH (%) across all patient rooms and nurse stations. 116

77. Correlation matrix for daily average absolute humidity across lower level nurse station and patient rooms. 119

78. Correlation matrix for daily average absolute humidity across upper level nurse station and patient rooms. 119

79. Correlation matrix for daily average absolute humidity across all nurse stations and patient rooms. 120

80. Correlation matrix for daily average light intensity across lower level nurse station and patient rooms. 123

81. Correlation matrix for daily average light intensity across upper level nurse station and patient rooms. 123

82. Correlation matrix for daily average light intensity across all patient rooms and nurse stations. 124

83. Correlation matrix for daily total IR beam-break across lower level patient rooms. 126

84. Correlation matrix for daily total IR beam-break across upper level patient rooms. 126

85. Correlation matrix for daily total IR beam-break across all patient rooms and nurse stations. 127

86. Correlation matrix for daily average CO_2 across lower level patient rooms.....129

87. Correlation matrix for daily average CO_2 across upper level patient rooms.....129

88. Correlation matrix for daily average CO_2 across all patient rooms 130

89. Correlation matrix for daily average CO_2 minus supply air CO_2 (limited to occupant-generated CO_2) across lower level patient rooms.....133

90. Correlation matrix for daily average CO_2 minus supply air CO_2 (limited to occupant-generated CO_2) across upper level patient rooms.....134

91. Correlation matrix for daily average CO_2 minus supply air CO_2 (limited to occupant-generated CO_2) across all patient rooms.....135

92. Variations between floors for temperature, RH, absolute humidity, light intensity, CO_2 and OA fraction; lower floor is denoted by 1, upper floor by 2. ...138

93. Variations between night and day for temperature, absolute humidity, light intensity, IR beam-break, CO2 and OA fractions; night is denoted by 0 and daytime is denoted by 1. 139

94. Seasonal average temperatures over all rooms and nurse stations. 141

95. Seasonal average RH over all rooms and nurse stations. 142

96. Seasonal averages absolute humidity over all rooms and nurse stations. 143

97. Monthly average absolute humidity over all rooms and nurse stations; each consecutive number denotes consecutive months beginning January 2013.....144

98. Seasonal average light intensity over all rooms and nurse stations. 144

99. Monthly average light intensity over all rooms and nurse stations; each consecutive number denotes consecutive months beginning January 2013.....145

100. Seasonal average daily IR beam-break over all rooms. 146

101. Seasonal average CO_2 concentrations over all rooms. 147

ABSTRACT

The Hospital Microbiome Project was designed to study the progression of microbial communities present inside and nearby patient rooms in a new hospital pavilion recently built at the University of Chicago, both before the hospital was occupied and for nearly one year after introduction of patients and hospital staff. A suite of building science measurements, which is the focus of this work, was also designed and implemented to provide potentially meaningful data on several building environmental and operational parameters that may have influenced microbial communities inside the hospital. The building science measurement plan included characterizations of indoor air temperature, relative humidity (RH), absolute humidity, light levels, outdoor air fractions in the HVAC systems, room pressurization, and human occupancy using both beam break counters and CO_2 concentrations in the 10 patient rooms and 2 nurse stations. Each parameter was measured at 5-minute intervals over the span of nearly one year, which resulted in more than 8 million collected data points.

Air temperatures varied more than expected for such a typically tightly controlled environment, with surprisingly low correlations between rooms. RH and absolute humidity were highly correlated between patient rooms, indicating a strong effect from the HVAC system and little effect from occupants. Humidity was more tightly controlled during summer and winter months when the weather was most extreme in Chicago. Light intensity levels were not found to be very different between rooms and floors (which received similar solar exposure), but large seasonal patterns were apparent. CO_2 was moderately correlated with non-directional IR beam-break counts at times, but not consistently. IR beam-break counters revealed large variations in patient room occupancy

patterns throughout the study. In the HVAC systems serving each floor, outdoor air (OA) fractions were successfully calculated using CO_2 concentrations measured in the outdoor air intake, recirculation air, and supply air, albeit only after periodic calibrations with data from the building automation system. OA fractions also showed distinct patterns of economizer usage with outdoor temperatures. Ultimately, this large suite of building science data will be used alongside microbial diversity data to explore correlations between indoor microbiology and the built environment.

CHAPTER 1

INTRODUCTION

Because we spend nearly 90% of our time indoors on average (Klepeis et al., 2001), much of our exposure to both airborne and surface-bound pollutants of physical, chemical and biological origin occurs inside buildings. Hospitals represent a particularly important indoor environment for human exposure to biological contaminants, with the potential for contracting a microbial pathogen while inhabiting a hospital being quite high. The number of healthcare associated infections (HAIs) in the United States was estimated to be 1.7 million in 2002, revealing a rate of 4.5 infections per 100 hospital admissions that led to nearly 100,000 deaths (Klevens et al., 2007). This has placed HAIs as the sixth leading cause of death in the U.S., ahead of diabetes, influenza, pneumonia, and Alzheimer's disease (Anderson & Smith, 2005). Many HAIs can be traced back to exposure to specific microbial pathogens in patient rooms in hospitals. Therefore, hospitals are a prime ecosystem for studying the transfer of microorganisms between humans and the built environment.

The Hospital Microbiome Project (HMP) was designed to study the growth and diversity of microbial communities present inside a new hospital pavilion recently built at the University of Chicago. The study's primary focus was to characterize the indoor microbiome within and nearby patient rooms in a brand new hospital immediately before it was occupied and for nearly one year after introduction of patients and hospital staff. This biological sampling design provided a unique scenario under which to observe the spatial and temporal progression of microbial communities in a brand new, high-occupancy and high-turnover hospital environment. In addition to the microbiological

sampling campaign being conducted simultaneously by project partners at Argonne National Laboratory and the University of Chicago (data for which are still being analyzed using a number of culture-independent sequencing techniques), a suite of building science measurements was also designed and implemented to provide potentially meaningful data on several building environmental and operational parameters that may have influenced microbial communities inside the hospital. This provides an extensive environmental context for microbial samples and may lead to more biologically significant discoveries and may allow for comparisons to other indoor environments (Corsi, Kinney, & Levin, 2012). These kinds of data are also commonly referred to as "built environment metadata" in the microbial ecology literature (Glass et al., 2013).

This work first reviews recent indoor microbial community research, highlights the lack of built environment metadata collection in many previous investigations, and describes some potentially important built environment factors that can influence microbial communities in indoor environments. Based on this review, this work then describes in detail a building science measurement plan that was developed in order to address the need for accurate, long-term environmental and operational measurements within the Hospital Microbiome Project (HMP), which has applicability to other indoor environments as well. Within the hospital, the measurement plan included characterizations of indoor air temperature, relative humidity, light levels, outdoor air fractions in the HVAC systems, and human occupancy in the 10 patient rooms and 2 nurse stations that were also simultaneously sampled for microbial communities. Each parameter was measured at 5-minute intervals over the span of nearly one year while project partners took concurrent daily and weekly microbial samples from a variety of

surfaces. The field equipment, calibrations, installation, data retrieval, analysis methods, and results are presented in this work, and the constraints and significance for building science characterization are also discussed. Although the microbial samples are still being sequenced and analyzed, these building measurements are intended to provide a robust set of environmental data that will provide valuable context to the microbial community samples once analyzed.

CHAPTER 2

BACKGROUND & LITERATURE REVIEW

The study of microbial communities has historically relied on culture-based methods, yielding only partial or biased assessments of microbial community structure and failing to detect fragments of organisms that may influence the larger microbial ecology and potentially human health. In recent years, metagenomics has enabled culture-independent analytical methods, allowing microbes to be sampled directly from their habitats. This, along with faster and cheaper sequencing technologies has significantly increased our knowledge related to microbial communities and diversity (Wooley, Godzik, & Friedberg, 2010). The following subsections describe (1) previous indoor microbial community research and the importance of hospital environments in particular, (2) the prevalence of built environment metadata collection in recent indoor microbial ecology studies, (3) the importance of building environmental and operational characteristics in microbial survival and pathogen transmission, and (4) the methods typically used to robustly measure individual building science parameters, all of which inform the building science measurement plan implemented in the Hospital Microbiome Project (HMP) described in Chapter 3.

2.1 Previous indoor microbial community research and the importance of hospital environments

The development of computational methods for measuring and analyzing microbial diversity has led to a rapid increase in the number of studies exploring microbial diversity within the built environment (Humphries, 2012; Scott T Kelley &

Gilbert, 2013). Recent studies have characterized microbial diversity in offices and other commercial buildings (Hewitt, Gerba, Maxwell, & Kelley, 2012; Tringe et al., 2008), classrooms (Hospodsky et al., 2012; Meadow et al., 2013; J. Qian, Hospodsky, Yamamoto, Nazaroff, & Peccia, 2012), healthcare facilities (Hewitt et al., 2013; Kembel et al., 2012; Lee, Tin, & Kelley, 2007; Oberauner et al., 2013; Poza et al., 2012; Rintala, Pitkaranta, Toivola, Paulin, & Nevalainen, 2008), homes (Dunn, Fierer, Henley, Leff, & Menninger, 2013; Flores et al., 2013; Jeon, Chun, & Kim, 2013; S. T. Kelley, Theisen, Angenent, St. Amand, & Pace, 2004; Medrano-Félix et al., 2011), and transportation environments (Korves et al., 2013; Robertson et al., 2013), which all represent indoor environments where people spend much of their time. Particular attention has been paid to surface sampling, with few studies focused on indoor or outdoor air sampling. Many of these studies have shown that humans are the main source of microbial diversity in many indoor environments. Others have shown that outdoor microbial communities can also play a role, depending on specific types of microbes and particular building design and operational characteristics. For example, many bacterial communities in occupied environments appear primarily dominated by human skin, gut, nasal, and/or oral sources (Hewitt et al., 2013; Hospodsky et al., 2012), with some variability attributed to building ventilation strategies and occupancy characteristics (Kembel et al., 2012; Meadow et al., 2013). Conversely, fungal communities appear primarily dominated by local outdoor environments (Adams, Miletto, Taylor, & Bruns, 2013; Amend, Seifert, Samson, & Bruns, 2010).

Beyond fundamental microbial community characteristics, human exposure and susceptibility to specific pathogens is of great concern for public health, and previous

research has shown that the built environment plays a significant role in the transmission of many pathogens. Hospitals are particularly sensitive indoor environments for pathogen transmission. Hospitals implement strict surface cleaning procedures and hygiene protocols in order to decrease microbial contamination and reduce the chance of transmitting infections, but hospital-acquired infections (HAIs) continue to persist. The indoor environment acts as a reservoir for pathogens that are often capable of prolonged survival, possibly months. For example, Kramer et al. (2006) reported that hospital surfaces with hand contact are often contaminated with nosocomial pathogens and may serve as vectors for transmission (Kramer, Schwebke, & Kampf, 2006). Stiefel et al. (2011) found that healthcare workers are just as likely to contaminate their hands (gloves) from commonly touched surfaces as from direct contact with patients' skin sites (Stiefel et al., 2011). Sharpe et al. (2011) found that everyday levels of surface contamination in intensive care units (ICUs) are significantly higher than levels considered to represent a risk for the transmission of infections. Other studies suggest that more attention is needed toward building design and environmental factors that can facilitate and enhance environmental disinfection (Sharpe & Schmidt, 2011).

As an indoor study site, hospitals offer the advantage of having many built environmental characteristics that are relatively constant across individual patient rooms, including building materials, square footage, furniture, and cleaning procedures and schedules. Additionally, the absence of macrofauna such as pets and insects enhances our ability to measure the effect of a defined set of sources responsible for the introduction of microorganisms, namely air, water, and occupants. Other environmental variables such as air temperature, relative humidity, ventilation air sources, HVAC airflow rates, and

human occupancy are typically assumed to be rather tightly controlled, particularly in newer hospital facilities, although there is a general lack of data to support this assumption in the peer-reviewed literature.

2.2 Building science measurements in recent DNA-based indoor literature

While recent studies utilizing culture-dependent molecular techniques and metagenomic computational tools for measuring and analyzing microbial diversity have greatly advanced our knowledge of the diversity and dynamics of microbial communities in indoor environments, accurate and meaningful characterizations of the building and indoor environmental conditions in which sampling takes place remain limited. Insufficient descriptions of these conditions may limit our ability to accurately compare microbial ecology results from different indoor environments (Corsi et al., 2012).

Early DNA-based studies of microbial diversity in the built environment focused primarily on surfaces, followed by a larger (albeit still limited) number of studies that also incorporated indoor air sampling. Many of these studies have failed to characterize local indoor environmental and operational parameters that may greatly affect microbial diversity. For example, Kelley et al. (2004) analyzed microbes from four used vinyl shower curtains from different Colorado households. Each community was highly complex with no identical sequences between them. However, no building environmental conditions, such as shower usage and cleaning procedures, was reported to potentially explain some of the observed variation. Lee et al. (2007) used both culture and culture-independent molecular methods to determine bacterial diversity in a child-care center over a six-month period with surface samples taken from toys and furniture in

four daycare classrooms. The study showed certain bacteria types consistently found on all surfaces with some variability in other sequences with time (particularly during cold and flu season). However, no information on building design, operation or occupancy was reported, limiting our ability to make comparisons to other environments.

There have been several studies in hospital facilities using similar methods. For example, Poza et al. (2012) compared bacterial diversity on surfaces in intensive care units (ICUs) to diversity in an open, crowded entrance hall of a hospital (Poza et al., 2012). Bacterial diversity detected in the ICU was different from that in the hall, suggesting that high human occupancy in close proximity within the hall may have played an important role. Hewitt et al. (2013) surveyed bacterial diversity in two neonatal intensive care units (NICUs) and tracked the sources of microbes (Hewitt et al., 2013). Many of the bacteria genera included known pathogens and many were skin-associated. Fecal coliform bacteria were also detected in high proportions of surface samples in one of the units. Although the authors maintained a particular focus on commonly touched surfaces in the units, no quantitative measures of human occupancy were noted, which may have helped further explain or extrapolate their results. In another study of ICUs in a hospital, Oberauner et al. (2013) sampled floors, medical devices, and workplaces (Oberauner et al., 2013). They found that microbial diversity between the three areas were distinct and overall, bacterial communities were not as diverse as other indoor environments. Floor-associated communities formed distinct clusters compared to devices, whereas workplaces and devices were similar, again suggesting occupancy influences. The authors noted that the ICU had both air conditioning and window

ventilation, but other environmental conditions or operational characteristics were reported.

Other recent DNA-based microbial diversity studies have given more attention to building environmental and operational characteristics that could potentially have an effect microbial diversity, and many have shown these variables to be influential. For example, a study by Rintala et al. (2008) investigated bacterial communities in settled dust in two similarly aged buildings in Finland over the course of a year (Rintala et al., 2008). Four samples were taken in each building, one per season. Differences between buildings were found to be greater than differences between seasons. They described several building characteristics, including construction, HVAC system, age, history of problems, and also reported that a civil engineer performed a technical inspection on both buildings. Both buildings had a mechanical exhaust ventilation system, although it is not clear how it actually performed during the field campaign. One building, built in 1920, had local signs of moisture and microbial damage in the bathrooms on both floors; additionally, the authors noted that employees in the building had complained of building-related symptoms and indoor air problems. The other building, built in 1940, had undergone a thorough restoration in 1982 and had no visible signs of moisture damage; occupants reported no problems related to the building or indoor air.

Several other recent studies have gone even further, providing more information about HVAC systems and ventilation strategies, occupant behaviors, and basic indoor environmental parameters such as temperature (T) and relative humidity (RH). For example, Kembel et al. (2012) studied the relationship between building attributes and airborne bacterial communities at a hospital by quantifying airborne bacterial

communities and environmental conditions in patient rooms exposed to mechanical or window ventilation and in outdoor air on the roof near the HVAC system outdoor air intake. The rooms were classified as “exposed to mechanical ventilation” or “exposed to window ventilation.” The mechanically ventilated rooms had ventilation air supplied by the HVAC system and removed by a return duct and a bathroom exhaust duct. The window ventilated rooms had ventilation air supplied directly from the outside through a window and removed through a return duct, bathroom exhaust, and by any outflow through portions of the same window. Diversity of airborne bacterial communities was found to be lower indoors than outdoors, and communities in mechanically ventilated rooms were less diverse than window-ventilated rooms. Bacterial communities found indoors contained many taxa that are absent or rare outdoors, including those closely related to potential human pathogens. Building characterizations included the source of ventilation air, airflow rates, relative humidity and temperature. They correlated that relative abundance of bacteria closely related to human pathogens was higher indoors than outdoors, and higher in rooms with lower airflow rates and lower relative humidity (Kembel et al., 2012).

Several recent studies have also incorporated detailed information about human activities in their sampled environments. Medrano-Feliz et al. (2010) investigated human activities in terms of cleaning behaviors and identified the presence of *Escherichia coli*, *Staphylococcus aureus*, *Salmonella*, hepatitis A, and norovirus in 60 homes in Mexico and assessed the effect of chlorine and ammonium based disinfectants on these communities (Medrano-Félix et al., 2011). Surface sample sites included kitchens (counter top, sponge, dishcloth, cutting board, and sink), bathrooms (sink, toilet bowl,

toilet seat, and shower tile), pet areas (toy sites) and children's areas (toy sites). In 30 homes that followed a disinfection protocol, there was a significant reduction in the presence of the study's target microbes compared to a control group that did not utilize a disinfectant protocol, suggesting that cleaning patterns are very important to assess accurately for better interpretation of surface sample results.

Qian et al. (2012) took a closer look at bioaerosol dynamics and was the first study to quantify size-resolved emission rates of biological (bacteria and fungi) particles in indoor air inside a 30 m^2 classroom measuring under both occupied and vacant conditions. The reason that the authors were able to calculate emission rates is because they sufficiently characterized detailed building operation, including air exchange rates, HVAC operation, and the number of occupants during sampling. Human occupancy was assessed visually, and position of windows and doors and HVAC system operational characteristics were noted. AER was measured using CO_2 decay techniques and T/RH was also measured during testing. They demonstrated that human occupancy resulted in significant emissions of airborne particle mass, bacterial genomes, and fungal genomes.

In the same university classroom, Hospodsky et al. (2012) also collected bioaerosol samples during both occupied and vacant periods in order to characterize total particle mass concentrations, bacterial genome concentrations, and bacterial phylogenetic populations indoors, outdoors, and in ventilation duct supply air concurrently. HVAC filter dust and floor dust were also sampled. They measured several environmental parameters, including T/RH and CO_2 concentrations. They characterized the HVAC system as operating under economizer conditions, varying the fraction of outdoor airflow rate to total airflow from 25% to 100% depending on heating and cooling needs. OA

fraction measurements were not made, but the authors suggested it would have been near 50% OA during test conditions based on outdoor climatic conditions. The HVAC system passed through a MERV 8 particle filter before entering the classroom; authors measured the in-situ size-resolved filtration efficiency of this filter using an optical particle counter. $PM_{2.5}$ and PM_{10} air samples were taken in indoor, outdoor, and HVAC supply environments; HVAC filter and floor dust was mechanically extracted and then sieved and resuspended to obtain $PM_{2.5}$, PM_{10}, and PM_{37} mass fractions. The authors noted that there was no visible water damage or known history of water damage in the building. The room was cleaned every second day by vacuuming and semiannually by wet carpet cleaning. Students and teachers were asked not to open windows and doors during the sampling campaign. Air exchange rates were measured using CO_2 injection and decay during several distinct periods, with an average AER of 5.5 per hour. Human occupancy was also the same as in Qian et al. (2012). Comparisons between bacterial populations in indoor air and during unoccupied and occupied periods further suggested that resuspended floor dust and direct human shedding were important contributors to bacterial populations in indoor air. These very detailed building characterizations again allowed for unprecedented quantitative estimates and interpretations of their results.

2.3 Building environmental and operational factors influencing microbial survival and pathogen transmission

While contact transmission of disease is likely responsible for the majority of HAI cases in hospital environments, transmission through the air may be more difficult to control. However, measures can be made to limit the spread. Aside from personal and administrative measures, engineering control methods including building ventilation, use

of HEPA and other air cleaning methods, can play a significant role in infection control in hospital environments and other buildings. Eames et al. (2009) identified three basic elements of building ventilation, including (i) the ventilation rate (i.e., the amount of outdoor air provided to a space), (ii) airflow direction, which should be from clean to dirty zones in a hospital, and (iii) air distribution or indoor airflow patterns (i.e., efficient air delivery and removal, which all play a role in infection control) (Eames, Tang, Li, & Wilson, 2009). Several studies have also sought to quantify the risks associated with airborne transmission of respiratory diseases. One often-used approach is the Wells-Riley model, which is based on a concept of a "quantum of infection", whereby the rate of generation of infectious airborne particles can be used to model the likelihood of an individual in a steady-state well-mixed indoor environment being exposed to the infectious particles and subsequently succumbing to infection (Riley, Murphy, & Riley, 1978).

Qian et al. (2009) integrated the Wells-Riley equation into computational fluid dynamics (CFD) models to predict the spatial distribution of infection risk, analyzing the 2003 SARS outbreak in a hospital in Hong Kong. The spatial distribution of infected cases was shown to be related to the airflow pattern and the outbreak was very likely transmitted via airborne routes and related to the ward ventilation system (H. Qian, Li, Nielsen, & Huang, 2009). Knibbs et al. (2011) assessed the effect of ventilation rates on influenza, tuberculosis, and rhinovirus infection risk within three distinct rooms in a major urban hospital: a lung function laboratory, an emergency department negative-pressure isolation room, and an outpatient consultation room. They measured air exchange rates (AER) using CO_2 as a tracer and used a model developed by Gammaitoni

and Nucci to estimate infection risk (Gammaitoni & Nucci, 1997). The study showed that the isolated nature of the first two rooms limited infection risks to 0.1-3.6%, but for individuals entering an outpatient consultation room after an infectious individual departed ranged from 3.6-20.7%, depending on occupant duration (Knibbs, Morawska, Bell, & Grzybowski, 2011).

Blachere et al. (2009) measured size-fractioned airborne particles in a hospital to identify airborne influenza viruses using real-time polymerase chain reaction (PCR), a method to amplify and quantify targeted DNA molecules. They found that ~53% of the detectable influenza virus particles they found were within the respirable aerosol fraction (i.e., less than 4 µm). More specifically, 46% were in the >4 µm stage; 49% were found on the 1-4 µm stage; and 4% were collected on the back-up filter (<1 µm). Temperature, relative humidity, and air pressure differentials were measured and design air-exchange rates were noted in the study (Blachere et al., 2009). Particle size is an extremely important parameter governing removal by HVAC filters and deposition to surfaces (Nazaroff, 2004).

King et al. (2013) measured spatial deposition of aerosolized *Staphylococcus aureus* in an aerobiology test room arranged in three different layouts: an empty room, a single-bed, and a two-bed hospital room. They demonstrated that small particle bioaerosols are deposited throughout a room with no clear correlation between relative surface concentration and distance from the source. However, a physical partition separating patients was shown to be effective at reducing cross-contamination of neighboring patient zones. The results also validated the use of CFD techniques for

modeling bioaerosol behavior in indoor environments (King, Noakes, Sleigh, & Camargo-Valero, 2013).

Overall, these studies and others point to the large influence that a number of building environmental conditions, operational conditions, and design and construction characteristics can have on indoor microbial communities, microbe survival, and pathogen transmission and infectious disease risk.

2.4 Built environment metadata parameters and collection methods

A large number of building science measurements that may influence microbial communities in indoor environments can be described generally by the following categorizes: (i) building characteristics and basic indoor environmental conditions, (ii) human occupancy measurements, (iii) HVAC system characterizations and ventilation rate measurements, (iv) air-sampling and aerosol dynamics, and (v) surface characterizations. These parameters are informed in large part by evidence of their importance for influencing microbial communities on indoor surfaces and in indoor air, as well as their importance for general building characterizations in other indoor environmental research. This work was designed to incorporate most of the above building science measurements in order to adequately support the microbial measurements in the Hospital Microbiome Project.

2.4.1 Building characteristics and basic indoor environmental conditions. Several basic building characteristics and indoor environmental measurements are fundamental to any indoor environmental investigation. Important building characteristics include age of

construction, floor areas and volumes, material descriptions, type of use, typical occupancy, history of water damage, occupant complaints, HVAC system type and operation (i.e., in heating or cooling modes), the use of humidifiers, and many others. Important indoor environmental conditions, including air temperature (T), relative humidity (RH), absolute humidity, and light levels in the sample space, may have particular influence on microbial diversity outcomes. Portable, off-the-shelf battery-powered sensors can accurately and inexpensively measure and log these data for long periods of time. Long-term data logging is important for assembling a history of indoor environmental conditions that may affect microbial growth and survival, rather than relying upon spot measurements during the time of testing.

Indoor T/RH has been shown to be an important influential parameter in a number of previous field studies of indoor microbial ecology. For example, indoor temperatures have been positively associated with fungi and negatively associated with bacteria and total inflammatory potential (TIP) of cell assays in several homes in Denmark (Frankel et al., 2012). In the same study, indoor RH was also positively correlated with indoor fungi concentrations. In a study of child day-care centers in Turkey, differences in airborne bacterial communities were seen with some (varying) outdoor environmental conditions, which could also have manifested in differences in indoor environmental conditions such as temperature, relative humidity, or HVAC operation (Aydogdu, Asan, & Tatman Otkun, 2009). For example, the amount of endospore-forming Gram-positive bacteria increased as the amount of sunlight and temperature increased and as relative humidity decreased (all measured outdoors). In fact, it has long been thought that sunlight (in addition to increased ventilation) could reduce the spread airborne infections in hospitals,

although evidence is quite limited and suspected mechanisms are not entirely environmental (Hobday & Dancer, 2013). More recently, a study in primary schools in Australia found that air temperature (measured over the previous 24 hours) was negatively associated with concentrations of endotoxin in indoor air and positively correlated with endotoxin loads in floor dust (Salonen et al., 2013). Additionally, lower airborne endotoxin concentrations were observed during periods of higher levels of relative humidity, and T and RH appeared to act separately.

Measurements of T/RH may be particularly important inside HVAC systems as well; bacteria and fungi have been shown to grow at an accelerated rate with higher temperatures and higher RH in air-conditioning ducts subjected to dust deposition (A. Li, Liu, Zhu, Liu, & Wang, 2010). Other studies have shown that a substantial amount of dust can accumulate due to particle deposition on air-conditioning ducts (Sippola & Nazaroff, 2004; Brent Stephens & Siegel, 2012; Waring & Siegel, 2008). There are complex interactions between moisture and building materials that may be important to characterize as well. For example, in a recent study of day care centers in Sweden, fungal DNA levels were shown to be higher in buildings at risk of dampness, in rooms with linoleum flooring materials, and in buildings with rotating heat exchangers (Cai et al., 2011). T/RH measurements should also be used to calculate absolute humidity ratios, or the mass of water vapor per mass of dry air, regardless of temperature (ASHRAE, 2013a), as there is some evidence that absolute humidity can influence microorganism survival (Baughman & Arens, 1996), mold growth on building materials (Nielsen, Holm, Uttrup, & Nielsen, 2004), airborne endotoxin (Park et al., 2000), and the inactivation or survival of influenza viruses on surfaces (McDevitt, Rudnick, First, & Spengler, 2010; J.

Shaman & Kohn, 2009; Jeffrey Shaman, Pitzer, Viboud, Grenfell, & Lipsitch, 2010). Thus, at a minimum, long-term measurements of T/RH and possibly artificial and/or natural light levels should be made and recorded in microbial diversity studies, as many have already done. Long-term data logging is important for characterizing changes in environmental conditions over time, within a study space. Relying on spot measurements can significantly reduce the information with which to correlate biological data.

2.4.2 Human occupancy measurements. Human occupancy and activity are major factors influencing indoor microbial communities. Studies have suggested that the presence of people, their activities, and the surfaces with which they come in contact are important drivers of microbial diversity. There are many ways to measure human occupancy, with the simplest method being physical counting and recording of people in the sample space. However, such a method is only successful in small-scale, short-term studies and does not allow for larger, long-term studies, which require more sophisticated methods and equipment for accurately capturing human occupancy and activity. The method of choice often depends on the design and construction of the study environment and may include video cameras equipped with people-counting software (Chen, Chen, & Chen, 2006; Erickson et al., 2009; Liu, Guan, Du, & Zhao, 2013; Terada, Yoshida, Oe, & Yamaguchi, 1999), optical and infrared tripwires that count people crossing a particular area, such as a doorway (Dong & Andrews, 2009; Meyn et al., 2009), proximity or light sensors that can detect movement or lack of movement near a specific location (Dodier, Henze, Tiller, & Guo, 2006; Jennings, Rubinstein, DiBartolomeo, & Blanc, 1999; Rubinstein, Colak, Jennings, & Niels, 2003), CO_2 sensors coupled with dynamic mass

balances on indoor CO_2 concentrations (Bartlett, Martinez, & Bert, 2004; Cornaro, Paravicini, & Cimini, 2011; Lawrence & Braun, 2007; Wang, Burnett, & Chong, 1999), radio-frequency identification (RFID) (Gillott, Holland, Riffat, & Fitchett, 2006; N. Li & Becerik-Gerber, 2011; N. Li, Calis, & Becerik-Gerber, 2012) and Bluetooth tracking systems (Bruno & Delmastro, 2003; Kjærgaard, Treu, Ruppel, & Küpper, 2008; Naya, Noma, Ren Ohmura, & Kogure, 2005), or even acoustic sensors that detect noise levels (Dong & Andrews, 2009). Even with more sophisticated methods, it may be difficult to make accurate measurements when the study involves large volumes of people. Measurements can also be combined with sophisticated algorithms to provide robust determinations of time-varying human occupancy and/or activity (Hutchins, Ihler, & Smyth, 2007; Ihler, Hutchins, & Smyth, 2006; Lam et al., 2009; Page, Robinson, Morel, & Scartezzini, 2008).

The choice of occupancy measurement technology may depend on the environment in which sampling is taking place. For example, IR beam-break sensors installed at doorways are most appropriate for smaller volume environments with limited numbers of entrances and exits, and where location inside the room may not be as significant as mere presence in the room. Video camera systems, on the other hand, may provide location detection in smaller environments, but result in higher costs in larger environments. Proximity sensors can help determine occupancy near a particular location, but can suffer from inaccuracy, with a lack of movement not necessarily equating to a lack of occupancy, and vice versa. Both beam-break sensors and video camera systems are more appropriate for environments with limited entryways.

Upgrading from non-directional to directional beam-break sensors makes them more utilizable in environments with multiple doorways, but can increase costs significantly.

CO_2 sensors can be good identifiers of human occupancy as they can be highly accurate, but suffer from high costs and variable correlation with human occupancy as emission rates vary between individual people. Additionally, reliance on CO_2 measurements requires sufficient characterization of HVAC system characteristics and a well-mixed environment in order to complete a mass balance. Several options allow users to choose depending on specific needs and budget.

2.4.3 HVAC system characterizations and ventilation rate measurements. Another set of parameters that are essential in characterizing building operation are HVAC system airflow rates and ventilation rates in the sample space. These factors greatly impact indoor concentrations of particles, including those of biological origin. Many HVAC-related factors have been linked to microbial growth, including air temperature, humidity, air velocity, and filter media location and characteristics (Bluyssen et al., 2003). Air exchange rates (AERs) have also been shown to correlate with indoor microbial communities. Particle filtration efficiency and HVAC recirculation rates (the airflow rate through an HVAC system divided by the volume of the space it serves) can impact the amount of biomass that settles on surfaces, depending on particle size and surface characteristics; biomass is decreased when particles are removed at a greater rate than their deposition to surfaces. This factor becomes less important when sampling in spaces that are frequently cleaned. Additionally, the effects of air speed, amount of mixing in the environment, and surface area-to-volume ratio will also have an effect on

deposition rates, and therefore the amount of settled biomass (He, Morawska, & Gilbert, 2005; Lai, 2002).

There are a variety of tools to measure airflow rates through HVAC systems, many with varying degrees of accuracy, complexity, and equipment requirements (ASHRAE, 2013b). Airflow rates can be measured either within air handling units or at individual supply diffuser and return grilles, depending in large part on the size of the equipment. There are many valid and accepted ways to measure airflow rates at or near the air handling unit, including: (i) pressure readings can be correlated to fan curve data provided by the fan manufacturer; (ii) flow metering devices such as venturi meters, flow nozzles, orifice meters, or rotameters can be installed directly into the HVAC system; (iii) air velocity can be measured using pitot tubes or hot-wire anemometers traversing the entire area of a duct system, particularly if general guidelines for the number and spacing of measurement points are followed (i.e., equal-area or log-Tchebycheff methods can take into account the distribution of air velocity from bulk air in the duct to the velocity near the edges and corners of ducts), or (iv) pressure matching with a calibrated fan (The Energy Conservatory, 2007). Particularly for small and medium sized HVAC systems, there are also highly accurate airflow metering plates available for rapid measurements of air handler flow rates (Francisco & Palmiter, 2003).

Additionally, there are ways to measure airflow rates leaving supply diffusers or entering return grilles, including: (i) airflow capture hoods; (ii) air velocity readings correlated to diffuser characteristics provided by the manufacturer; (iii) duct traverse air velocity measurements; and (iv) pressure matching with a calibrated fan. Once specific airflow rates have been characterized in an environment, there are several methods to

continue to record flow data over time without the need for interventions by field-workers. For example, airflow rates, which are invasive to measure, can be correlated to duct pressure measurements, which can be easily measured and recorded on a data logger (Stephens, Siegel, & Novoselac, 2010; Brent Stephens, Novoselac, & Siegel, 2010; The Energy Conservatory, 2006; Walker, Dickerhoff, Faulkner, & Turner, 2012).

Once airflow rates are measured, the rate of outdoor air supplied by the ventilation system can also be measured. Although many building automation systems can report these values, accuracy is often an issue. The fraction of outdoor air in an air stream can be measured in several ways, including measuring CO_2 concentrations in recirculation, outdoor and supply air streams of an air handling unit (A. K. Persily, 1997). Knowing both supply flow rate and outdoor air fraction, outdoor air ventilation rates can be calculated. Another way of measuring ventilation rates and air flows directly in test environments is using a tracer gas (ASTM E 741, 2006; Miller, Leiserson, & Nazaroff, 1997; Sherman, 1989, 1990; Wallace, Emmerich, & Howard-Reed, 2002). Tracer gas methods include simple injection and decay, constant injection, and constant concentration (ASTM E 741, 2006). Both active and passive tracer gas injection and sampling methods can be used as well. Active techniques allow for time-varying AER measurements but involve real-time monitoring of tracer gases, which can introduce prohibitive costs and labor requirements for large field studies. Passive techniques such as the perfluorocarbon tracer (PFT) method utilize inexpensive passive tracer sources and samplers, but are limited to measuring longer-term time-averaged AERs (Lunden et al., 2012). Particular care should be taken to achieve proper mixing and tracer gas

distribution, as well as selection of a nonreactive, nontoxic, inexpensive, and easily detectable tracer gas.

2.4.4 Air sampling and aerosol dynamics. A wide range of air sampling devices have been used in recent studies to measure microbial abundance and diversity in indoor air. These methods have included liquid impingers (Kembel et al., 2012; Robertson et al., 2013), filter-based size-resolved impactors (Hospodsky et al., 2012; J. Qian et al., 2012) and non-size-resolved impactors (Meadow et al., 2013), petri dishes suspended in air (Adams et al., 2013), HVAC particle filters installed in air handling units (Korves et al., 2013; Tringe et al., 2008), and an experimental sampler similar to a wetted wall cyclone (Gaüzère et al., 2013). These methods may vary widely in their collection efficiencies and DNA extraction efficiency. Additionally, they vary in terms of some practical concerns with airflow rates, noise levels, and introducing potential bias. Bioaerosol samplers operate at airflow rates ranging from 4 L min^{-1} (Meadow et al., 2013) to as much as 300 L min^{-1} (Robertson et al., 2013) or even 1000 L min^{-1} (Gaüzère et al., 2013). Higher airflow rates have the advantage of collecting more biomass, but can also compete with air exchange rates in smaller volume environments, which could alter aerosol dynamics in the space. Additionally, larger pumps used for higher flow rates introduce practical size and noise concerns. Passive sampling techniques, such as suspended petri dishes, avoid these concerns but may introduce bias by oversampling larger particle sizes that are more likely to settle than smaller particles.

A recently developed technique in air sampling mechanisms has been the use of HVAC filters to passively collect bioaerosols. The advantage of this method is the

extremely large volume of air that passes through filters on a daily basis. Tringe et al. (2008) used HVAC particle filters installed in air handling units to sample air microbiota in two shopping centers in Singapore. Over a period of 90 days, with air passing through filter for 14 hours per day, approximately 6×6^6 m^3 of air passed through the filters (Tringe et al., 2008). Traditional bioaerosol sampling techniques utilizing flow rates of 4-1000 L min^{-1} would have provided a maximum of 75×10^3 m^3 of air for sampling, reducing the amount of biomass available for analysis significantly. Noris et al. (2011) conducted a study that compared bacterial and fungal communities on residential HVAC filters and found that microbial communities on the filters were not different from those obtained from impingers that sampled air for a month (Noris, Siegel, & Kinney, 2011). Additionally, dust from the HVAC filters were found to be similar to those collected on surfaces. This suggests that high efficiency HVAC filters could be used as a long-term integrated measure of microbial communities in indoor air.

2.4.5 Surface characterizations. Finally, the last type of building environmental characterization that we should mention involves meaningful characterization of surfaces from which microbes are sampled. Surfaces can harbor an array of adsorbed compounds and settled dust that may affect the growth and diversity of microbial communities on them. Basic surface characteristics such as porosity, composition, and environmental conditions immediately adjacent to surfaces can all affect microbial communities. Water activity, or the relative humidity at equilibrium, of a building material is a major determining factor for fungal growth (Nielsen et al., 2004). Water activity varies with temperature and the type of material; the longer a material's water activity is over 75%,

the greater risk of fungal growth (Viitanen et al., 2010). Water activity may also vary with surface temperatures, which may or may not correlate well with nearby air temperatures.

Another important parameter when sampling microbial communities on surfaces is the frequency of cleaning. Cleaning impacts settled dust, adsorbed compounds, and the microbial mass found on surfaces. The effect of cleaning frequency has been demonstrated in a recent study showing that the microbial community composition on people's hands is highly influenced by time since their last hand washing (Fierer, Hamady, Lauber, & Knight, 2008). Similar studies involving building materials have shown the same (Adams et al., 2013; Flores et al., 2013; Medrano-Félix et al., 2011).

CHAPTER 3

METHODOLOGY

Using information from the review in Chapter 2 combined with realities of budget constraints in the HMP, a suite of building science measurements was designed to support the simultaneous microbial sampling by providing meaningful data on several building environmental and operational parameters that may serve to influence microbial communities in the hospital. The suite of measurements was informed by several initial walkthroughs of the hospital during construction, evaluations of mechanical and floor plans, and several baseline measurements during unoccupied periods of parameters that were predicted to be challenging to acquire once the hospital was occupied, including supply and return airflow rates in each patient room. Subsequently, long-term measurements of parameters including indoor air temperature, relative humidity, light intensity, HVAC outdoor air fractions, room pressurization with respect to the hallways, and human occupancy inside the patient rooms were conducted. An assortment of off-the-shelf sensors was selected to measure each of these parameters, giving consideration for accuracy, ease of data retrieval, aesthetic impact, battery life, and budgetary constraints. This chapter describes (1) basic patient room characteristics, (2) instrumentation, (3) instrument calibration procedures, (4) data collection procedures, and (5) data analysis procedures.

3.1 Patient room and mechanical room characteristics

Ten patient rooms were selected for sampling on two floors, with five consecutive adjacent rooms on the 9th floor located directly below five identical rooms on the 10th

floor. All ten rooms were identical, single-occupancy, west-facing, adult inpatient rooms and classified as “neutral pressure” rooms on the mechanical plans. While all ten rooms were patient care units, the 10th floor was devoted to oncology patients, who typically had longer stays than patients on the 9th floor. Each room had a floor area of approximately 360 square feet (33.4 m^2), including a bathroom of 50 square feet (4.6 m^2). Ceiling heights were 9.5 feet (2.9 m), providing a volume of approximately 3420 ft^3 (96.8 m^3). Large windows spanned the width of the west side of each room, opposite the sole doorway on the east side. Two 1.5 m slot supply diffusers were located at the ceiling near the windows, spanning the width of the room. The design supply airflow rate was 450 cfm (765 m^3/hr) according to detail drawings and schedule sheets, with summer and winter minimum flows of 390 cfm (663 m^3/hr). Although the HVAC systems conditioned air centrally, reheat coils were also installed at the supply diffusers for greater temperature control within individual rooms. A single 2 ft x 2 ft (0.6 x 0.6 m) return grille was located at the ceiling near the doorway with a design airflow rate of 350 cfm (595 m^3/hr) and a minimum of 290 cfm (493 m^3/hr), according to the schedule sheets. An additional exhaust was located in the bathroom with a constant design airflow rate of 100 cfm (170 m^3/hr). Two large nurse stations located across the hallway from the patient rooms on each floor were also selected as sampling locations.

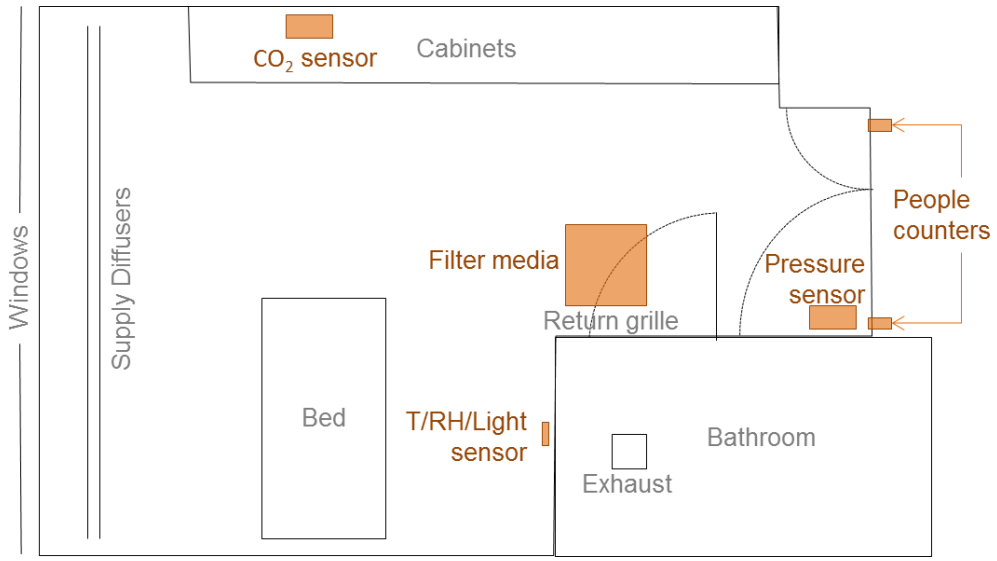

Figure 1. Diagram of sensors and locations in hospital patient rooms.

Each floor was served by air handling units (AHUs) located in the two-level mechanical penthouse on the 11th and 12th floors. The 10th floor was served by a single AHU with a design airflow rate of ~50,000 cfm (85,000 m^3/hr), while the 9th floor was served by a combination of four connected ~50,000 cfm (85,000 m^3/hr) AHUs that also served the 8th floor (for a total of ~200,000 cfm or 340,000 m^3/hr). These four AHUs met at a common return plenum, mixed with outdoor air, and split into four different supply plenums after conditioning and filtration. Each AHU had MERV 7 and MERV 13 pre-filters installed before the heating and cooling coils and supply fans, as well as HEPA filtration installed just before entering the supply plenum. Dampers at the outdoor air intakes were automated to adjust the intake flow rate depending on outdoor air temperature. AHU detail drawings are shown in Figure 2.

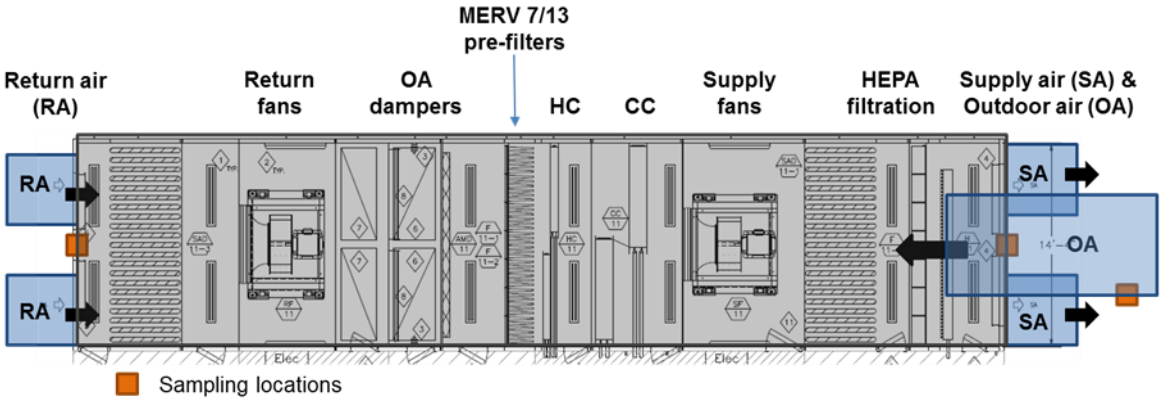

Figure 2. Air handling unit showing outdoor, return, and supply air streams.

3.2 Patient room and mechanical room coding for identification and confidentiality

In order to de-identify patient rooms for purposes of patient confidentiality, a naming convention was created to refer to rooms on the 9th and 10th floors of the hospital. Numbers 101-105 referred to consecutive rooms on the 9th floor, with 100 referring to the nurse station on the same floor. Numbers 201-205 refer to the rooms on the 10th floor, directly above those on the 9th, with 200 referring to the nurse station on the 10th floor.

AHU 6 refers to the single AHU that served the 10th floor. AHU 11 refers to the combination of AHUs 11, 12, 13, and 14, which combine to serve the 8th and 9th floor. For the purposes of our sampling, we are only concerned with the 9th floor and do not refer to the 8th floor. Each of the two AHUs had three sampling locations (outdoor air intake, recirculation air, and supply air), giving a total of six sampling locations within the mechanical rooms. Here, we specify AHU 6 OA, RA and SA and AHU 11 OA, RA, SA to refer to the AHU number and outdoor air, return air, and supply air streams, respectively.

3.3 Sensor instrument selection and installation

Environmental conditions within each patient room and nurse station were measured continuously using a combination of sensors and data loggers operating at 5-minute intervals for the span of one year. The location of each sensor is shown in Figure 3. Data was retrieved on a weekly basis, concurrent with weekly microbial sampling by project partners. Onset HOBO U12-012 data loggers, which recorded air temperature, RH, and light intensity, were installed on the wall adjacent to patient beds and at a central location at each of the two nurse stations. These locations were chosen primarily by giving consideration for likely light exposure, aesthetic impact, invasiveness, and ease of access. CO_2 was measured in each room as one of two surrogates for occupancy using PP Systems SBA-5 analyzers connected to Onset HOBO U12 data loggers installed on a shelf located near an electrical outlet. A differential pressure transducer (Onset T-VER-PXU-X) was also installed at each doorway connected to a large battery pack and another Onset HOBO U12 data logger with sampling lines placed on each side of the doorway to measure the pressure differential between the patient rooms and the adjacent hallway. Each of the aforementioned devices that were connected to HOBO U12 data loggers was synchronized to collect data simultaneously throughout the project.

To further characterize human occupancy and activity, non-directional infrared beam-break people counters (SenSource PC-TB12-R) were installed at each patient room doorway (there was only one doorway for each room). These sensors recorded the number of beam breaks that occurred over each 5-minute sample interval, although they were not synchronized with the HOBO data loggers. Finally, a thin sheet of synthetic filter media was placed on the exterior of each patient room return grille and attached

with custom fit magnets in order to sample airborne microbial communities (Hoisington, Maestre, Siegel, & Kinney, 2014; Noris et al., 2011). The media was removed, preserved for microbial extraction, and replaced every week. This was the only airborne microbial sampling method utilized in this project.

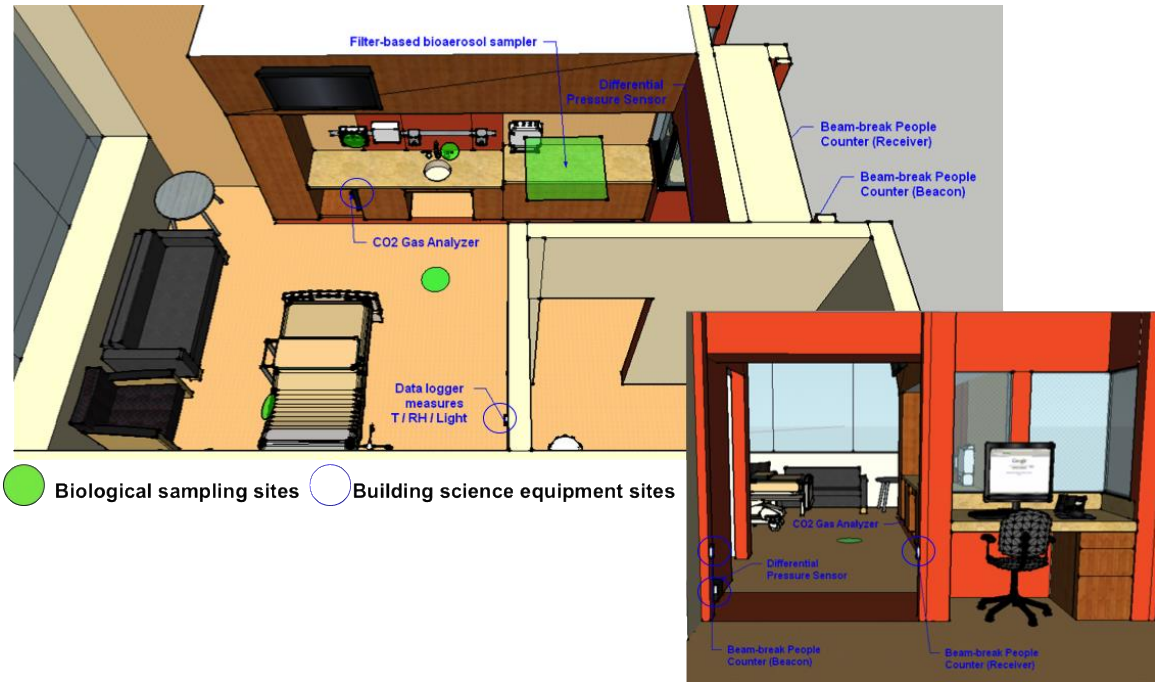

Figure 3. Typical patient room showing locations of building science sensors and microbial sampling

All of the building science equipment is listed in Table 1. Individual parameter measurements are described in more detail in the following subsections.

Table 1. Building science instruments

Parameter	Instrument	Sampling Location	Make/Model
T/RH/Light	Data logger	Patient rooms, Nurse stations	Onset HOBO U-12-012
Room Pressurization	Differential Pressure Sensor	Patient Rooms	Veris Industries PX Series Digital Pressure Transducer
Room Occupancy	IR Beam-break People Counters	Patient Rooms	Sensource PC-TB12-R People Counter Non-Directional Wireless Sensor
	CO_2 sensors	Patient Rooms	PP Systems SBA-5 CO_2 Analyzer
OA Fraction	CO_2 sensors	AHUs	PP Systems SBA-5 CO_2 Analyzer

3.2 Data collection procedures

Many environmental sensors do not have built-in data logging capabilities, so additional hardware was required to record and store data. Onset HOBO data loggers were selected for their compatibility with indoor environments, large memory for long-term sampling, ability to simultaneously launch and log, and aesthetic appearance. Wireless versions were considered, but proved probability expensive. Therefore, we utilized small, battery powered HOBO data loggers that required a USB interface cable to periodically offload data using HOBOware software. In addition to temperature, relative humidity and light intensity measurements, the data loggers are also equipped with external port(s) to store data from other external sensor(s) that output voltage or current correlating to their measurement. In total, three types of HOBO data loggers were selected based on different needs for logging requirements throughout this project.

Table 2. Types of data loggers used

HOBO data logger	Supported measurements	Range	Accuracy
U12-012	Temperature, Relative Humidity, Light Intensity, 1 external	-20° to 70°C (-4° to 158°F) - RH: 5% to 95% Light intensity: 1 to 3000 foot candles (lumens/ft^2) External input: 0 to 2.5 VDC	Temp: ± 0.4°C @ 25°C (± 0.7°F @ 77°F) - RH: ± 2.5% from 10% to 90% - External Input: ± 2 mV ± 2.5% of absolute reading
U12-013	Temperature, Relative Humidity, 2 external	Temp: -20° to 70°C (-4° to 158°F) - RH: 5% to 95% - External input channels: 0 to 2.5 VDC	Temp: ± 0.35°C from 0° to 50°C (± 0.63°F from 32° to 122°F); RH: ± 2.5% from 10% to 90%; External Input: ± 2 mV ± 2.5% of absolute reading
U12-006	4 external	0 to 2.5 VDC	± 2 mV or ± 2.5% of absolute reading

Figure 4. 3 types of Onset HOBO data loggers

3.2.1 Indoor environmental conditions. Onset HOBO U12-012 data loggers were used to record temperature, relative humidity and light intensity in each of the ten patient rooms. Areas that could capture the amount of light exposure within the main sampling space, including both natural and artificial light, were considered as potential locations for installation. Because much of the microbial sampling would occur at or around the

patient beds, data loggers were installed on the wall adjacent to patient's bed and across from the large windows. They were installed directly next other room controls to blend in and satisfy aesthetic requirements. Additionally, they were installed far enough away from patient beds to allow access with minimal invasiveness and were attached by 3M Command strips for easy removal and re-attachment during data collection.

Figure 5. HOBO data loggers located on a wall in patient room measure temperature, relative humidity and light intensity.

Figure 6. HOBO data logger located on a wall in patient room blended in with other room controls.

3.2.2 Room Pressurization. Differential pressure sensors were installed just inside each patient room immediately behind one of the doors with sampling lines on each side of the doorway (one was run underneath the gap between the door and floor to obtain measurements of room pressurization with respect to the hallway). This measurement was designed to serve primarily as an indicator of whether the rooms were being operated at neutral pressure, positive pressure isolation (i.e., with airflow moving from patient rooms toward the hallway, protecting patients from airborne hallway interactions), or negative pressure isolation (i.e., with airflow moving from the hallway toward patient rooms, protecting the hallway and other environments outside of the patient room from a particular patient). The pressure sensors required 12 VDC power supply and drew approximately 35 mA when operating. Therefore, the pressure sensors were connected to battery packs with 8 D batteries and housed together in a nondescript black plastic project enclosure box. This box was mounted on the wall with 3M Command strips. Clear vinyl tubing was used to measure the pressure differential and data were logged to an Onset HOBO data logger at 5-minute intervals, synchronized with other HOBO loggers throughout the hospital. Field measurements using an Energy Conservatory DG-700 differential pressure sensor confirmed very low, typically neutral pressures with respect to the hallway, so the pressure transducers were set to bi-directional operation with a maximum range of 0.1 in. W.C. (25 Pa). These sensors have an accuracy of ±1% of full scale, or 0.25 Pa.

Figure 7. Differential pressure sensor; inside enclosure, attached to external data logger and two tubes for differential pressure measurement between inside and outside of room.

Figure 8. Differential pressure sensor located behind door, enclosed in box, external data logger, two tubes: short tube inside room, long tube extending outside room.

3.2.3 Human Occupancy Measurements. Patient room occupancy was measured using two methods. The primary method was the installation of single infrared (IR) beam-break people counters mounted at each doorway to detect the combined number of entrances and exits through the patient room doorways, again at 5-minute intervals (although we were not able to synchronize with the Onset HOBO data loggers). These battery powered sensors and loggers were installed on the door frames using 3M Command strips. While logging at 5-minute intervals, their data storage reached capacity after approximately 10 days, thereby providing the limiting factor to how often data had

to be acquired by an individual from our team. These measurements were most helpful for inferring the level of activity in each room (i.e., the combined number of entrances and exits), but not necessarily the time-varying occupancy on its own. Dual-direction beam break counters and other methods exist, but were out of range of the budget for this project. However, when summing over an entire 24-hour day, if one assumes there is roughly the same number of entrances and exits through the doorway, one can find a reasonable estimate of the total number of people (not individual people) that had been in the room during that day.

Figure 9. Beam-break people counter components and configuration

Figure 10. Location of beam-break people counters at patient room doorways

To support these beam break measurements, CO_2 was also measured in each patient room using PP Systems SBA-5 CO_2 analyzers. These analyzers were installed in another nondescript black plastic project box on a small shelf within the rooms with clear vinyl tubing running out to the soda lime absorber columns (for zeroing) and to the sample area (at approximately counter height near the edge of the sink). This location was chosen primarily because of easy access to power; the units require 12 VDC power supplies and could not operate for very long on batteries. Data from the CO_2 analyzers were output to another Onset HOBO data logger attached to the side of the project box to allow for easy retrieval. A mass balance on carbon dioxide provided a method for checking beam break room occupancy counts and also supported ventilation information by allowing for estimation of AERs using periods of concentration decay following periods of concentration build-up.

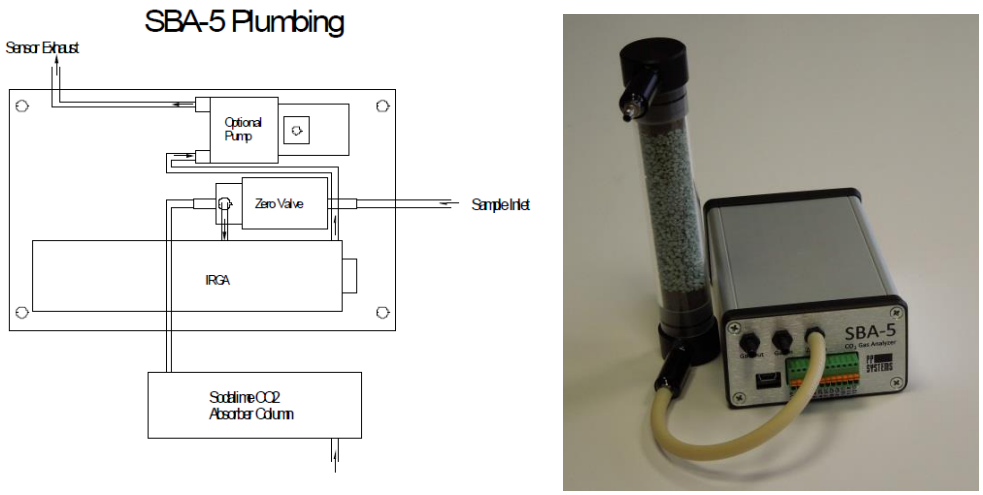

Figure 11. SBA-5 CO_2 sensor with absorber column filled with self-indicating soda lime.

Figure 12. SBA-5 CO_2 sensor set-up and location in patient room.

3.2.4 HVAC system characterizations and ventilation rate measurements. It is also essential to know the amount of outdoor air being provided to each room and how it may vary hourly, daily, monthly, or seasonally. To assess outdoor air ventilation rates, CO_2 concentrations were measured jointly in the outdoor air, recirculated air, and supply air in the air handling units (AHUs) in the mechanical systems that serve the patient rooms. Measurements were made using the same type of analyzers as in the patient rooms (PP System SBA-5) connected to Onset HOBO U12 data loggers in each of the outdoor, recirculated, and supply air streams at each of the two AHUs serving the patient rooms. These measurements were also synchronized with the patient room and nurse station measurements and logged at 5-minute intervals.

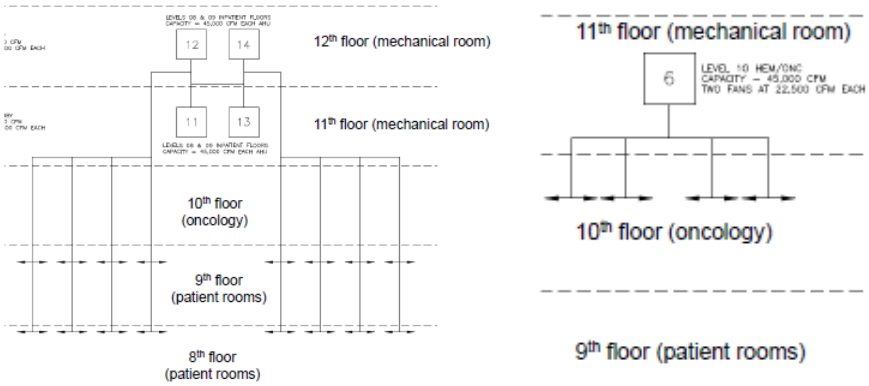

Figure 13. Diagram showing how AHU's are connected to patient care floors 9 and 10.

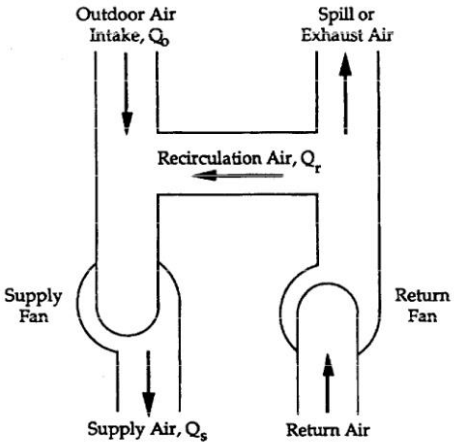

Figure 14. Air-handling system schematic (A. Persily, 1997).

Figure 15. CO2 sensors installed at AHUs

Finally, only spot measurements of the airflow rates in individual patient rooms were made prior to the hospital opening because of the level of invasiveness of these measurements. Both return airflow rates and exhaust airflow rates were measured using a pressure-matching technique combined with a calibrated fan (Energy Conservatory Duct Blaster). These measurements were generally in line with the design flow rates on the hospital plans and schedule sheets. Similar measurements were also performed at the two slot supply diffusers, although we have less confidence in their results.

3.2.5 Passive Air Sampling with HVAC Filter Media. In addition to the long-term building science data collection mentioned in sections 3.2.1 through 3.2.4, we also used a single sheet of filter media as a passive sampler to collect airborne particle-bound microbes in each patient room. A thin-sheet of medium efficiency filter media was selected, cut into 2 x 2 ft. pieces, and placed on the exterior of each patient room return grille on the ceiling and attached with custom-built magnets that resembled the white drop ceiling frame. The filter media was removed and replaced on a weekly basis and

preserved for microbial extraction. A photo of a roll of media is shown in Figure 16; this media came courtesy of Kevin Kinzer at 3M.

Figure 16. Roll of filter media used for filter-based air sampling

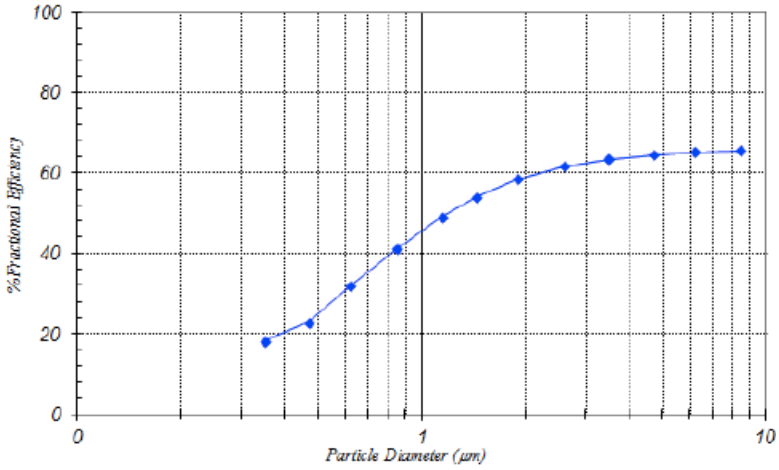

Figure 17. Efficiency curve for filter media used in filter-based sampling.

Figure 18. Placement of magnetic filter frame for filter-based air sampling.

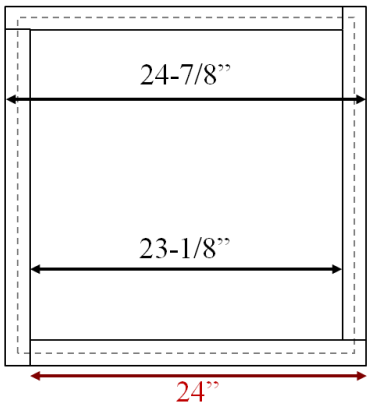

Figure 19. Magnetic frame design for filter-based air sampler

3.3 Instrument Calibration and Initial Measurements

Prior to installation, all CO_2 sensors and differential pressure sensors were calibrated against one another using separate co-location experiments in the laboratory. Calibration factors were estimated using linear regression analyses and applied to data

retrieved from the sensors. The calibrated CO_2 sensors were also used during a short field campaign in February 2013 (prior to the hospital opening) to assess mixing characteristics in one of the patient rooms. An additional co-location calibration procedure was later conducted with all of the temperature and relative humidity loggers used in the patient rooms and nurse stations. The next subsections describe each of the calibration procedures and results, as well as the results of initial hospital measurements during unoccupied periods.

3.3.1 CO_2 Sensor Calibrations. Before installation in the hospital, all 17 SBA-5 CO_2 sensors were calibrated using co-located measurements in the laboratory. Data from each sensor was analyzed and calibration factors were determined for each sensor using linear regressions. An additional co-location experiment was also later conducted during the field sampling campaign, albeit only for the six SBA-5 CO_2 sensors installed in the mechanical rooms (where accurate CO_2 measurements were most useful for calculating OA fractions). This was performed by connecting all sampling lines from the six instruments in a single small cardboard box with a mixing fan operating. CO_2 was injected and allowed to decay; new calibration factors were estimated for use with these sensors from that point forward (around week 8). A final calibration was performed again in the lab at the end of the project, after sensors were disconnected and removed from hospital locations. Table 4 shows results from the regression analysis for the three calibrations performed throughout the project.

Figure 20. Co-location calibration of 17 SBA-5 CO2 sensors

Table 3. Calibration factors for 17 SBA-5 CO_2 sensors

SBA-5 Serial ID	Location	Calibration Factor, initial	Calibration factor, starting at visit 8	Calibration factor, final
32	AHU6 OA	1.004x-0.39	0.962x + 2.29	0.983x+20.18
29	AHU6 RA	1.014x+8.37	1.020x – 4.78	0.923x-11.48
27	AHU6 SA	1.079x-16.23	0.999x – 10.32	0.969x-6.83
46	AHU11 OA	1.048x+36.06	1.002x+36.44	1.004x+7.20
30	AHU11 RA	1.021x+7.87	0.994x+5.11	*
26	AHU11 SA	1x+0	1x+0	1x+0
50	101	1.034x+18.56		1.036x+14.78
47	102	1.036x+10.79		1.003x+8.05
65	103	1.010x+2.07		0.937x-52.91
51	104	1.006x+16.05		0.956x-2.77
28	105	1.007x+9.21		0.930x-42.01
44	201	1.006x+10.99		0.967x-8.16
33	202	1.020x+32.72		1.090x+30.15
45	203	1.030x+10.31		*
49	204	1.036x+19.58		1.041x+1.25
31	205	1.001x+12.98		0.966x-3.74 **
64	spare	n/a		0.963x-12.93 **

* Not available for calibration
** Changed location since initial installation

Calibration factors appeared to have drifted considerably for most of the sensors over the course of the project. The final data set was analyzed using a combination of one or more of these calibration factors for each sensor, depending on how well it correlated with related data, particularly by comparing supply air CO_2 measurements with room air CO_2 measurements made during known unoccupied periods.

3.2.2 Pressure Sensor Calibrations. The 10 differential pressure sensors used in this work were also calibrated by co-location methods in the lab alongside a DG-700 differential pressure gauge. This was performed using a simple pressurized cardboard box connected to both the DG-700 and the pressure sensors to be launched in the field. Calibration factors were again estimated using linear regression and applied to raw data after collection.

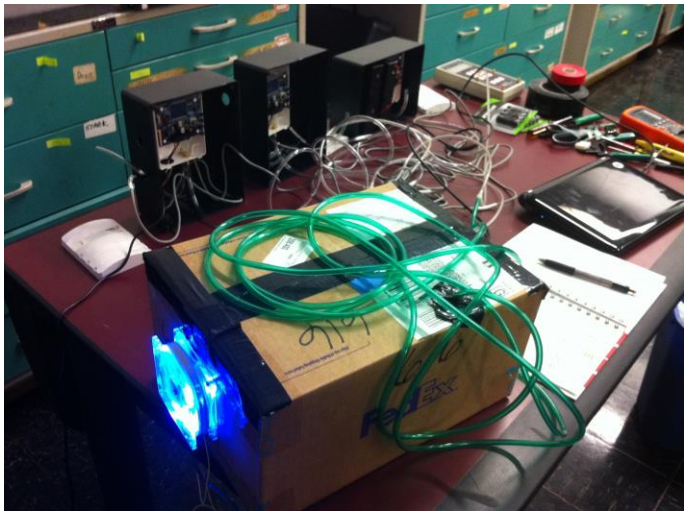

Figure 21. Co-location calibration of pressure sensors

Table 4. Calibration factors for 10 differential pressure sensors

Room	Calibration factor
101	(x+0.2812) / 0.9987
102	(x+0.4673) / 1.0017
103	(x-0.4578) / 1.0092
104	(x+0.4673) / 1.0017
105	(x+0.3145) / 1.0109
201	(x-0.0058) / 0.9896
202	(x-0.5254) / 0.9937
203	(x+0.2500) / 0.9999
204	(x+2.9207) / 0.9933
205	(x-1.4710) / 1.0044

3.2.3 Temperature and RH Calibrations. A co-location calibration of the temperature and RH sensors used in the patient rooms and nurse stations was also conducted at the end of the project. The calibration factors shown in

Table 5, revealing that most of the temperature and RH sensors were within the range of uncertainty stated for each of the sensors (±0.4°C for temperature, 2.5% for RH). Using these calibration factors over the range of patient room temperatures measured herein (i.e., 17°C to 31°C), the temperature sensors appear more accurate than suggested by the manufacturer-reported uncertainty. Calibrated temperatures were within 0.07°C of each other on average, with the highest deviation being approximately 0.2°C. Calibrated RH responded similarly, with mean deviations of 0.2-0.4% RH and a maximum deviation of 0.8% RH using calibrated data over the range of RH values measured throughout the project. Without applying calibration factors, the units were still well within the range of manufacturer-reported uncertainty in the co-location experiment: the mean temperature

deviation was only 0.06°C (ranging from 0.01°C to 0.14°C) and the mean RH deviation was only 0.19% RH (ranging from 0.04% to 0.32% RH). Given these strong correlations with raw sensor data, calibration factors were not used for T/RH data in this work.

Table 5. Calibration factors for temperature and RH sensors

	Temperature calibration			RH calibration		
Room	Slope	y-intercept	R^2	Slope	y-intercept (%)	R^2
100	1	0	1	1	0	1
101	1.00	0.086	0.999	0.991	0.224	0.999
102	1.00	-0.017	0.999	0.993	*0.428*	0.999
103	0.984	0.421	0.999	1.003	0.186	0.999
104	0.979	0.420	0.999	0.994	0.637	0.999
105	0.981	0.417	0.998	0.985	0.372	0.999
200	0.994	0.193	0.999	0.995	-0.041	0.999
201	0.998	0.120	0.999	0.990	0.317	0.999
202	0.993	0.128	0.999	0.996	0.102	0.999
203	0.994	0.167	0.999	0.994	0.175	0.999
204	0.995	0.149	0.999	0.993	0.334	0.999
205	1.003	-0.015	0.999	0.987	0.112	0.999

3.2.4 Initial Patient Room Measurements. In order to test the extent of mixing inside the patient rooms, five calibrated CO_2 sensors were installed in five separate locations within just one patient room (Room 102) and measured simultaneously for approximately 24 hours. Photos of this experiment are shown below. Measurement locations were chosen to cover a wide range of distances from each other within the relatively small patient room. These simultaneous calibrated data are shown in Figure 23 versus time and in Figure 24 with four sensors calibrated against one sensor in the center of the room.

Figure 22. Well-mixed test using 5 CO2 sensors

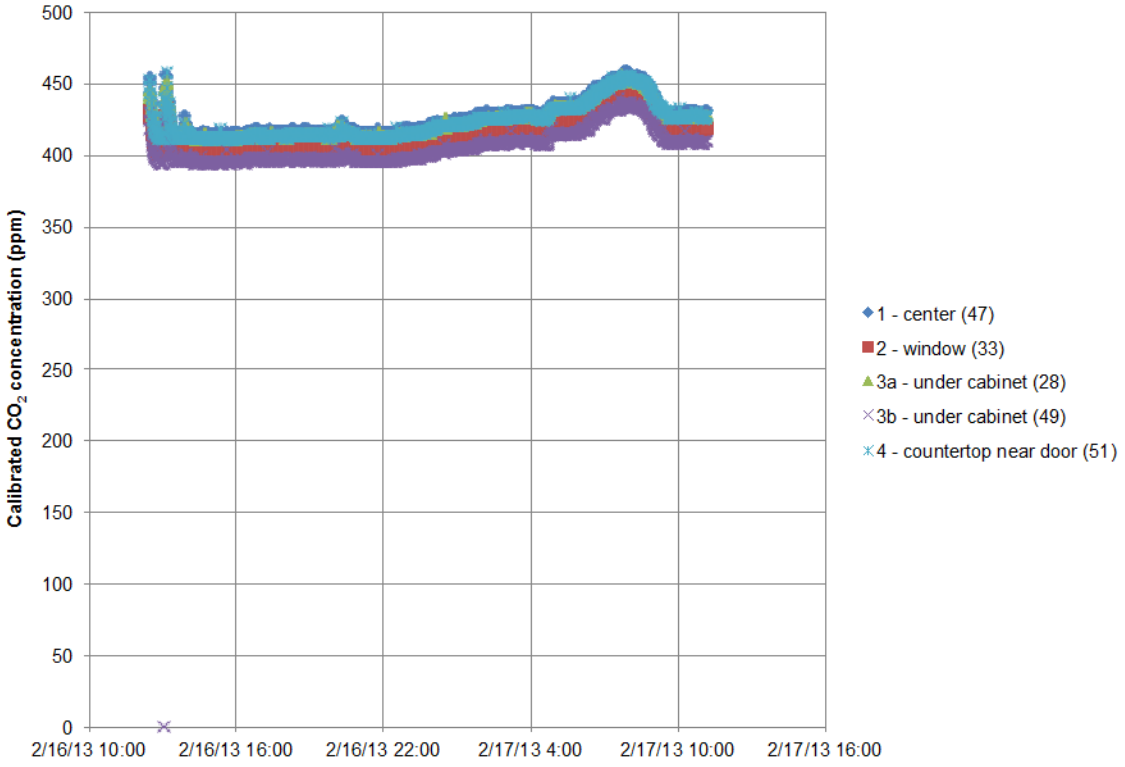

Figure 23. Time-series of 5 CO2 sensors used in well-mixed test

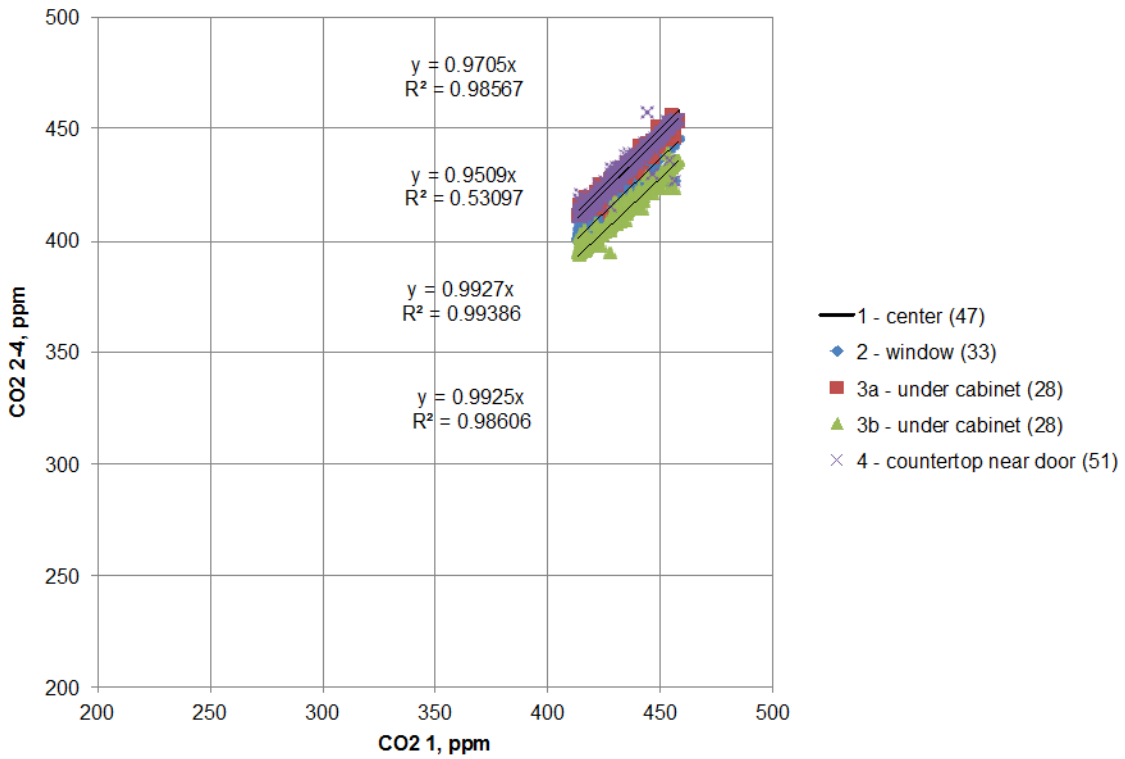

Figure 24. Regression analysis for 5 CO2 sensors used in well-mixed test.

Regression analysis shows that the room was reasonably well mixed throughout the duration of testing, even while unoccupied. CO_2 measurements from each of the five locations were all within 5% of each other, including measurements taken under the counter in an exposed cabinet where the CO_2 sensors were ultimately installed for long-term measurements.

During this same visit, baseline airflow rates were also measured in a number of the rooms. We used a pressure matching technique whereby a duct blaster was connected to a 2 ft × 2 ft × 2 ft cardboard box and held against supply diffusers, return grilles, and bathroom exhaust grilles in most of the patient rooms.

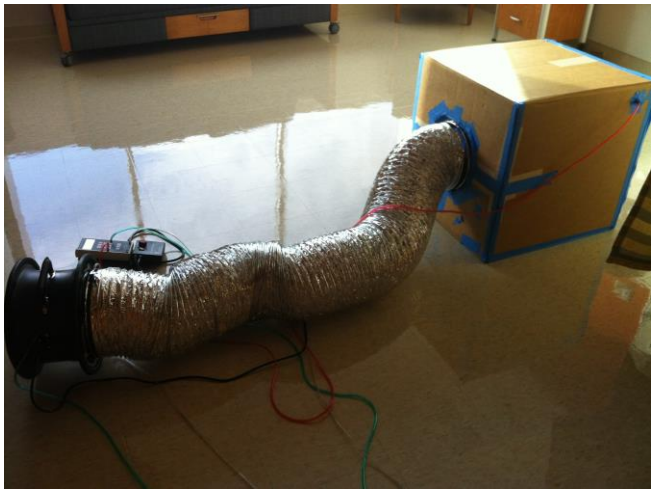

Figure 25. Duct Blaster pressure matching flow meter for measuring airflow rates through supply diffusers and return grilles.

Flow measurements obtained from supply diffusers were difficult to obtain with high accuracy, given the nature and shape of the supply diffusers. Therefore, we considered these values to be somewhat suspect compared to the return and exhaust grill measurements

3.3 Data Collection Procedures

This section describes the actual data collection procedures utilized in this work.

3.3.1 Data logger settings. In order to maximize quantification of building environmental and operational parameters within reasonable bounds of data storage capacity of the data loggers and our capacity to manually retrieve data, data loggers were set to record measurements every 5 minutes. HOBO data loggers are capable of synchronizing to computer time and logging on exact 5-minute intervals (e.g. 00:05, 00:10, 00:15, etc.), allowing all data loggers to log simultaneously. The beam-break

people counters, with built-in logging capabilities, are able to log at an interval frequency of 5 minutes but are unable to log on exact intervals (e.g. 00:02, 00:07, 00:12, etc.), unlike HOBO data loggers. Due to the limited memory capacity of the people counters, the maximum-frequency logging interval of 2 minutes would require data offloading after 4 days and 5-minute logging intervals would log 10 days of data before reaching capacity. In order to coincide with weekly microbial sampling, a 5-minute logging interval was selected to allow for weekly data collection with the maximum data acquisition. Data files acquired from each data logger were immediately transferred to a password protected online repository and named with the sensor type, room code and visit number according to an internal file naming convention.

3.3.2 Weekly data collection. Concurrent with microbial sampling, building science data was downloaded on a weekly basis. A data collection team entered patient rooms along with the microbial sampling team to briefly remove HOBO data loggers from the three sampling locations within the patient room (CO_2 sensor, differential pressure sensor, and independent T/RH/light data logger on wall). The data loggers were brought outside the room, connected via USB, and data downloaded onto a laptop computer. Once data was downloaded, the data logger memory was cleared, re-launched for the next week of sampling, and then put back and reconnected to their locations within the patient room. In addition to the patient rooms, two data loggers were located at the nurse stations, one on each floor. These were also removed briefly for data collection and re-launched.

Data from beam-break people counters are also collected at that time, but did not require entry into the patient room. As these sensors were more or less permanently attached to doorframes just outside patient rooms, data was downloaded without removing the sensor from its location. Once data was downloaded, the history was cleared, and sensors were re-launched for another week of data collection.

Data from the mechanical rooms were also collected at the same time period of the weekly visit. There were six data collection sites located in the mechanical rooms, three for each AHU corresponding to each floor. Data was collected from HOBO data loggers and re-launched in the same manner as described above. Several equipment checks were also conducted during each weekly visit. These checks included data logger battery levels, placement and integrity of all sensors, cables and tubing, and adhesives for mounted equipment, and the condition of self-indicating soda lime in the absorber columns connected to CO_2 sensors. Each weekly visit typically took between two and four hours, depending on the pace of the microbial sampling team and the accessibility of each room. If a patient room was not accessible during the weekly visit, only the beam break people counters were collected and reset and the other data loggers inside the room were allowed to continue monitoring until the following week.

3.4 Analysis procedures

Once data were acquired from the hospital during each visit, the data were sorted into folders labeled according to sensor type. Stata Version 13, a data analysis and statistical software package, was used to manage and analyze the data. Data measured within 15 minutes of data collection period for each sensor and logger combination were

dropped to account for the time it takes to disconnect and reconnect data loggers. Additionally, the data were inspected visually by plotting time-series of each parameter and obvious errors resulting from sensor or logger malfunctions were flagged and noted in a visit log. After each visit, newly retrieved data was simply merged with previous visit data to produce a file containing time-series data from the beginning of the project for each sensor.

Once all of the 5-minute data for the entire duration of the project (from as early as January 22, 2013 for some sensors but as late as February or March 2013 for other sensors, to a final collection date of January 15, 2014) were stored, merged, and cleaned for quality assurance and quality control (QA/QC), data were summarized over a wider range of time-scales. For example, most data were summarized on an hourly basis, and again summarized over daily and weekly bases since microbial samples were only taken on a daily and weekly basis. To provide meaningful data to the biological sampling team, we have provided a variety of summary statistics over each time scale, including means, medians, standard deviations, minimum and maximums, and percentiles in between.

Because we had no direct, accurate measure of time-varying human occupancy in the patient rooms, we primarily summarized the beam break data into daily total counts, describing the total number of entries and exits during the day. This may be considered more a metric of *activity* than actual occupancy, but still may be useful for interpreting microbial community results. We also used the beam break counters in addition to the patient room CO_2 measurements in order to explore correlations between the two as another indicator of occupancy. Finally, we also explored the use of CO_2 sensors alone in estimating time-varying room occupancy using mass balance models.

Last, in order to determine the fraction of outdoor air being supplied to patient rooms at each measured 5-minute interval, data from all three air streams (outside, supply and recirculation air) from each air handling unit are merged together. The percent of outside air is supply air is calculated using the following equation (A. K. Persily, 1997).

$$\%OA = 100 \times \frac{(C_r - C_s)}{(C_r - C_{out})} \tag{1}$$

Where

%OA = percent outdoor intake,

C_r = CO_2 concentration in the recirculation airstream of the air handler,

C_s = CO_2 concentration in the supply airstream of the air handler,

C_{out} = CO_2 concentration in outdoor air.

Uncertainty in each estimate of OA fraction was made using the following equation, which takes into account the uncertainty of the CO_2 sensors in each location.

$$\Delta\% = \%OA \sqrt{\frac{(\Delta C_r^2 + \Delta C_{out}^2)}{(C_r + C_{out})^2}} + \sqrt{\frac{(\Delta C_r^2 + \Delta C_s^2)}{(C_r + C_s)^2}} \tag{2}$$

Where

$\Delta\%$ = precision of the percent outdoor air intake,

ΔC_r = precision of the measured carbon dioxide concentration in the recirculation air

ΔC_s = precision of the measured carbon dioxide concentration in the supply air

ΔC_s = precision of the measured carbon dioxide concentration in the outdoor air

Additionally, temperature and humidity measurements from each AHU air stream are also merged together in a similar manner to validate these outside air fraction calculations. Finally, to validate and calibrate OA fraction data from the air handling units, the hospital facilities department occasionally provided information on AHU damper positions over brief 24-hour periods.

The next chapter describes results from each of these measurements performed in the hospital over the duration of the project.

CHAPTER 4

RESULTS

4.1 Initial Visit and Further Calibration

The following section describes results from measurements prior to the hospital opening as well as the calibration procedures for measuring OA fractions.

4.1.1 Initial Airflow Measurements

Table 6. Flow schedule and baseline measurements

Room	Measured (CFM)*			Schedule (CFM)			
	Supply	Return	Bathroom	Supply		Return	
				Max	Min	Max	Min
101	*372*	*412*	100	450	390	350	290
102	*340*	*400*	100	450	390	350	290
103	*345*	*400*	100	450	390	350	290
104	*345*	*380*	100	450	390	350	290
105	*374*	*375*	100	450	390	350	290
201	401	*380*	100	450	390	350	290
202	411	*380*	100	450	390	350	290
203	395	*390*	100	450	390	350	290
204	400	*370*	100	450	390	350	290
205	*380*	*405*	100	450	390	350	290

*Italicized values may be suspect because they are out of the range described in the schedule

Initial airflow measurements were made in mid-February 2013, several days before the hospital opened. Values in italics were found to be out of the range specified in the hospital's airflow schedule. On the ninth floor, both supply and return airflow

measurements were found be outside the range of the flow schedule. Return grille air flow measurements on the ninth floor were shown to be consistently higher than supply air flow measurements, suggesting additional flow coming in from outside the patient room, although we have limited confidence in our supply measurement data because of difficulties in measuring flow accurately using the pressure matching technique with the slot diffuser. We have more confidence in the return and exhaust measurements because the flow measurement device fit entirely over the grilles. The total return + exhaust airflow rates were near 500 CFM in each of the patient rooms. Considering the rooms to be operating at neutral pressure, supply airflow rates may have been closer to 500 CFM as well. For the patient room indoor air volume of 3420 ft^3 (96.8 m^3), the rate of supply airflow to room volume (effectively the recirculation rate of the room) was approximately 8.8 per hour. Additionally, the volume of indoor air passing through the HVAC filter media based passive air sampler installed on the return grill and replaced on a weekly basis was approximately 4.0×10^6 ft^3 (1.14×10^5 m^3).

On the tenth floor, with the exception of the last room, only the return flow measurements were found to be outside the range identified the schedule. In the last room, both supply and return flow was found to be outside the schedule. Most of supply airflow rate measurements were found to be higher than those at the return grille, but again values are suspect. Additionally, we have no way of knowing whether airflow rates were adjusted between the time we made our measurements and the time the hospital actually opened.

4.1.2 OA Fraction: Calibration and Results. Raw outdoor air (OA) fractions were often outside of the bounds of theoretical limits (0 to 1) because uncertainties associated with very low differences in concentrations between the three airstreams in each AHU. An example of this is shown in blue in Figure 26. The estimated OA fraction shows clear changes in damper position for this particular day, but the OA fraction impossibly exceeds 100%. However, we periodically retrieved short-term records of OA damper positions from the facilities manager at the hospital for our measured AHUs, which allowed for periodic calibration of our absolute values against their data. Unfortunately their system only stored the previous 24-hours of data, so long-term calibration was not feasible. However, as Figure 26 shows (orange line), we were able to provide an approximate calibration of our OA fractions to known damper positions show in Figure 27.

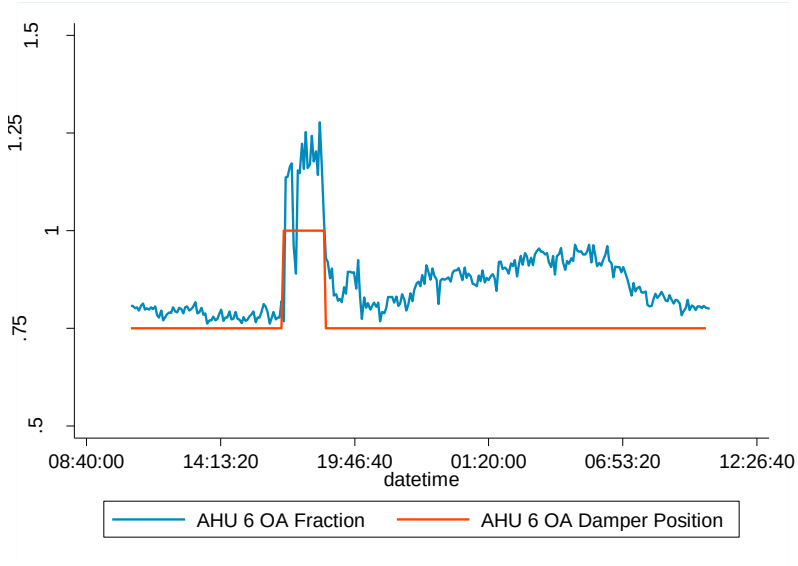

Figure 26. OA damper position from UCMC Facilities Department and measured OA fraction from AHU 6

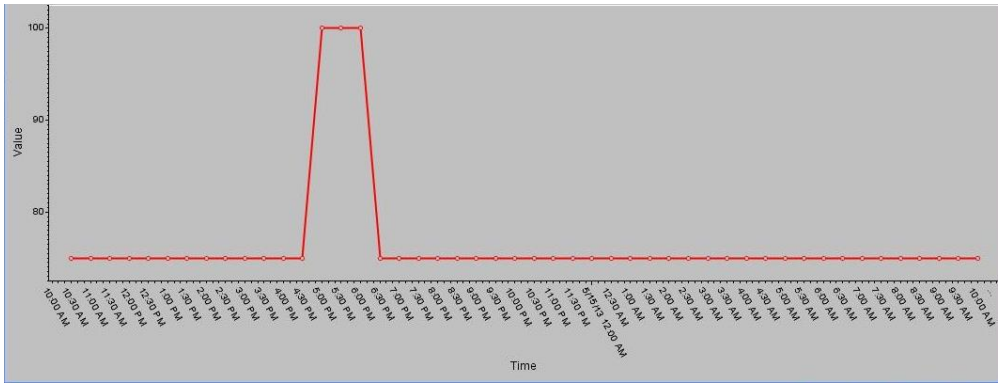

Figure 27. Damper position (% open) of outside air to supply air in AHU 6 for 24-hour period starting 5/14/2013 10:30am from hospital facilities department.

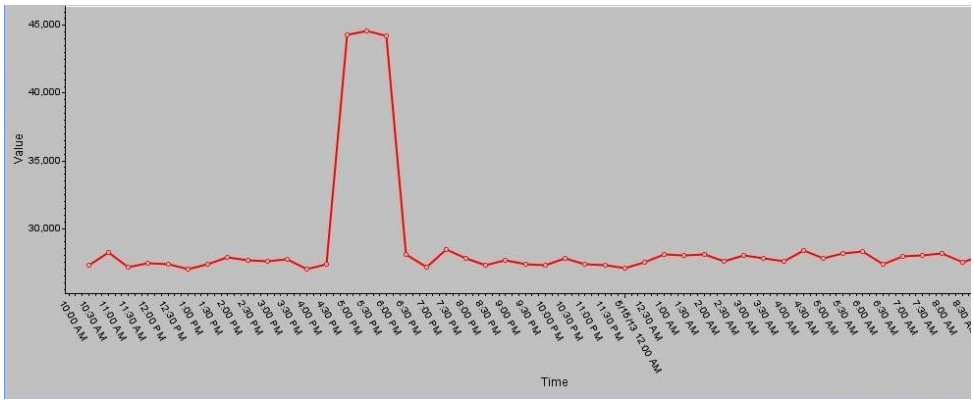

Figure 28. Flow at outside air intake of AHU 6 for 24-hour period starting 5/14/2013 10:30am from hospital facilities department (units are CFM).

Additionally, because we measured temperature in the outdoor air stream and the hospital HVAC system operated with an economizer, we have another method of estimating OA fractions based on outdoor temperature alone. Figure 29 shows outdoor air temperature measured by the hospital's building automation system during one 24-hour period retrieved from facilities. Figure 30 shows the same data using our measurements.

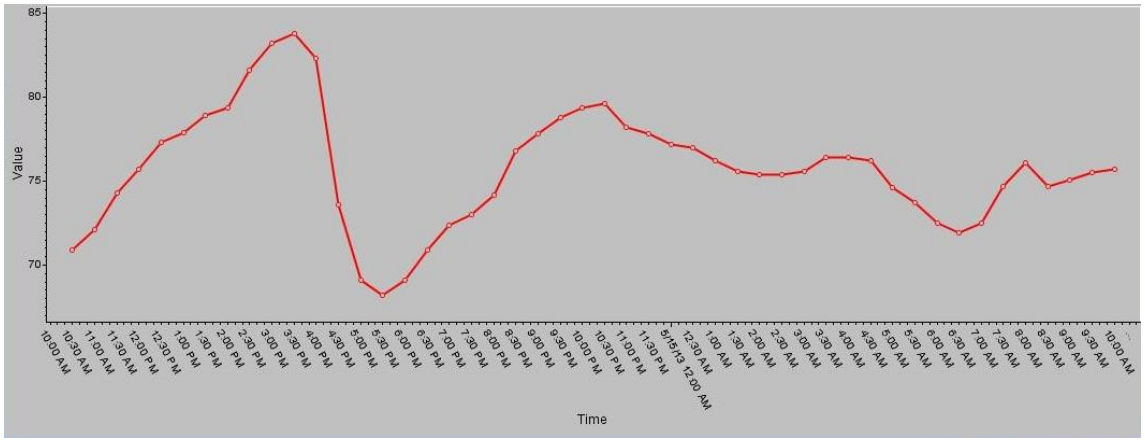

Figure 29. Temperature at outside air intake of AHU 6 for 24-hour period starting 5/14/2013 10:30am from hospital facilities department.

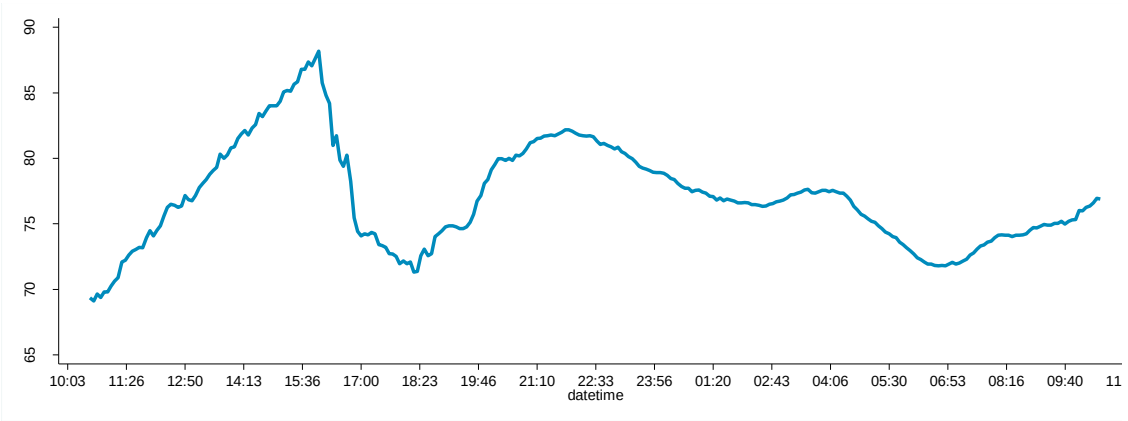

Figure 30. Temperature at outside air intake of AHU 6 for 24-hour period starting 5/14/2013 10:30am from project measurements

The two methods of outdoor temperature measurement correlate extremely well, showing that we could indeed trust our outdoor air temperatures. Although we were not able to retrieve the logic schedule for OA economizer operation, we plotted our estimates of OA fraction versus measured outdoor temperature and revealed intuitive results, as shown in Figure 31. One can see that both systems have a maximum OA fraction occurring when outdoor air temperatures are between approximately 7°C and 16°C,

consistent with typical economizer operation. We know through periodic facilities data that OA dampers were set at 100% during most of these periods.

Additionally, we also know that minimum OA damper settings were 75% in AHU 6, thus our minimum OA estimates made during the highest outdoor air temperatures likely correspond to 75% in that AHU. AHU 11-14 were more complicated. AHU 11 and 12 had minimum damper settings according to the facilities department of 50% each, while AHU 13 had a minimum of 75% and AHU 14 had a minimum of 70%. Because each of these AHUs had the same design airflow rate, we can reasonably assume that the minimum OA fraction for the combination of these four AHUs was the average of the four individual minimum OA fractions, or approximately 61.25%. Figure 31 shows correlations between OA fractions and outdoor air temperature, showing that OA fraction in AHU 11-14 appears to vary more widely when compared to AHU 6. This is consistent with the minimum damper position of 75% and 61.25% for AHU 6 and AHU 11-14, respectively. The figures show a strong correlation between OA fraction and temperature, with AHU 6 being clearer in this correlation. The extra noise in AHU 11-14 may also be an effect of the combination of the 4 AHUs.

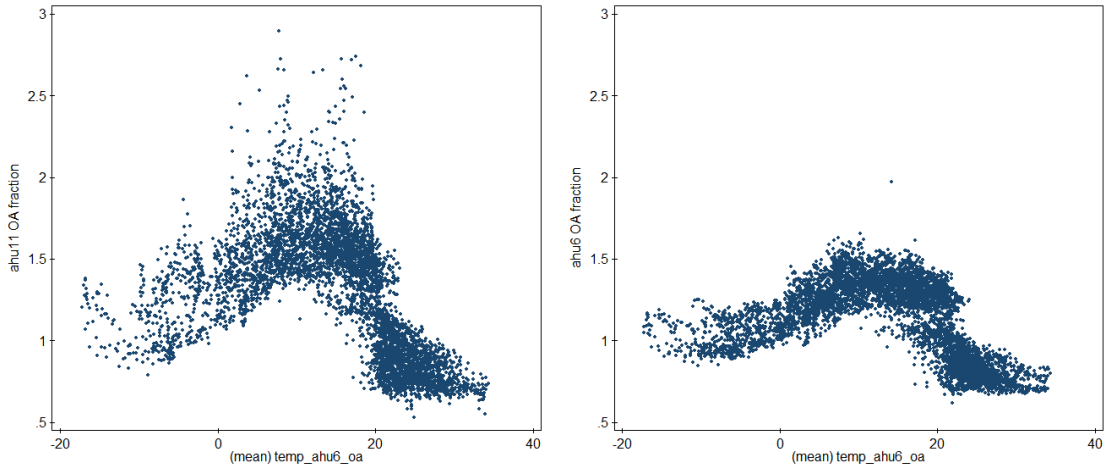

Figure 31. AHU 11-14 and AHU 6 correlated with outdoor air temperature

To gain a clearer look at the correlation between OA fraction and outdoor air temperature, OA fraction was averaged over a number of small temperature bins and plotted against the mean temperature in that temperature, revealing a tighter pattern.

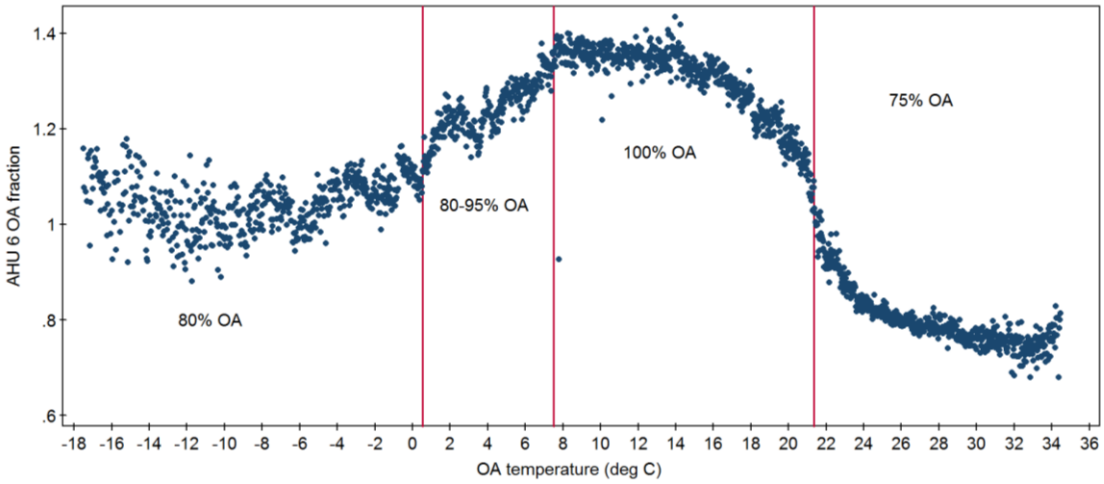

Figure 32. AHU6 OA fraction averaged over each temperature, correlated with temperature.

Using the known minimum damper positions of 75% and 61.25%, we can apply these to the lowest OA fractions which occur at higher temperatures, with a lower boundary of approximately 20°C. We can conclude that the highest OA fraction is 100%, occurring at moderate temperatures between 7°C and 20°C. Below 7° C, OA fraction appears to decrease linearly with temperature until about 0°C, where it plateaus.

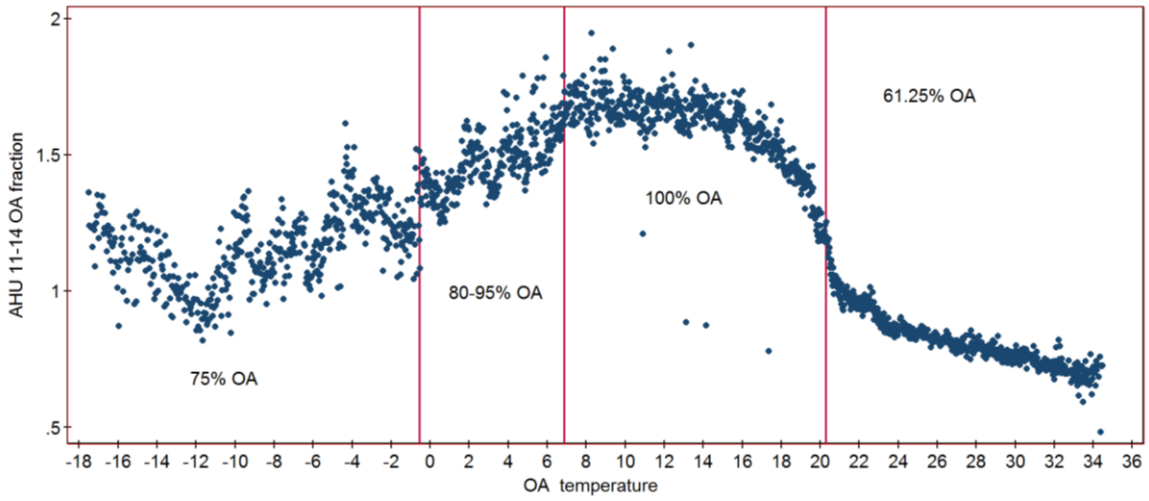

Figure 33. AHU 11-14 OA fraction averaged over each temperature, correlated with temperature

The same analysis was done using enthalpy instead of temperature, revealing a similar correlation, with minimum OA occurring at enthalpy values higher than 43. Like temperature, a wider range of OA fractions occurred with AHU 11-14, confirming a lower minimum OA fraction compared to AHU 6.

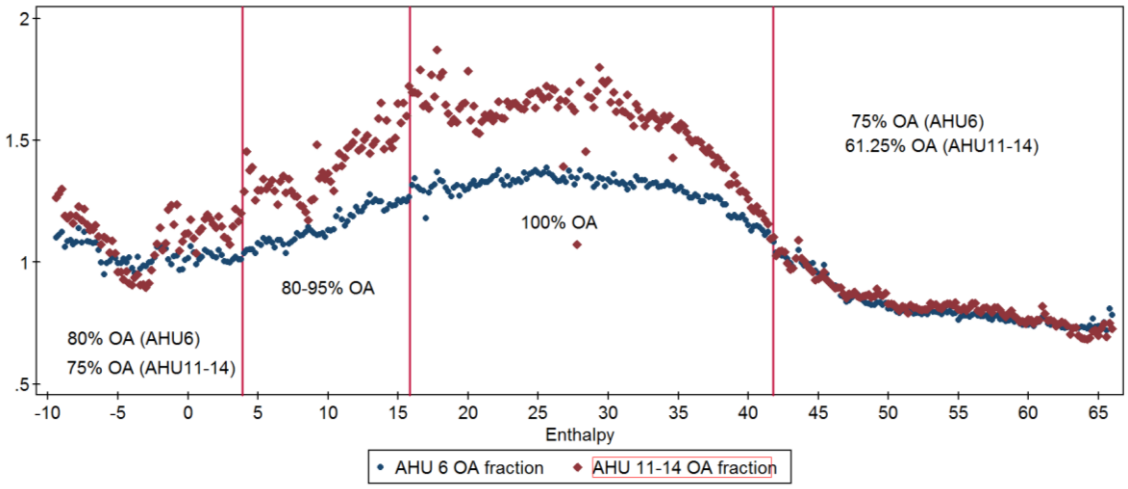

Figure 34. AHU 6 and AHU 11-14 OA fraction averaged over enthalpy

To further simplify our analysis and calibrate the raw data to reveal real OA fractions, raw OA fractions were averaged over 2°C wide temperature bins (Figure 35). The minimum and maximum raw OA fractions from these data, along with our known real OA fractions, were used to calculate a slope factor to obtain an estimation of real OA fractions over all temperatures.

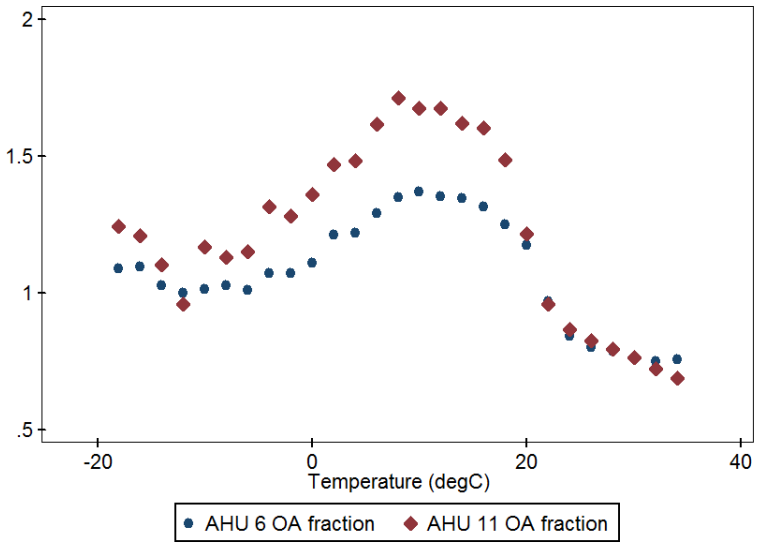

Figure 35. AHU 6 and AHU 11-14 OA fractions averaged over 2°C bins, correlated with temperature

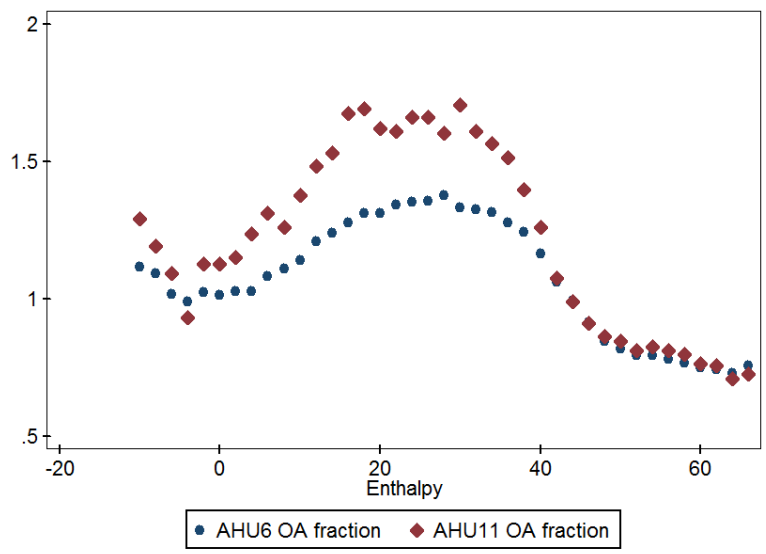

Figure 36. AHU 6 and AHU 11-14 OA fractions averaged over 2 units of enthalpy (kJ/kg), correlated with enthalpy

By setting highest OA fractions (7 data points) to 100% OA and lowest group of OA fractions (7 data points) to the stated minimums, 75% and 61.25%, for AHU 6 and AHU 11 respectively, slope factors shown in Figure 37 were determined and applied to all data points shown in Figure 35.

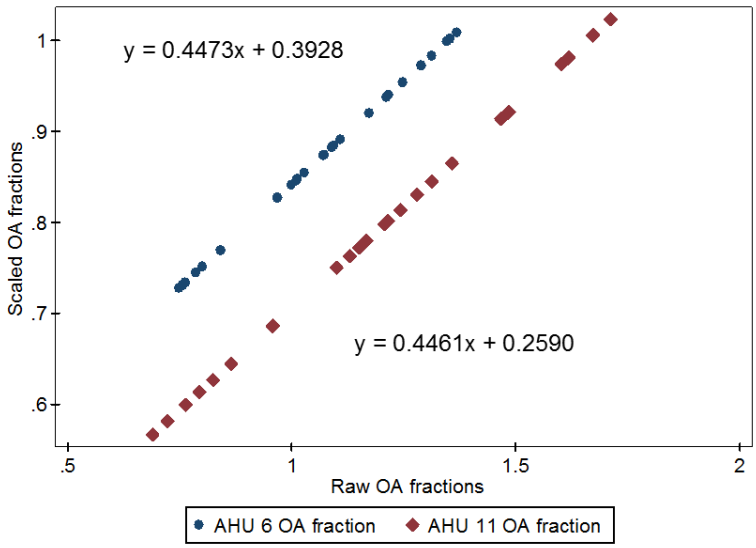

Figure 37. Regression analysis for AHU 6 and AHU 11 OA fractions.

The scaled data after applying the respective slope factors to the raw OA fractions are show below in Figure 38 and Figure 39.

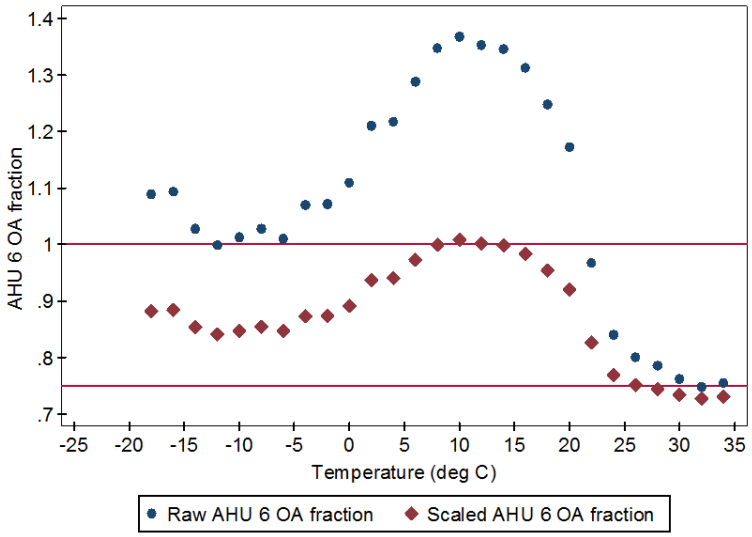

Figure 38. AHU 6 OA fractions before (raw) and after (scaled) applying slope factor.

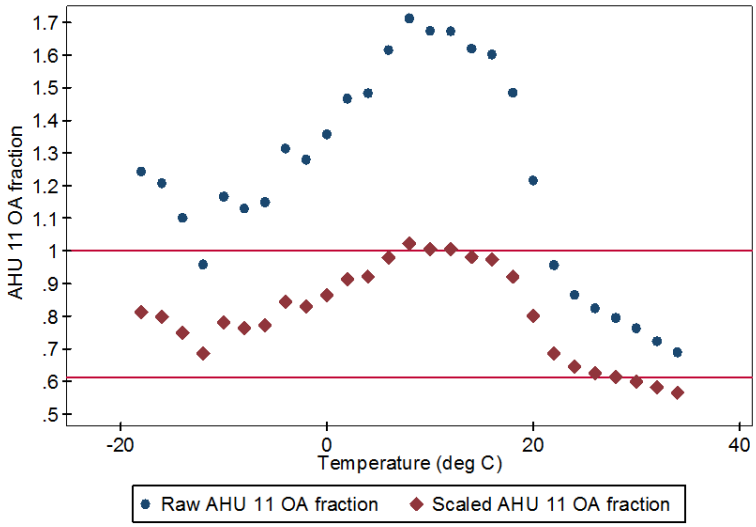

Figure 39. AHU 11 OA fractions before (raw) and after (scaled) applying slope factor.

Figure 40 shows scaled OA fractions for both AHU 6 and AHU 11 after applying slope factors. For both AHUs, OA fractions appear to drop below stated minimum OA fractions. Based on our analysis of data received from the hospital facilities department, OA fractions were at a minimum for all temperatures above ~21°C so slope factors were determined such that all of these data points were minimum OA fractions. Slope factors were also scaled considering OA fractions were between 80 and 90% for lowest temperatures, also based on data from hospital facilities department.

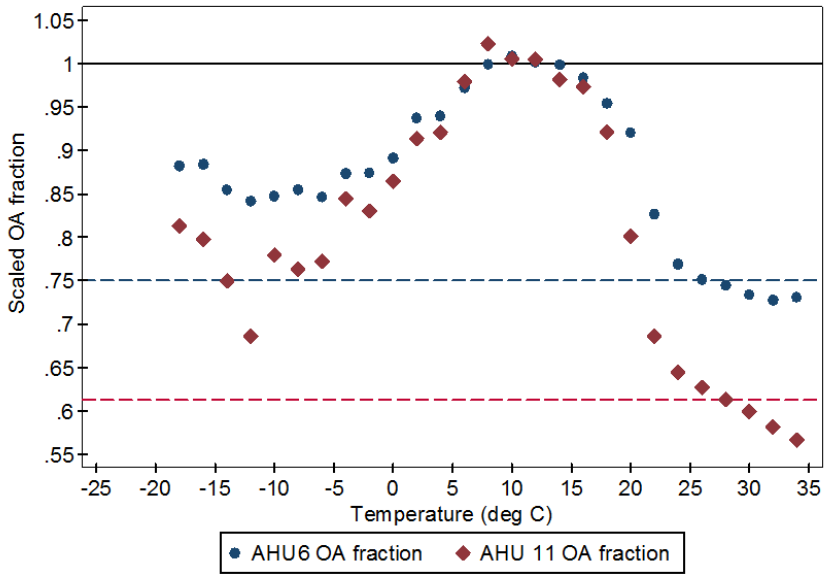

Figure 40. AHU 6 and AHU 11 OA fractions after applying slope factors.

Using 24-hour time-series data provided by the hospital facilities department, we were able to validate our method of measuring the fraction of outdoor air delivered to patient rooms. Using the minimum OA damper position limits for each AHU, also provided by the facilities department, we were able to calculate a slope factor to calibrate the raw data to reveal real OA fractions. These data reveal differences in the amount of outdoor air delivered to the two hospital floors used in the study. In general, rooms on the

tenth floor (AHU 6) received larger fractions of outdoor air during periods of both warm and cold weather than rooms on the ninth floor (AHU 11), although during moderate temperatures both units operated at 100% outdoor air fractions.

Combining these OA fractions with estimates of supply airflow rates at neutral pressure (where supply airflow rates equal the sum of return and exhaust flow rates in the patient rooms), room air exchange rates are estimated to vary from as low as ~5.2 per hour (at 60% OA) to as much as ~8.8 per hour (at 100% OA).

4.2 Example Time-series Data

This section describes example time-series data from each of the sensors and data loggers deployed in the hospital.

4.2.1 Time-series: Temperature in patient rooms and nurse stations. Within patient rooms, temperatures typically remained fairly steady over 24-hour periods, often oscillating over 0.2°C, as shown in Figure 41. However, throughout the entire measurement period, temperatures were found to vary by about 4°C, often within the same week (Figure 42).

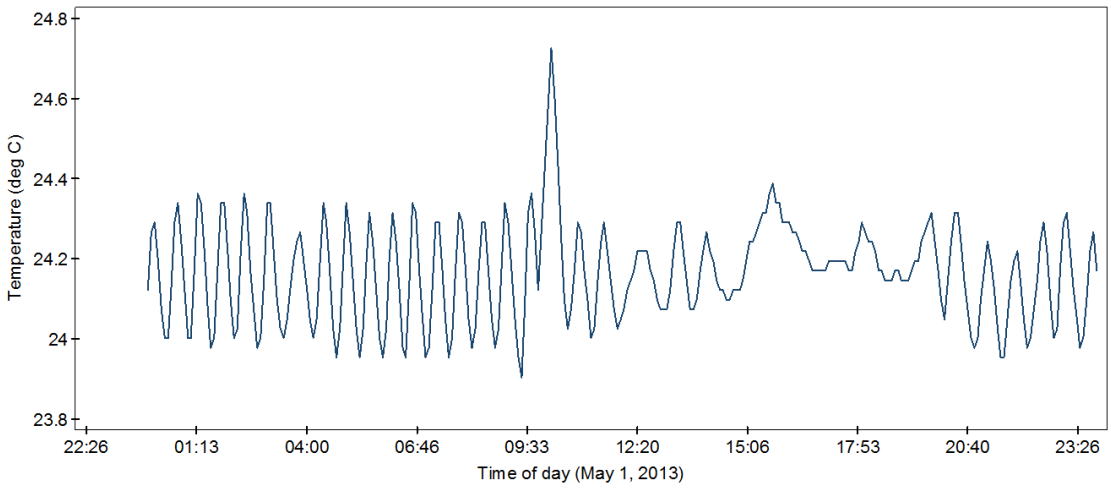

Figure 41. Temperature measured at 5-minute intervals in one patient room during the 24-hour period of May 1, 2013.

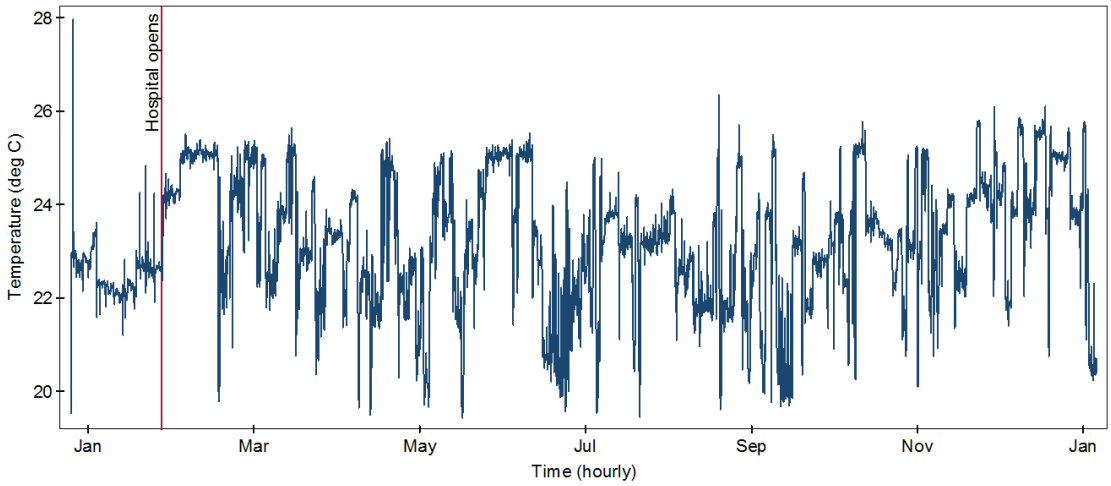

Figure 42. Hourly average temperature in one patient room over the duration of the measurement period (Jan 2013 to Jan 2014)

One thing to note is the wide variation in temperature in early January 2013, which was noticed during early data collection and attributed to in-hospital testing prior to the hospital's opening. Another thing to note is the increase in temperature that coincides with the opening of the hospital on February 23, 2013. Temperature increased

about 1°C and continued to vary widely over the course of the project, likely due to manual temperature controls within the individual patient rooms.

Figure 43 and Figure 44 show representative time-series data from one of the nurse stations. Compared to patient rooms, temperatures are less consistent throughout the day, showing patterns largely based on nighttime and daytime periods. However, temperatures are much more consistent throughout the duration of the project, following the same patterns at a daily frequency and a lower range of temperatures. A large increase in temperature can be noticed on the hospital's opening day.

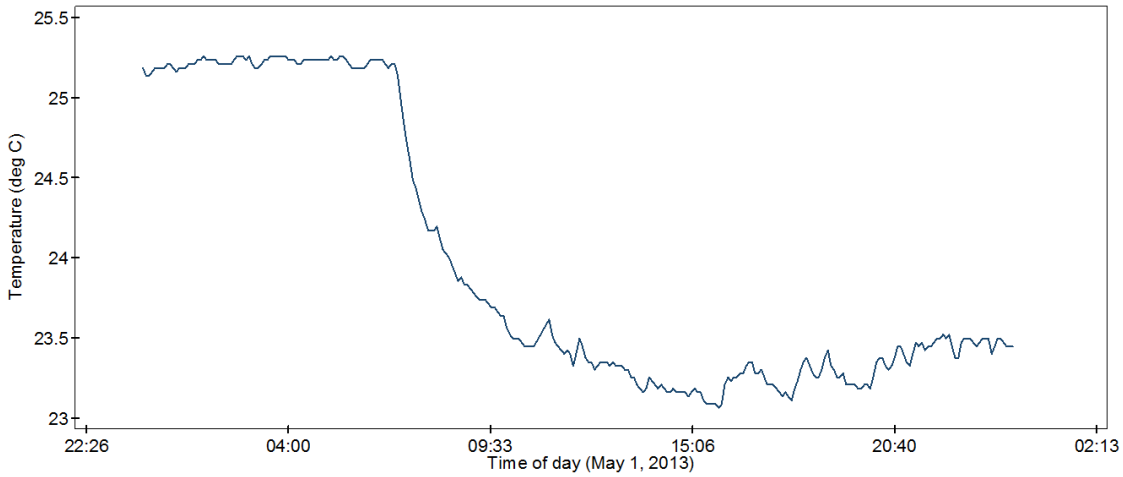

Figure 43. Temperature measured at 5-minute intervals at one nurse station on May 1, 2013.

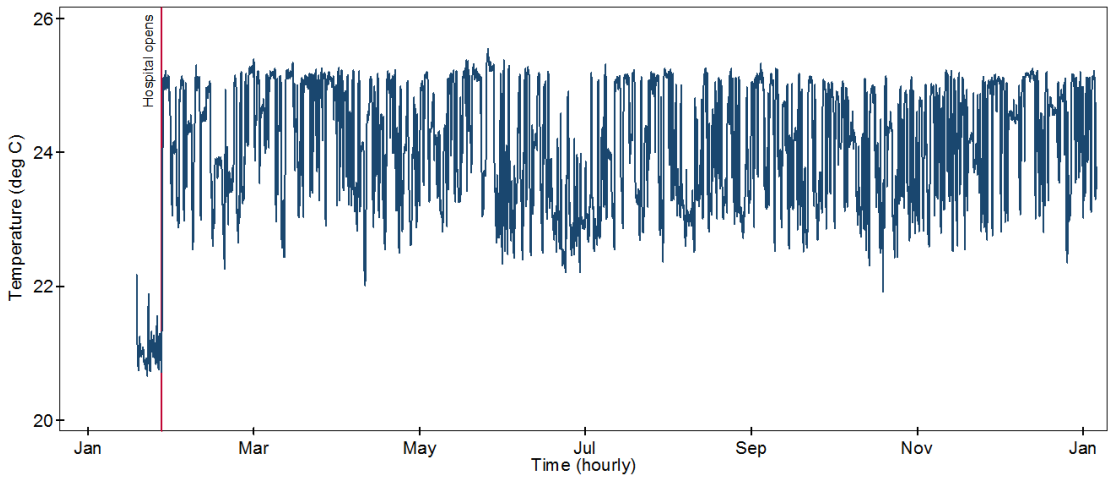

Figure 44. Hourly average temperature at one nurse station over the duration of the measurement period (Jan 2013 to Jan 2014)

4.2.2 Time-series: Relative humidity in patient rooms and nurse stations. RH varied little over 24-hour periods, often only by 3% or less (Figure 45). However, during the course of the year-long measuring period, average hourly RH varied over 30%, with typical high levels around 45-50% and low levels below 20% (Figure 46).

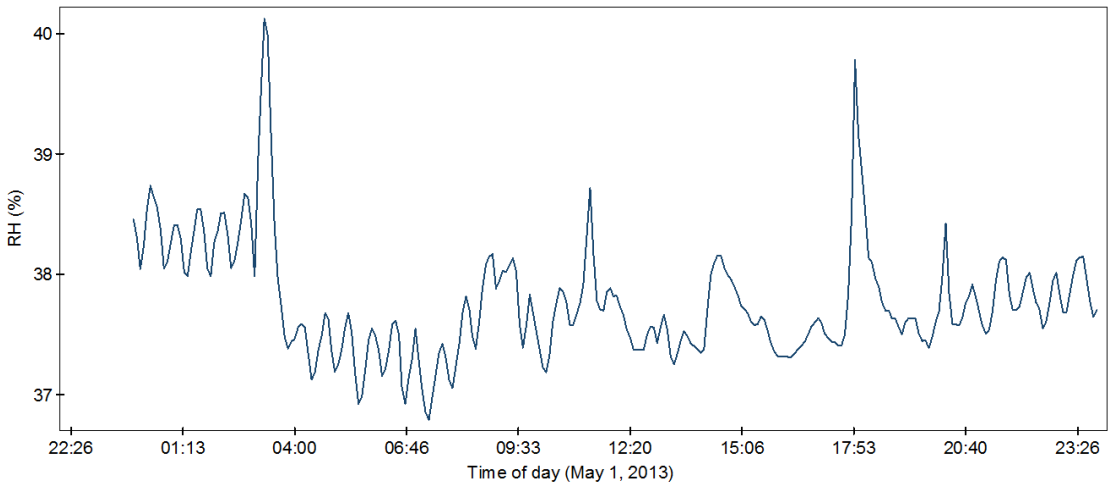

Figure 45. Relative humidity measured at 5-minute intervals in one patient room during the 24-hour period of May 1, 2013.

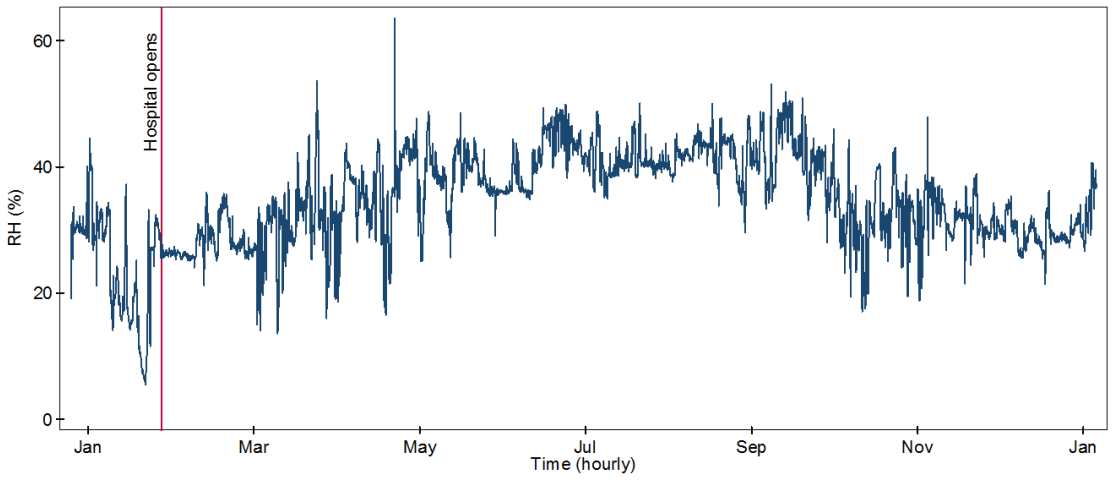

Figure 46. Hourly average RH (%) in one patient room over the duration of the measurement period (Jan 2013 to Jan 2014)

The weeks prior to the hospital opening showed RH values as low as 10%, showing that humidity controls were not in effect at that time. The data indicate the humidity controls were tightly regulated immediately after the hospital opened and became occupied.

Figure 58 and Figure 59 show representative time-series RH measured at a nurse station. Much like temperature, RH exhibited a night-day pattern, with values rising about 5% around 7:00am.

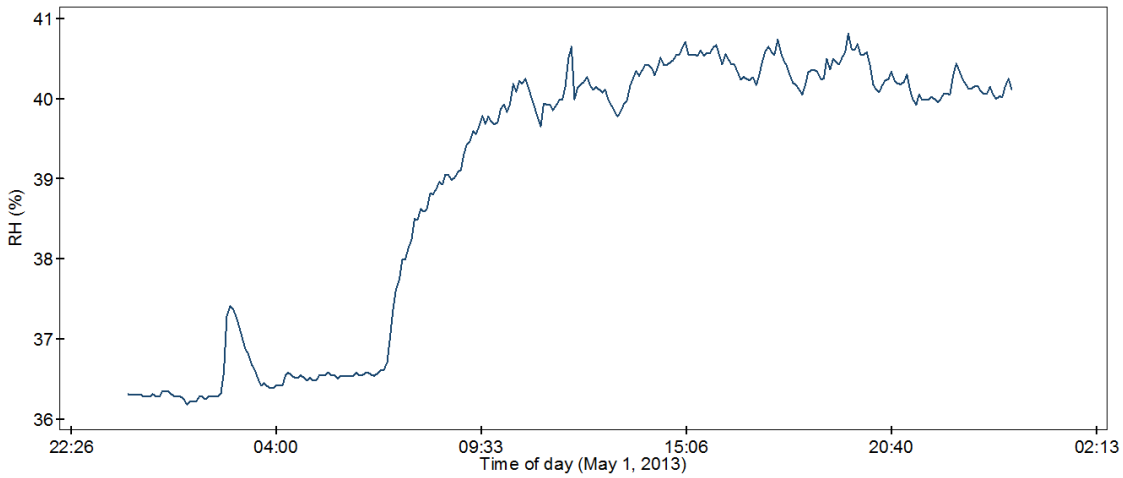

Figure 47. Relative humidity at one nurse station, measured at 5-minute intervals during the 24-hour period of May 1, 2013.

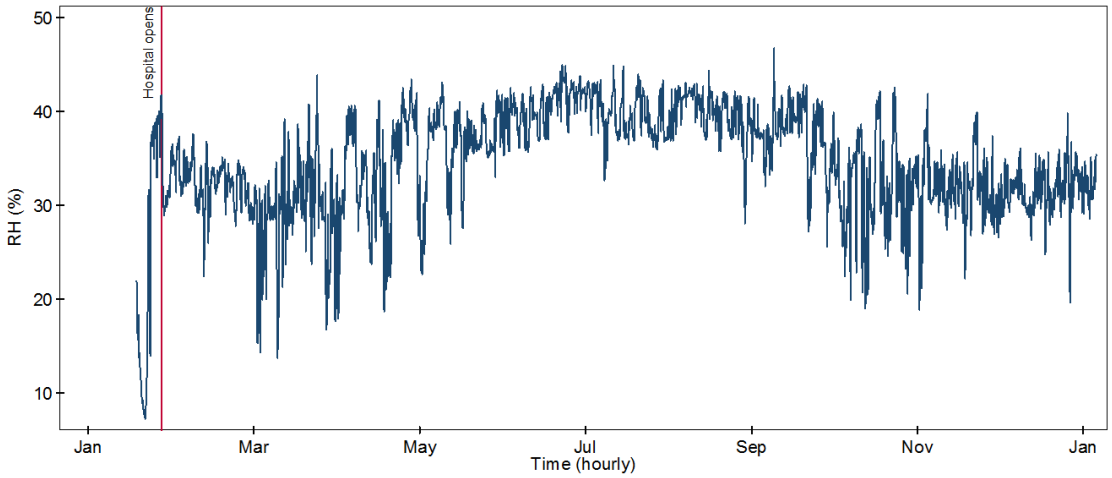

Figure 48. Hourly average RH (%) at one nurse station over the duration of the measurement period (Jan 2013 to Jan 2014).

Additionally, RH exhibited a seasonal pattern, with RH highest during the summer months, reaching above 40%, and lowest in winter months (with a mean around 30%). Both summer and winter months appear to be highly regulated, while months in between are not. This is likely due in part to changes in OA fractions; during summer

and winter months OA fractions are limited while OA fractions are closer to 100% during swing seasons and likely more subject to fluctuations in outdoor RH. Like temperature, a large increase in RH occurs just prior to the hospital's opening day.

4.2.3 Time-series: Absolute humidity in patient rooms and nurse stations. Using temperature and relative humidity data, absolute humidity ratios were also calculated. As with relative humidity, absolute humidity ratios were shown to vary little over 24-hour periods.

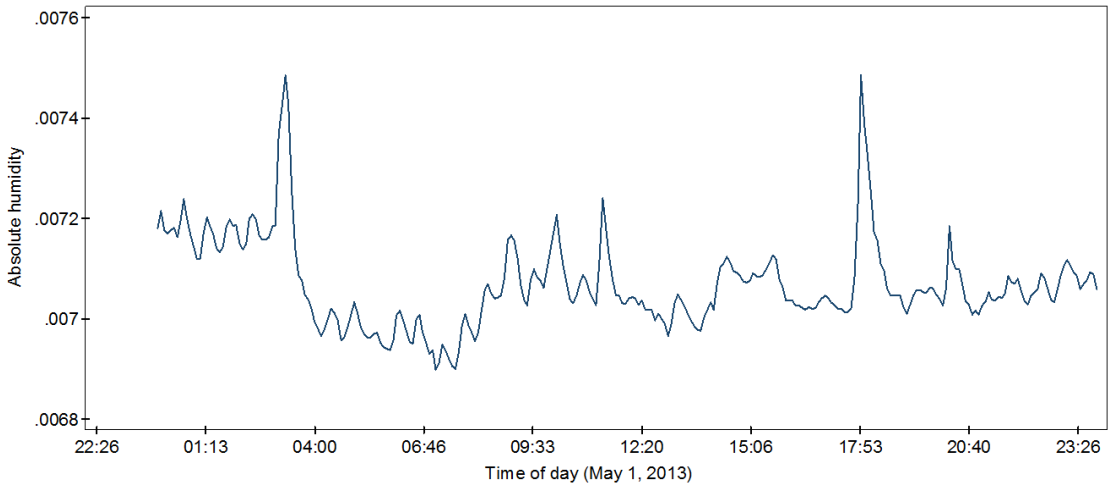

Figure 49. Absolute humidity measured at 5-minute intervals in one patient during the 24-hour period of May 1, 2013.

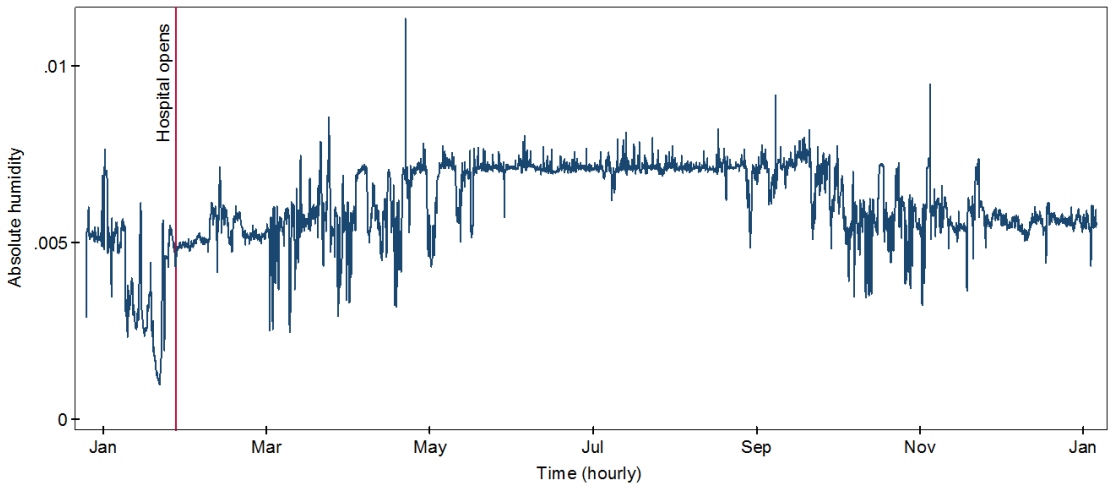

Figure 50. Hourly average absolute humidity in one patient room over the duration of the measurement period (Jan 2013 to Jan 2014)

The data clearly shows tight humidity control in the winter months following the opening of the hospital, as well as the summer months. It also clearly shows the dehumidification over the weeks prior to the hospital opening. Absolute humidity at nurse stations, shown in Figure 51 and Figure 52 follow a very similar pattern to that in patient rooms, showing that humidity is highly affected by the central HVAC system, without any large effects from occupancy.

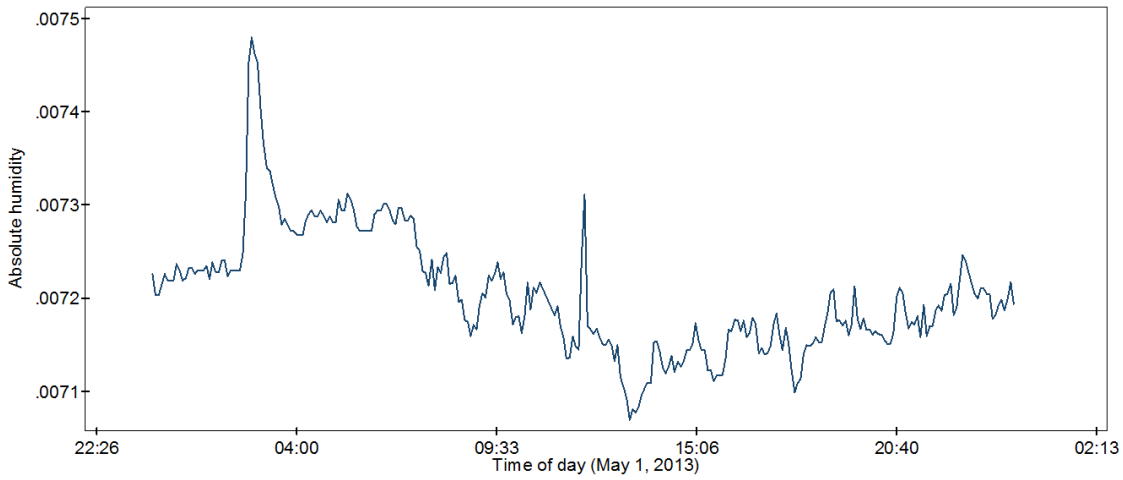

Figure 51. Absolute humidity at a nurse station measured at 5-minute intervals during the 24-hour period of May 1, 2013.

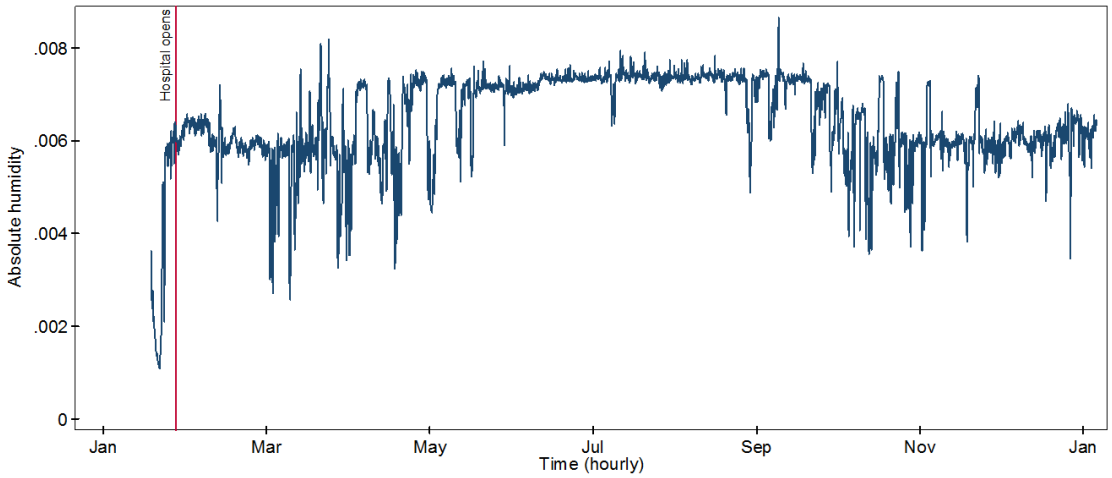

Figure 52. Hourly average absolute humidity at a nurse station over the duration of the measurement period (Jan 2013 to Jan 2014).

4.2.4 Time-series: Light intensity in patient rooms and nurse stations. Light intensity, including exposure from both natural and artificial light, exhibited a clear diurnal pattern as expected from the west-facing rooms. Light levels increased around the hours of sunrise and increase further in the afternoon as the sun appears from the west. The sharp increase intuitively occurs just before sunset when exposure to west-

facing surfaces is highest, then falls sharply as the sun sets. The step-change occurring at approximately 23:00 is likely a drop in artificial lighting within the patient room.

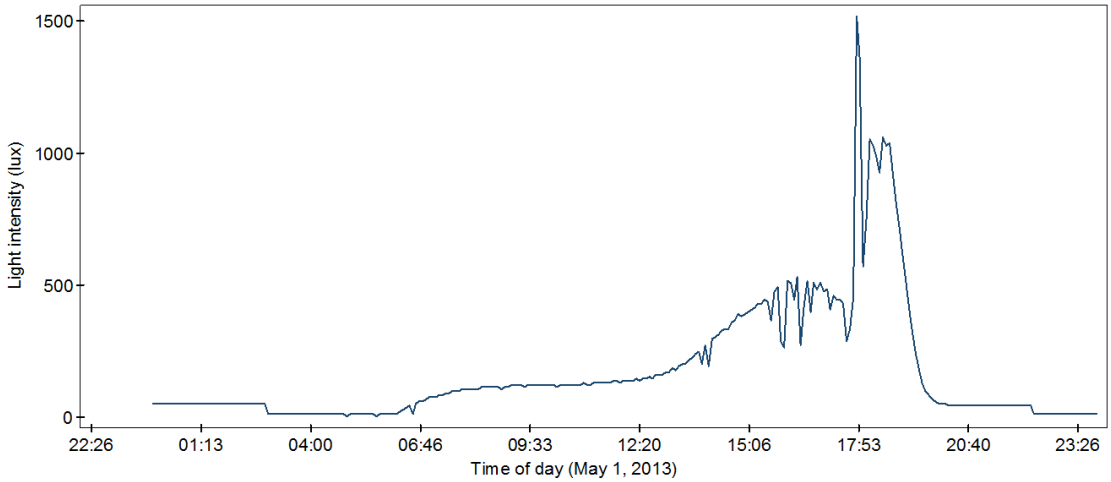

Figure 53. Light intensity (lux) measured at 5-minute intervals in one patient room during the 24-hour period of May 1, 2013.

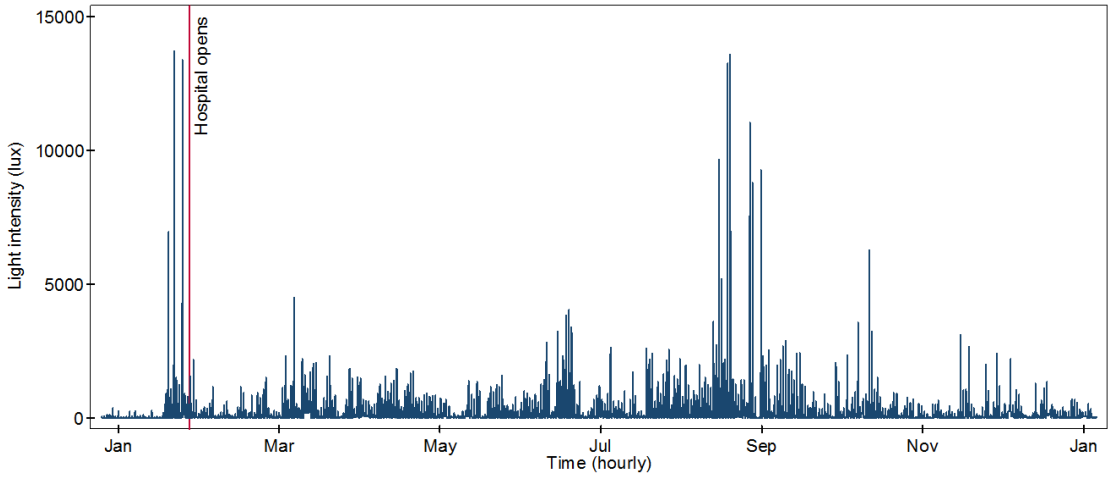

Figure 54. Hourly average light intensity (lux) over the duration of the measurement period (Jan 2013 to Jan 2014)

While the 24-hour example in Figure 54 shows a maximum of approximately 1500 lux, we see that much more variation exists over the span of the year, with hourly

average levels approaching 15,000 lux. The high variation in light intensity may be attributed to the fact that patients have control over some of the factors that affect light intensity, such as light switching and use of window shades.

Light intensity at nurse stations differed from patient rooms, spanning a much smaller range of 200 lux, compared to patient rooms, which could reach an hourly average approaching 15,000 lux. This is expected since nurse stations do not have windows and are not exposed to much natural light, aside from that which filters in through patient room doorways. The 24-hour time-series in Figure 55 shows a night-day pattern, with lights dimmed during the evening after about 19:00 and before 7:00.

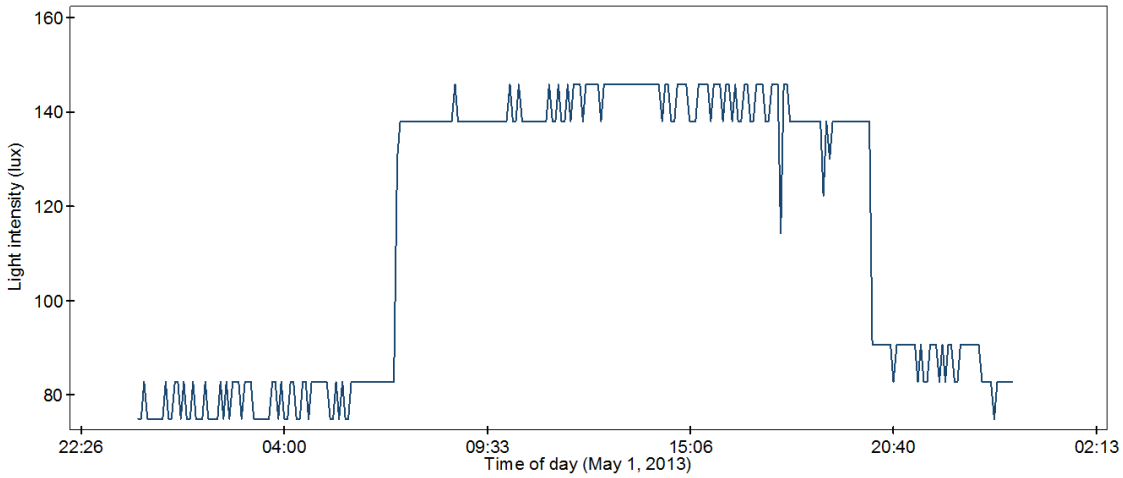

Figure 55. Light intensity (lux) at one nurse station measured at 5-minute intervals during the 24-hour period of May 1, 2013.

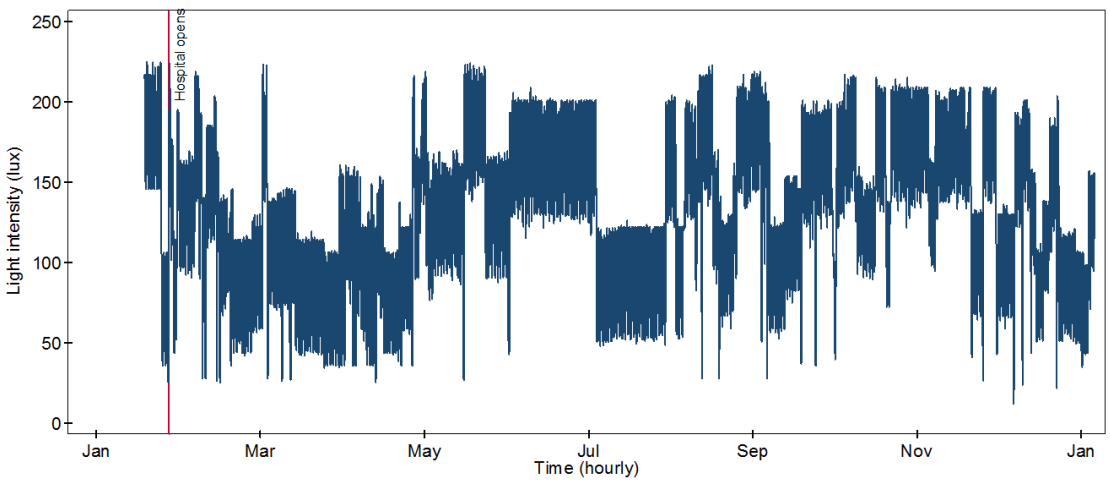

Figure 56. Hourly average light intensity (lux) at a nurse station over the duration of the measurement period (Jan 2013 to Jan 2014).

The pattern shown in Figure 67 is due to the placement of the light sensor during the duration of the project. The sensor was removed and replaced every week for data collection, and its placement at the nurse station was sensitive to objects in the surrounding area. The step changes are likely changes in sensor placement that occurred during weekly data retrieval. Nonetheless, we see a usual range of approximately 80 lux consistently during normal measurement periods.

4.2.5 Time-series: IR beam-breaks in the patient room doorways. The IR beam-break sensors attached to patient room doorways counted the number of beam-breaks (entries or exits) within 5-minute periods. An example of one 24-hour period in one patient room is shown in Figure 57. The data indicate that at least one beam-break occurred at least every 30 minutes, often more frequently. This is expected in a busy hospital environment, with patient-staff interaction occurring very frequently. As expected, no beam-breaks occurred between late night and early morning, during

sleeping hours. Without more information, it is difficult to determine the direction of persons passing through the doorway but it is reasonable to assume that any two beam-breaks can be attributed to one person. While the majority of measurements show no more than 4 beam-breaks per 5-minute period, it was not uncommon to see a much higher measurement with large groups of more than 5 people entering or exiting at once, but less likely to be within the same 5-minute period. Hourly totals over the entire measurement period from February 2013 to January 2014 are shown in Figure 58.

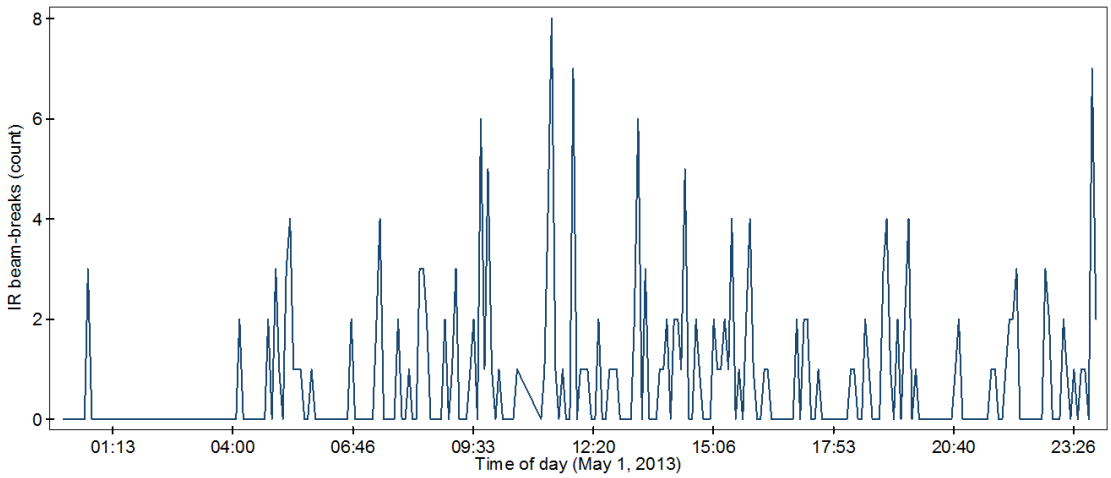

Figure 57. IR beam-breaks (count) measured at 5-minute intervals during the 24-hour period of May 1, 2013.

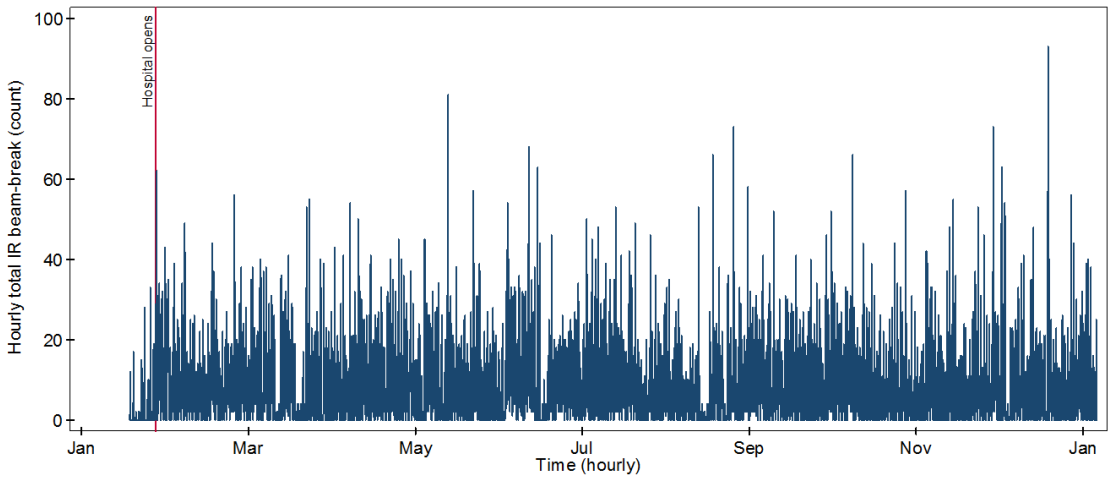

Figure 58. Hourly total IR beam-breaks (count) over the duration of the measurement period (Feb 2013 to Jan 2014) in one patient room.

Hourly total IR beam-breaks typically ranged from 0 to 20 counts per hour, with higher ranges occurring less frequently from 40 to 90 counts per hour. Small gaps indicate several hours and up to a couple of days with very low occupancy, likely with no patient occupying the room, although this occurred infrequently.

4.2.6 Time-series: CO_2 concentrations in the patient rooms. Patient room CO_2 concentrations over a 24-hour period in one patient room (Figure 59) follow a pattern similar to IR beam-break and light intensity, with higher values occurring in the early morning hours and lower values occurring during sleeping hours. Average hourly CO_2 concentrations over the entire measurement period in one room are shown in Figure 60. A sharp increase in concentration occurs upon the hospital opening and continues to fluctuate between 400 and 500 ppm.

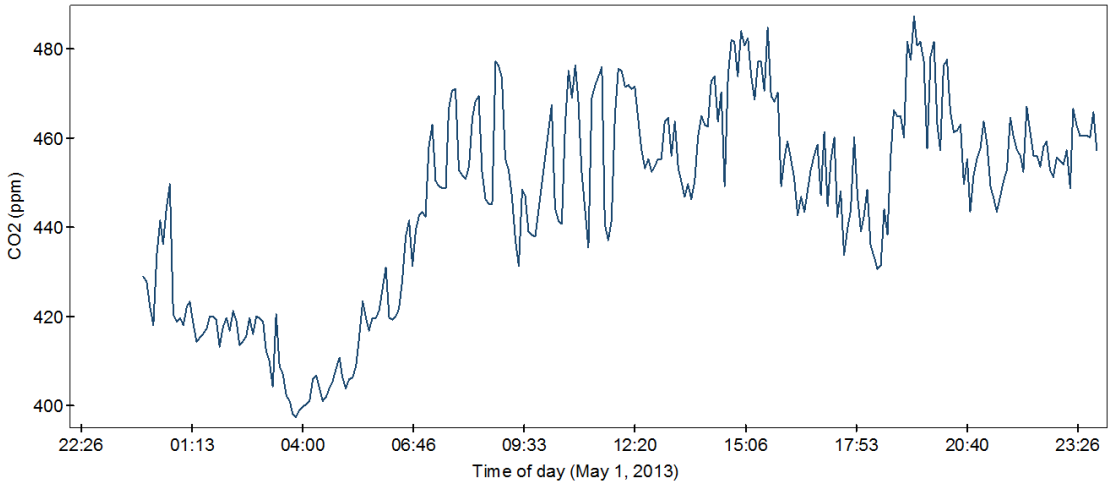

Figure 59. CO_2 (ppm) measured at 5-minute intervals during the 24-hour period of May 1, 2013.

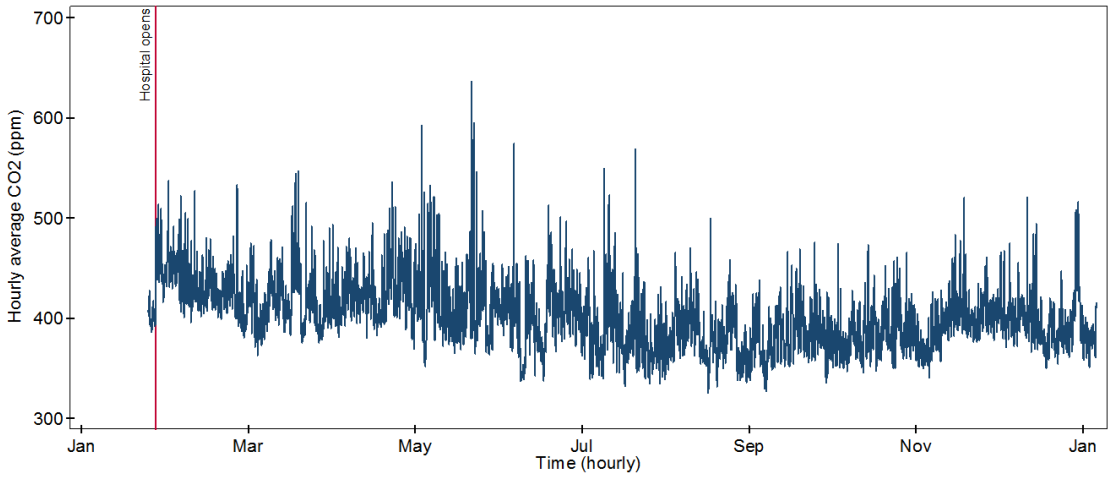

Figure 60. Hourly average CO_2 (ppm) over the duration of the measurement period (Feb 2013 to Jan 2014) in one patient room.

Taking the data from both IR beam-break sensors and CO2 sensors, we can explore correlations between the two parameters. Figure 61 shows total daily IR beam-break count with daily average CO_2 over a 3-month period, indicating a close correlation between the two.

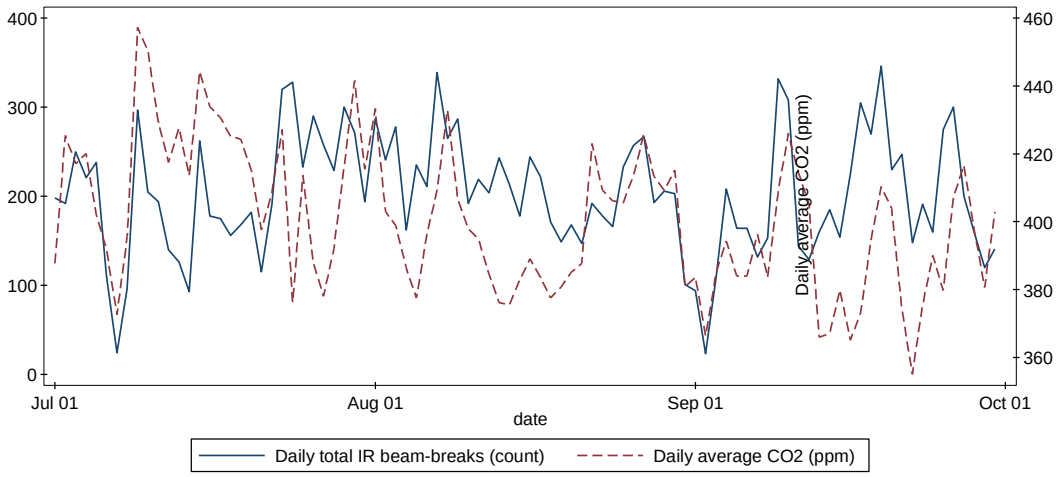

Figure 61. Daily IR beam-break data correlated with CO_2 in a patient room.

By taking daily average CO_2 concentrations from patient rooms and subtracting the concentration of CO_2 supplied to patient rooms through the HVAC system, we calculated the daily average CO_2 concentration originating from within the patient rooms. We correlated this with daily total IR beam-break data in all patient rooms and found a positive correlation between the two, shown in Figure 62, with the highest correlation coefficient of 0.53 in room 204 and the lowest of 0.28 in rooms 202 and 203. Table 7 shows these coefficients as well as R-squared values, slopes and y-intercepts for all the rooms. These data suggest that neither mean CO_2 concentrations nor daily total IR beam-break counts can serve as a perfect indictor of human occupancy but that the combination may be used as a general indicator of room occupancy.

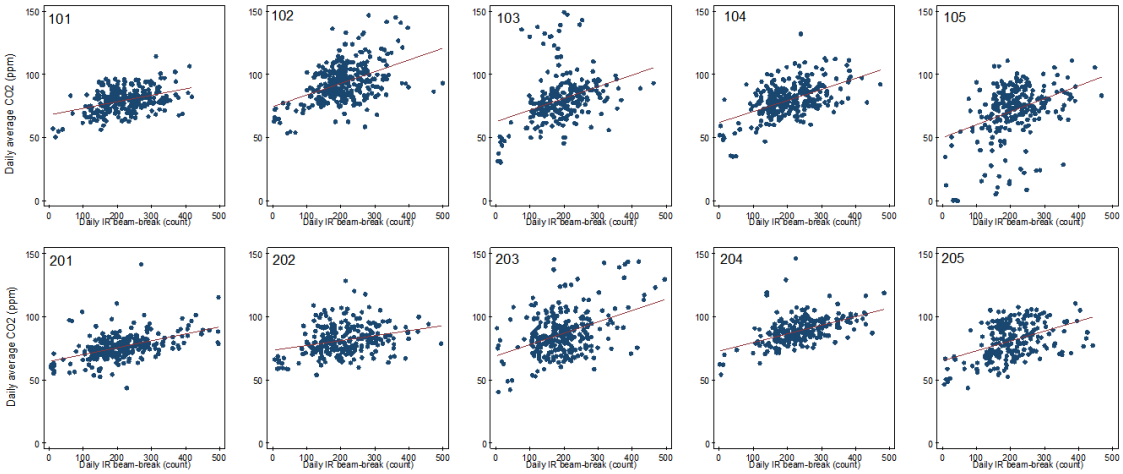

Figure 62. Daily total IR beam-break correlated with daily average CO_2, room source for all patient rooms

Table 7. Correlation coefficients, R-squared, slope and y-intercept for daily total IR beam-break correlated with daily average CO_2, room source for all rooms

Room	Spearman correlation coefficient	Pearson correlation coefficient	R^2	Slope	y-intercept
101	0.3426	0.4043	0.1603	0.0515	68.14
102	0.3757	0.4557	0.2077	0.0926	74.49
103	0.4470	0.3503	0.1227	0.0921	62.76
104	0.4251	0.5173	0.2679	0.0874	61.93
105	0.3157	0.3635	0.1322	0.1025	50.09
201	0.5051	0.4841	0.2343	0.0549	64.49
202	0.2757	0.2821	0.0796	0.0394	73.26
203	0.2753	0.4079	0.1663	0.0891	69.20
204	0.5307	0.5091	0.2592	0.0681	72.83
205	0.4084	0.4359	0.1900	0.0782	0.6524

4.2.7 Time-series: Differential pressure with respect to hallway. Differential pressure was measured at patient room doorways, with sampling lines both within the patient room and the hallway outside the room. Figure 63 shows a 24-hour time series in one room on May 1, 2013, which is generally representative of data collected across all

rooms throughout the course of the project. While data showed slight fluctuations, readings remained around zero, indicating no pressure differential between the room and hallway, and therefore likely no significant movement of air between the two. Average hourly differential pressure measurements from September 2013 to January 2014 (Figure 64) continue to show little fluctuation from zero, and likely no significant air movement between the room and hallway throughout the duration of the project. These sensors have uncertainties of ~0.25 Pa, so with data hovering around -0.25 to +0.25 Pa, room pressurization is considered neutral during the entire campaign. This is consistent with plan drawings for these rooms identified as neutral pressure rooms.

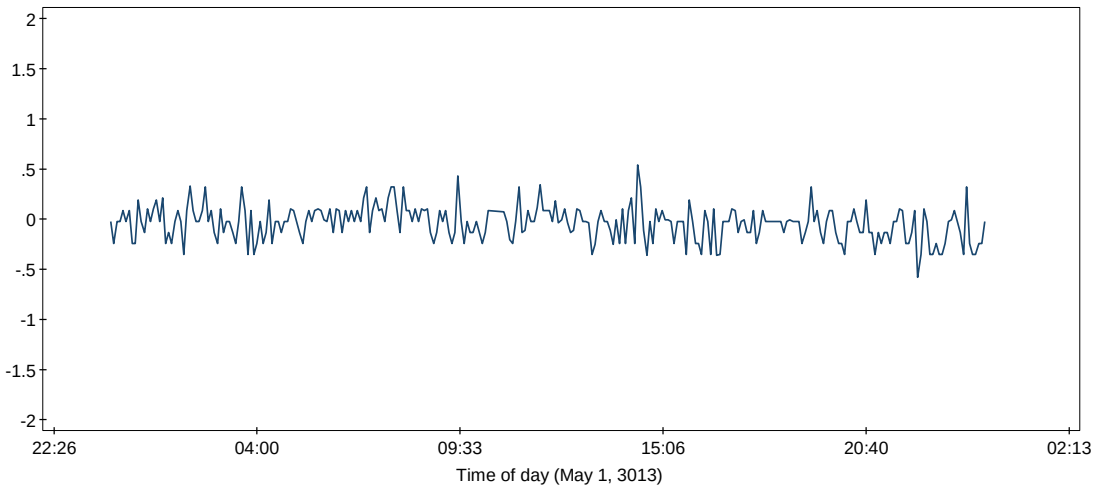

Figure 63. Differential pressure (Pa) measured at 5-minute intervals in one room during the 24-hour period of May 1, 2013.

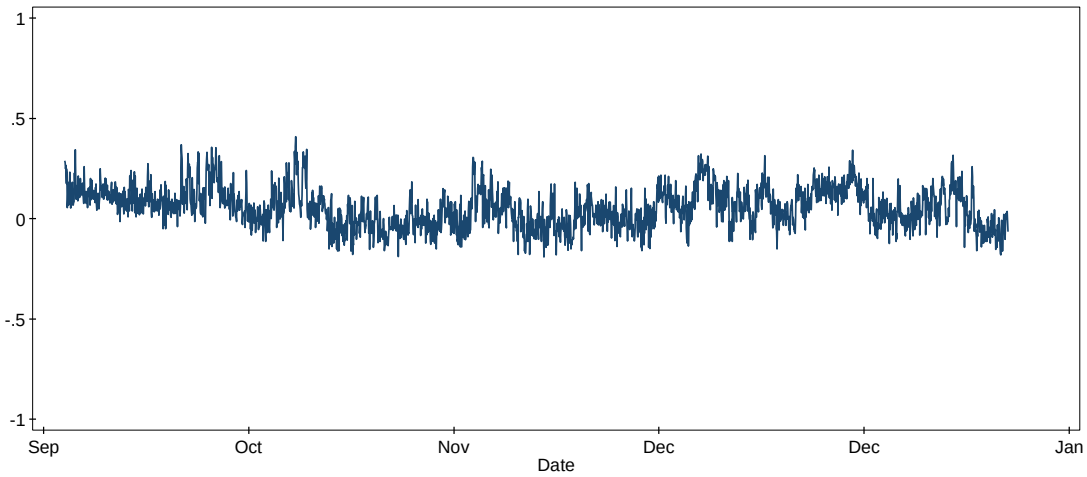

Figure 64. Hourly average differential pressure (Pa) over the period (Sept 2013 to Jan 2014) in one patient room.

To validate our long-term pressurization measurements, a DG-700 differential pressure sensor was used once a week for five weeks during hospital visits to manually measure differential pressure within all patient rooms. Measurements were taken with the door open and with the door closed to determine any changes in room pressurization pressure according to door position. Table 8 shows the representative results during one of the visits.

Table 8. Differential pressure measurements using a DG-700

Room	Pressure diff. w/ open door	Pressure diff. w/ door closed
101	0.1	0
102	0.1	-0.1
103	0.1	-0.1
104	0	0
105	0.1	0
201	0	0.2
202	0	0
203	0	0.1
204	0.1	0.2
205	0	0

These measurements confirmed that differential pressure truly hovered around 0, indicating no significant airflow between the spaces at the doorway or issues with pressurization or depressurization relative to the hallway.

4.3 Summary of Results

This section provides a general summary of all of the building science data collected over the course of the project.

Table 9. Summary statistics for all parameters measured within all 10 patient rooms

Parameter	N	Mean	S.D.	Min	Max
Temperature (°C)	1.20×10^6	23.6	1.4	13.4	31.6
RH (%)	1.20×10^6	34.8	6.8	5.2	88.0
Light intensity (lux)	1.20×10^6	173	448	4	32280
IR beam-break (counts/5 min.)	9.46×10^5	0.74	1.68	0	98
CO_2 (ppm)	8.63×10^5	416	40	325	699
Differential pressure	7.06×10^5	0.09	0.57	-1.78	1.77
TOTAL	6.12×10^6				

The total number of 5-minute data points approached 1.2 million for each measured variable. The mean (s.d.) temperature across all patient rooms and nurse stations in the hospital was 23.6°C (1.4°C). The mean (s.d.) relative humidity was 34.8% (6.8%). In addition to these measured parameters, absolute humidity was calculated using temperature and RH measurements, adding another 1.2 million data points to our analysis. These data suggest that the hospital was tightly controlled for thermal comfort, although the following sections will also explore variations both *within* individual rooms and *between* rooms.

Light intensity had a large range from 3.9 lux, up to 32280 lux, accounting for minimal light during nighttime hours and very high levels during daytime hours with high solar insolation. The mean (s.d.) light intensity was 173 lux (448 lux). The lower total number of 5-minute data points for IR beam-break and CO_2 data account for data dropped due to sensor and calibration issues throughout the project. Approximately 28% of the possible patient room CO_2 data points were either not collected or excluded for QA/QC reasons. Approximately 21% of the possible IR beam break data points were also lost or excluded. However, values for both of these parameters varied widely based on occupancy.

The total number of data points for differential pressure is much lower as these sensors were installed about 3 months after the beginning of our measurement period, and also account for data dropped due to sensor issues. Although the range is between about -1.8 and 1.8 Pa, the mean remained close to zero, 0.09 Pa. Due to the placement of these sensors next to patient room doorways, frequent interference caused some fluctuations in pressure, but overall patterns indicate values hovered close to zero.

The total number of 5-minute data points in the mechanical room approached 500,000 for both CO_2 and temperature measured in the OA, SA, and RA portions of two AHUs, or 6 air streams total. Since measuring OA fractions was the primary purpose in the mechanical room, only those CO_2 data for which all three OA, SA, and RA sensors were within reasonable bounds were included in this summary. RH was measured in both return air streams and the number of data points approached 110,000. Vapor pressure was measured directly using the SBA-5 monitors and compared to saturation vapor

pressure to estimate RH in the two supply air streams and one outdoor air stream, with the number of data points approaching 180,000.

Table 10. Summary statistics for all parameters measured in mechanical rooms

Parameter	N	Mean	S.D.	Min	Max
CO_2	4.78×10^5	393	37	309	594
Temperature	4.76×10^5	14.0	8.3	-24.7	34.5
RH	1.06×10^5	34.6	6.6	13.7	60.0
Vapor pressure	1.80×10^5	1.014	0.301	0.308	2.22
TOTAL	1.24×10^6				

In addition to these parameters in the mechanical room, absolute humidity, enthalpy and OA fraction were also calculated from temperature and RH or vapor pressure, adding another 1.2 million data points to our data set.

4.4 Variations *within* individual rooms and nurse stations

This section summarizes the variation in measurements for all parameters, both measured and calculated, over the duration of the project. Plots show both variation within rooms as well as between rooms and floors.

4.4.1 Air Temperature. Hourly average temperature (Figure 65) across all patient rooms typically varied between 19°C and 26°C, a range of about 7°C, with median temperatures between 22°C and 25°C. Nurse stations appeared to be more controlled, spanning a range of about 4°C. Median temperatures on the lower floor appeared more consistent than the upper floor. Slight differences between the lower and upper floor are apparent in both patient rooms and nurse stations, with median temperatures about 1°C

higher on the upper floor. One thing to note in Room 101 is that several hourly data points were greater than 30°C, well beyond the zone of thermal comfort (ASHRAE, 2013c). This can be attributed to systems testing done prior to the hospital opening.

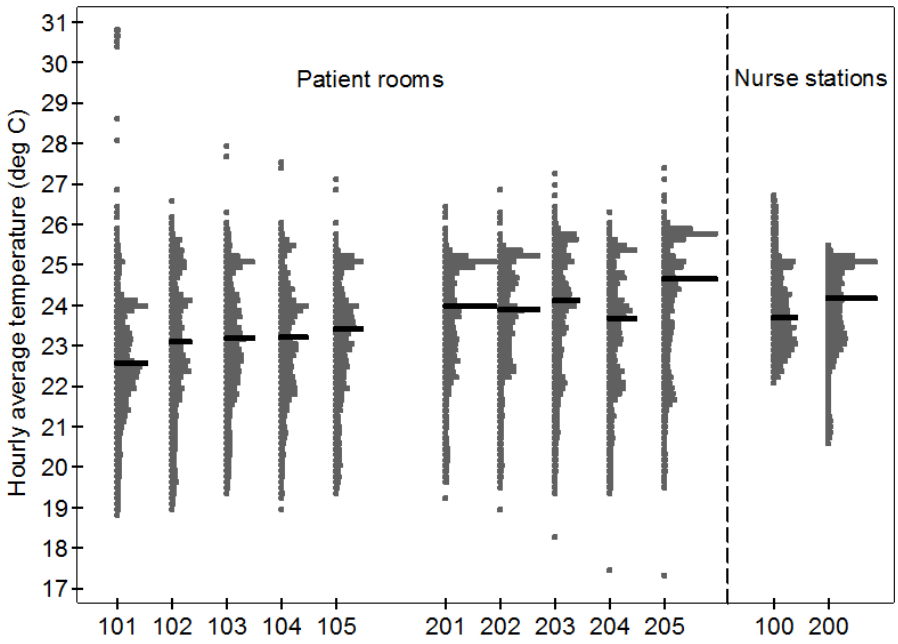

Figure 65. Variation in hourly average temperature (°C) in all patient rooms and nurse stations.

4.4.2 Relative humidity. Hourly average RH values shown in Figure 66 varied widely, by as much as 50% absolutely, although lower RH values occurred infrequently. The majority of measurements were between 25% and 50%, with median RH fairly consistent across all rooms and nurse stations, around 35%. It is important to note the similarities in variation within rooms as well as nurse stations, indicating the strong effect from the hospital HVAC systems and little effect from the local environment.

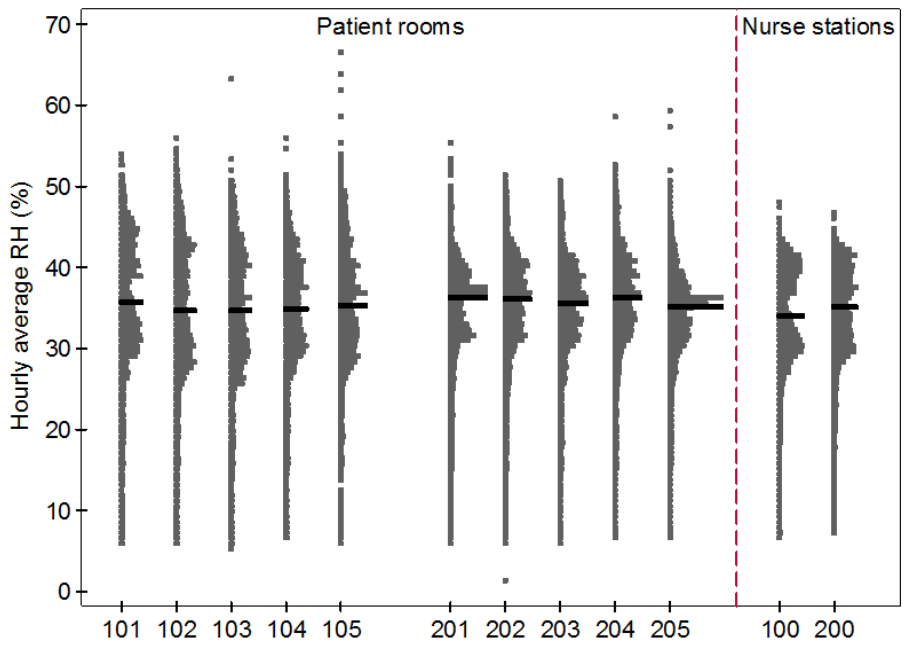

Figure 66. Variation in hourly average RH (%) in all patient rooms and nurse stations

4.4.3 Absolute humidity. Absolute humidity was calculated using temperature and RH data from patient rooms and nurse stations and the variation is shown in Figure 67. Variation within rooms and nurse stations appears consistent and similar across all rooms and nurse stations, with the majority of measurements occurring between 0.005 kg_w/kg_{da} and 0.008 kg_w/kg_{da}. However, there is a clear difference between floors, with humidity in the upper floors consistently higher than lower floors. Section 4.6 will explore these differences further.

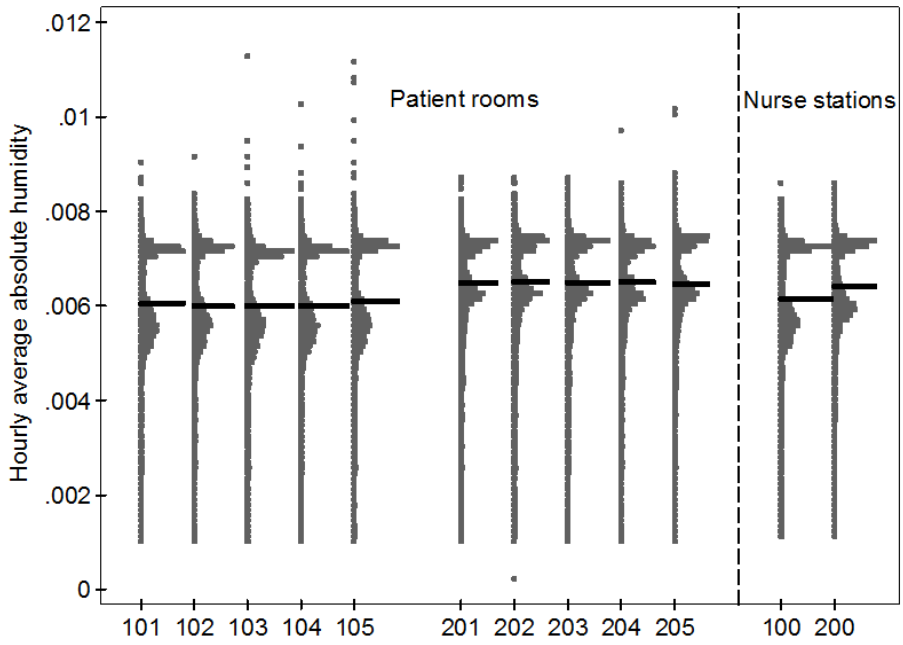

Figure 67. Variation in hourly average absolute humidity in all patient rooms and nurse stations.

4.4.4 Light intensity. Daily average light intensity across rooms and nurse stations (Figure 68) was analyzed to clearly show the highest occurrence of light levels. As demonstrated in the 24-hour time series plot (Figure 53), elevated light levels resulting from increased natural light occurred during afternoon hours as the sun went down, increasing exposure to west-facing surfaces. This period of increased exposure lasts approximately 6 hours, with highest levels occuring just before sunset over no more than 2 hours within a 24 hour period. Therefore, we would expect medians for daily average light levels to be closer to low level, artificial light, which is apparent in the following figure, where median light levels are similar to those of nurse stations. Nurse stations, with no exposure to natural light intuitively have a lower range of daily average light intensity, between 100 and 200 lux. Additionally, nurse station lights are dimmed during

evening hours, but are never completely turned off, so we do not see levels as low as those seen in patient rooms.

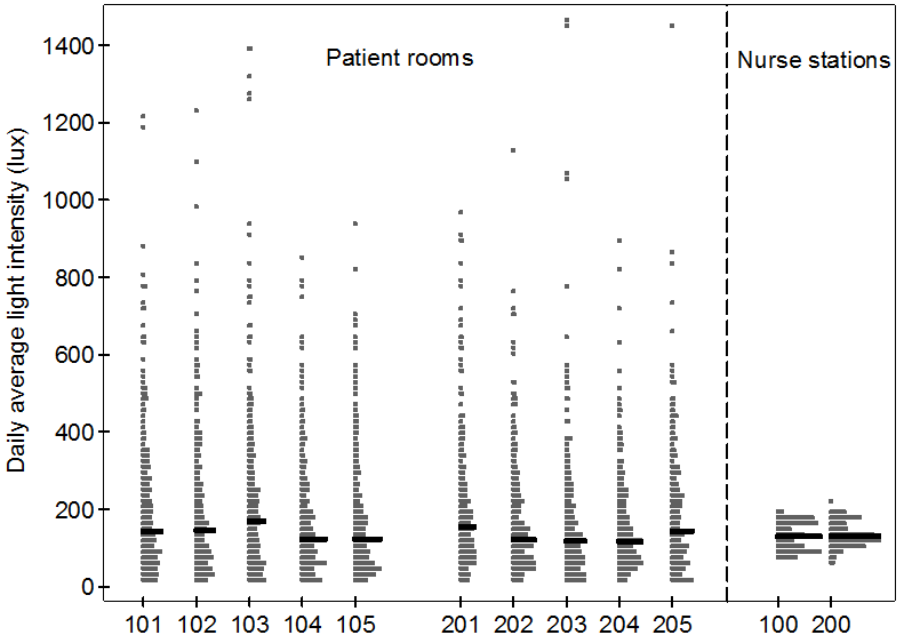

Figure 68. Variation in daily average light intensity (lux) in all patient rooms and nurse stations.

4.4.5 IR beam-break at patient room doorways. Daily total IR beam-break (counts), shown in Figure 69, varied similarly across all patient rooms with median daily total counts around 200 for all rooms. Room 204 appears slightly higher, with a median noticeably higher than all other rooms and several days averaging more than 500 beam-breaks per day. Over all rooms, few days had less than 100 beam-breaks, indicating that all patient rooms typically average at least 4 beam-breaks per hour, expected in a high occupancy/activity environment such as a hospital.

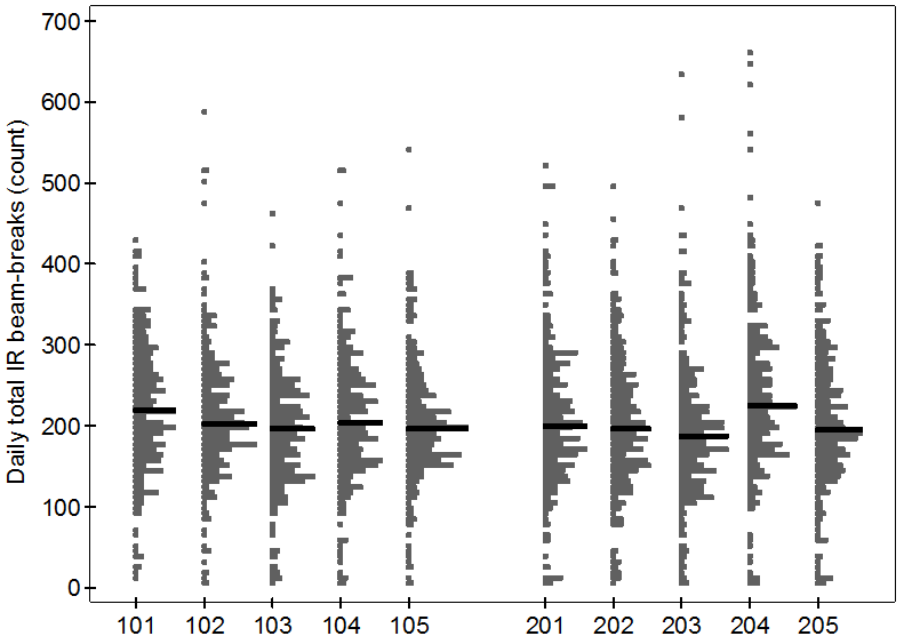

Figure 69. Variation in daily total IR beam-breaks (count) in all patient rooms.

4.4.6 CO_2 concentrations in patient rooms. Daily average CO_2 values varied similarly between rooms, typically spanning a range of 100 ppm. Figure 70 shows this variation, along with similar median values of about 375 ppm across all rooms, with the exception of room 102, which shows a slightly higher range.

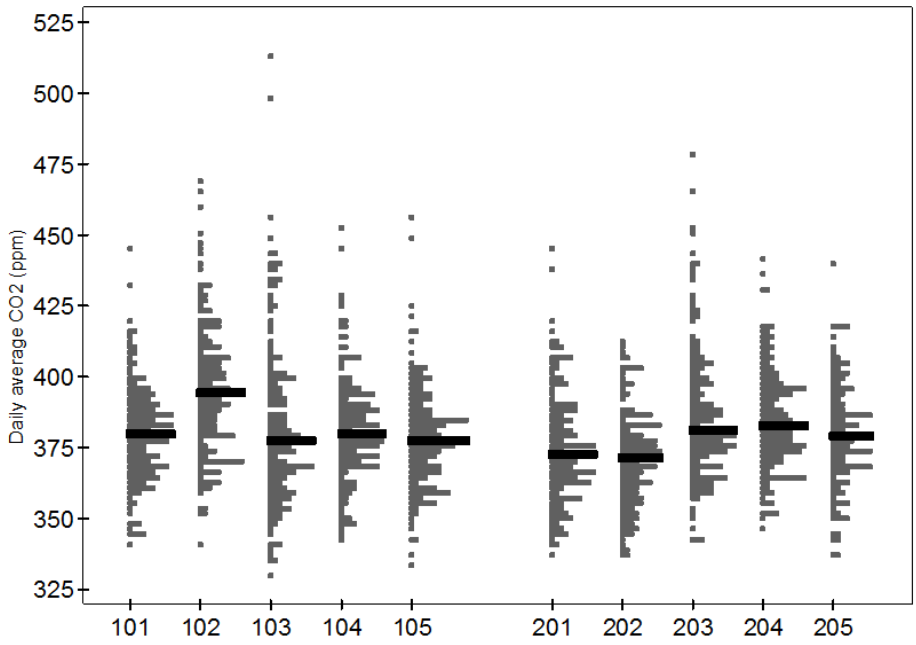

Figure 70. Variation in daily average CO2 (ppm) in all patient rooms.

4.5 Variations *between* individual rooms

To show variation between individual rooms, we analyzed how measurements from each room correlated with each other. The following plots show correlations between the nurse station and rooms on each floor, to focus on differences per floor, followed by a table showing correlation factors across all rooms and nurse stations.

4.5.1 Air Temperature. Daily average temperature in the lower floor (Figure 71) shows little correlation between rooms, in general. However, daily average measurements appear to cover the same range of temperatures among rooms, with the exception of Nurse Station 100 and Room 101. The lower range of temperatures in Nurse Station 100 correlate with relatively lower temperature in patient rooms. The

outlying high temperatures in Room 101 correlate with lower temperatures in all other rooms and nurse station.

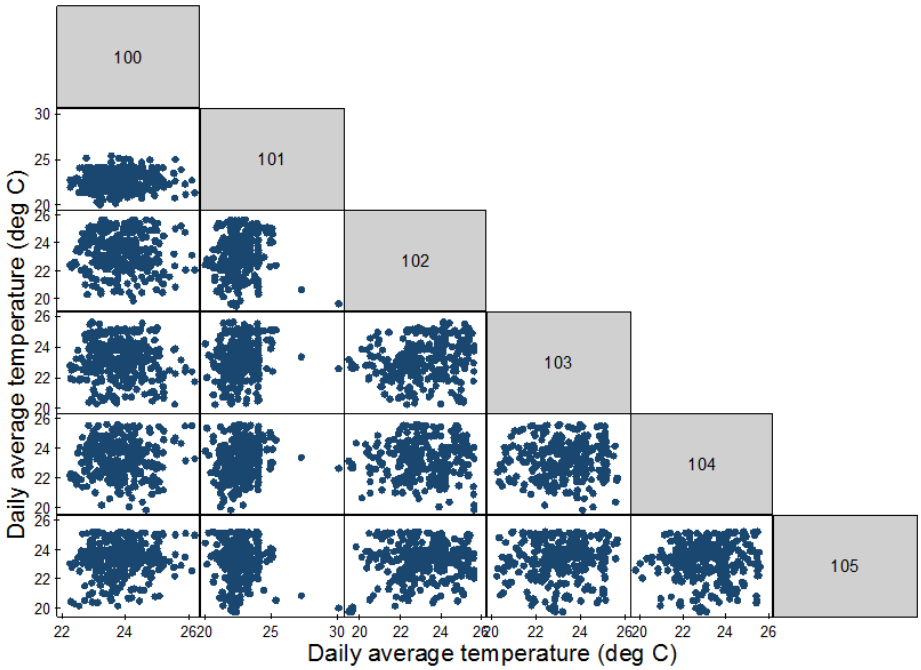

Figure 71. Correlation matrix for temperature in lower floor nurse station and patient rooms.

Correlations between rooms on the upper floor show a slightly stronger correlation between rooms than the lower level, with data points tending towards higher temperatures. Nurse Station 200 has a smaller range of temperatures relatively higher than patient rooms, with the exception of several outlying data points around 21°C, which correlate relatively well with similar temperatures in patient rooms.

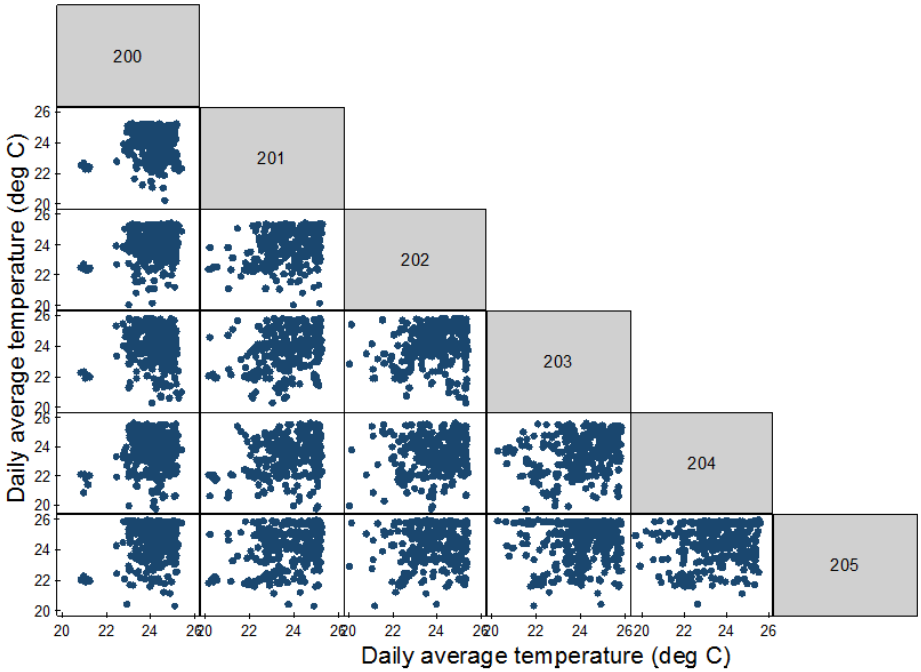

Figure 72. Correlation matrix for temperature in upper floor nurse station and patient rooms.

Figure 73 shows correlations between all rooms and nurse stations, showing similar correlations between all rooms, despite different floors. Table 11 shows correlation factors between all rooms and nurse stations, revealing the majority of the factors are less than 0.2, with the exception of a few, most of which occur among the upper level rooms. The highest correlation between two rooms is 0.289, between Room 201 and 203, with no obvious reason for the higher correlation.

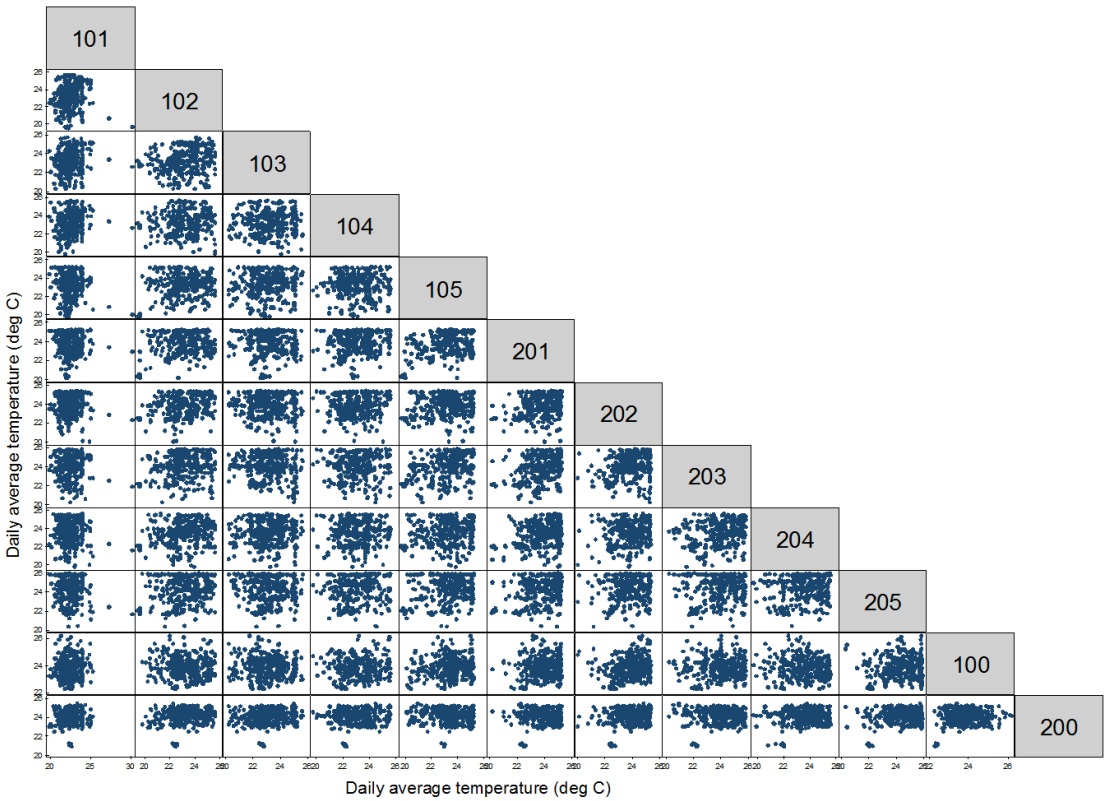

Figure 73. Correlation matrix for temperature in all rooms and nurse stations.

Table 11. Correlation matrix for all rooms and nurse stations.

	101	102	103	104	105	201	202	203	204	205	100	200
101	1											
102	0.142 *	1										
103	0.0593	0.146 *	1									
104	0.264 ***	0.0534	0.0377	1								
105	-0.109	-0.0340	-0.0253	-0.0669	1							
201	0.0358	-0.102	-0.236 ***	0.0707	0.0759	1						
202	0.0337	0.188 **	-0.0935	0.122 *	-0.0822	0.227 ***	1					
203	0.0884	0.0602	-0.252 ***	0.0190	0.177 **	0.289 ***	0.161 **	1				
204	0.0376	0.0873	-0.0644	0.0616	0.0301	0.220 ***	0.225 ***	0.184 **	1			
205	0.0479	-0.0358	-0.0562	0.0344	0.148 *	0.219 ***	0.117	-0.0108	0.0841	1		
100	0.0180	0.101	-0.0060	0.0307	0.0778	0.0338	0.153 *	0.105	0.0317	0.148 *	1	
200	0.0230	0.203 ***	0.144 *	0.148 *	-0.0565	0.0763	0.220 ***	0.0598	0.162 **	0.218 ***	0.208 ***	1

p<0.05 * p<0.01 ** p<0.001 ***

Table 12 shows the fraction of those measured differences in the correlations above that fell within the range of propagated instrument uncertainty (0.57°C), which was estimated by adding the manufacturer-reported uncertainty (0.4°C) in quadrature. Overall, 28.7% of all measured differences in daily averages were found to be within this range of uncertainty, with individual room comparisons ranging from 18.1% to 42.9%. This suggests that the weak correlations of temperatures between rooms are moderately impacted by sensor accuracy. However, we have good confidence that the true uncertainty in the temperature measurements is much lower according to our co-location calibration experiments. Therefore, the weak correlation observed is believed to largely stem from true differences in daily mean temperatures and not sensor uncertainty.

Table 12. Fraction of measured temperature differences between rooms that were within the range of propagated uncertainty

	101	102	103	104	105	201	202	203	204	205	100
101											
102	0.271										
103	0.301	0.312									
104	0.361	0.257	0.355								
105	0.281	0.341	0.315	0.263							
201	0.242	0.263	0.221	0.298	0.272						
202	0.276	0.265	0.281	0.303	0.295	0.391					
203	0.238	0.290	0.255	0.276	0.224	0.325	0.354				
204	0.238	0.281	0.275	0.256	0.275	0.319	0.320	0.317			
205	0.181	0.284	0.210	0.215	0.221	0.255	0.306	0.334	0.300		
100	0.268	0.265	0.307	0.279	0.321	0.353	0.387	0.315	0.303	0.306	
200	0.199	0.202	0.256	0.266	0.318	0.266	0.342	0.273	0.288	0.300	0.429

4.5.2 Relative humidity. In contrast with temperature, Figure 74 and Figure 75 show a strong correlation of daily average RH between rooms on each floor.

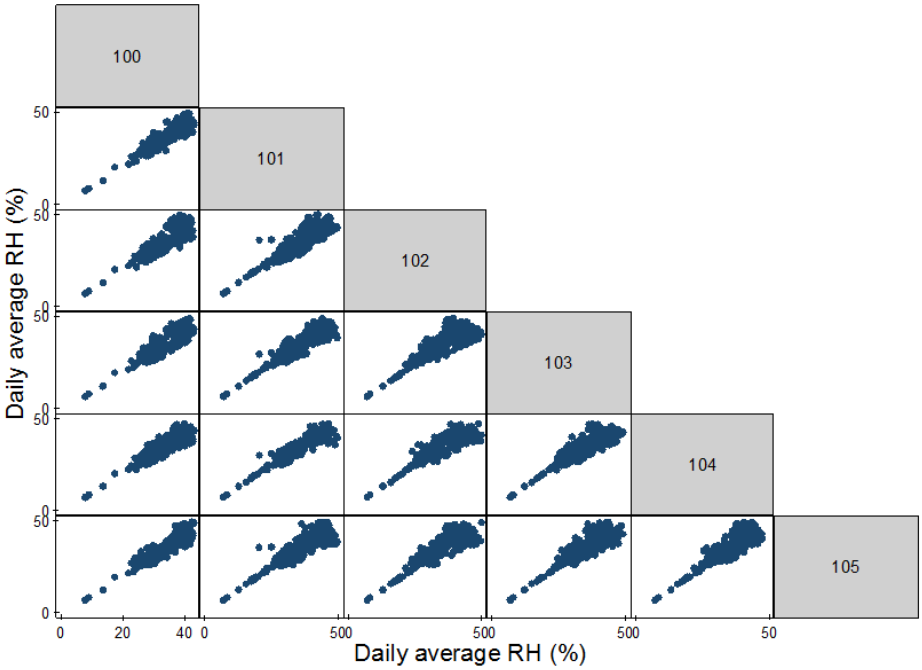

Figure 74. Correlation matrix for daily average RH (%) across lower level nurse station and patient rooms.

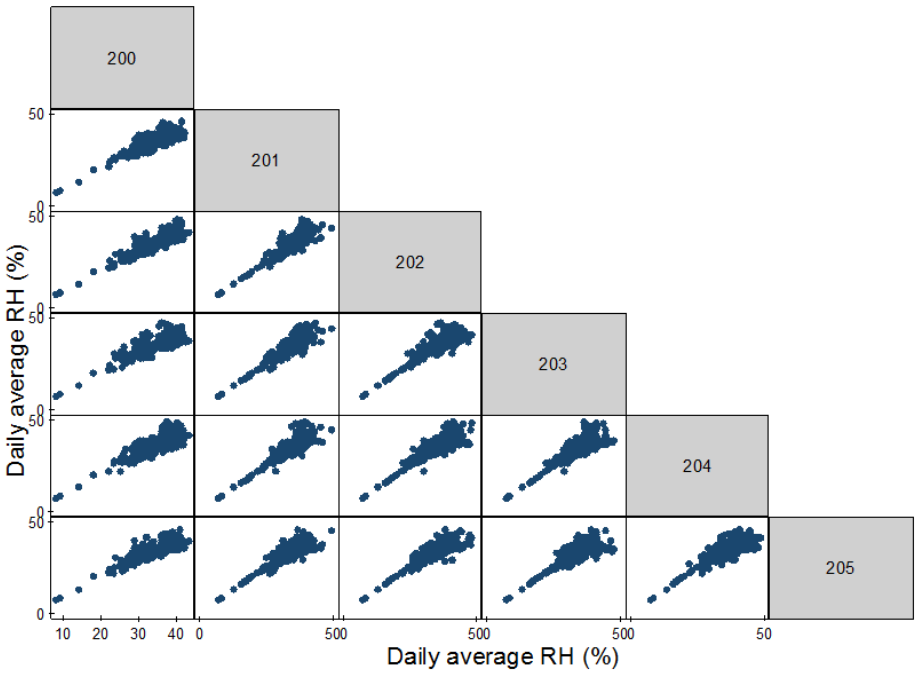

Figure 75. Correlation matrix for daily average RH (%) across upper level nurse station and patient rooms.

Furthermore, Figure 76 and Table 13 shows very strong correlations between rooms on each floor, with correlation factors between upper and lower level rooms typically between 0.7 and 0.8. Stronger correlations exist between rooms on the same floor, with factors greater than 0.8.

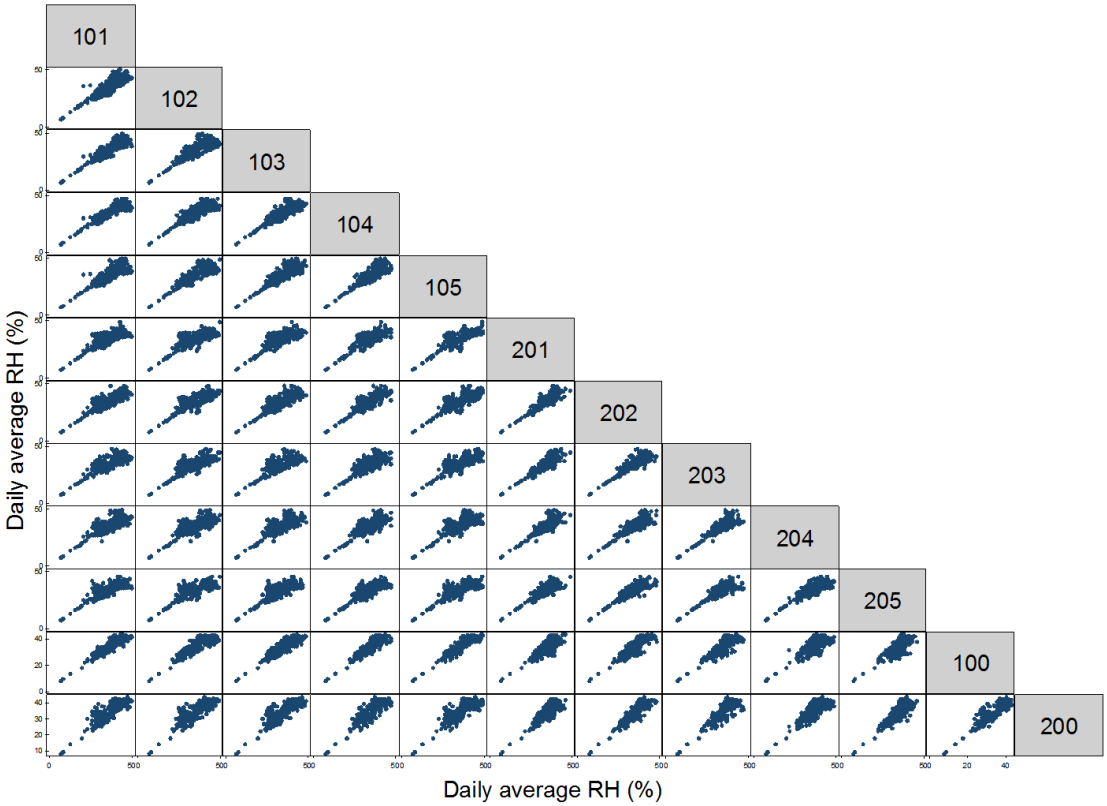

Figure 76. Correlation matrix for daily average RH (%) across all patient rooms and nurse stations.

Table 13. Correlation matrix for daily average RH (%) across all patient rooms and nurse stations.

	101	102	103	104	105	201	202	203	204	205	100	200
101	1											
102	0.892 ***	1										
103	0.886 ***	0.877 ***	1									
104	0.909 ***	0.865 ***	0.862 ***	1								
105	0.860 ***	0.855 ***	0.854 ***	0.837 ***	1							
201	0.731 ***	0.718 ***	0.687 ***	0.749 ***	0.739 ***	1						
202	0.777 ***	0.786 ***	0.747 ***	0.795 ***	0.754 ***	0.875 ***	1					
203	0.742 ***	0.738 ***	0.671 ***	0.737 ***	0.761 ***	0.851 ***	0.831 ***	1				
204	0.726 ***	0.729 ***	0.686 ***	0.736 ***	0.708 ***	0.825 ***	0.840 ***	0.786 ***	1			
205	0.729 ***	0.710 ***	0.696 ***	0.735 ***	0.729 ***	0.827 ***	0.831 ***	0.743 ***	0.764 ***	1		
100	0.917 ***	0.907 ***	0.901 ***	0.886 ***	0.908 ***	0.780 ***	0.834 ***	0.786 ***	0.762 ***	0.781 ***	1	
200	0.828 ***	0.839 ***	0.830 ***	0.829 ***	0.794 ***	0.852 ***	0.892 ***	0.817 ***	0.830 ***	0.829 ***	0.875 ***	1
p<0.05 *	p<0.01 **	p<0.001 ***										

Overall, RH correlates very highly between rooms, indicating high influence from the HVAC system, with little effect from local environmental conditions or occupancy. Table 14 shows the fraction of those measured RH differences in the correlations above that fell within the range of propagated instrument uncertainty (3.5%), estimated by adding the manufacturer-reported uncertainty of the RH sensors (2.5% RH) in quadrature. Overall, 66.8% of all measured RH differences were found to be within this range of uncertainty, with individual room comparisons ranging from 48.8% to 84.5%. Within patient rooms and nurse stations on the same floor, about 75% of the daily average measurements fell within this range of uncertainty. This supports the strong

correlations, showing that most of the observed differences were small and generally within the range of propagated uncertainty.

Table 14. Fraction of measured RH differences between rooms that were within the range of propagated uncertainty

	101	102	103	104	105	201	202	203	204	205	100
101											
102	0.700										
103	0.727	0.721									
104	0.772	0.676	0.728								
105	0.699	0.676	0.694	0.694							
201	0.558	0.509	0.567	0.630	0.618						
202	0.602	0.538	0.585	0.662	0.627	0.830					
203	0.558	0.521	0.555	0.632	0.609	0.818	0.802				
204	0.598	0.533	0.533	0.591	0.581	0.763	0.745	0.695			
205	0.544	0.488	0.544	0.600	0.567	0.751	0.725	0.718	0.683		
100	0.690	0.735	0.756	0.81	0.792	0.737	0.735	0.715	0.612	0.694	
200	0.568	0.568	0.690	0.666	0.685	0.792	0.789	0.758	0.721	0.755	0.845

4.5.3 Absolute humidity. Daily average absolute humidity showed very high correlations between rooms and nurse stations, more so than RH, in both upper and lower levels as shown in Figure 77 and Figure 78. Aside from a single outlier in Room 204, the correlations appear almost perfect.

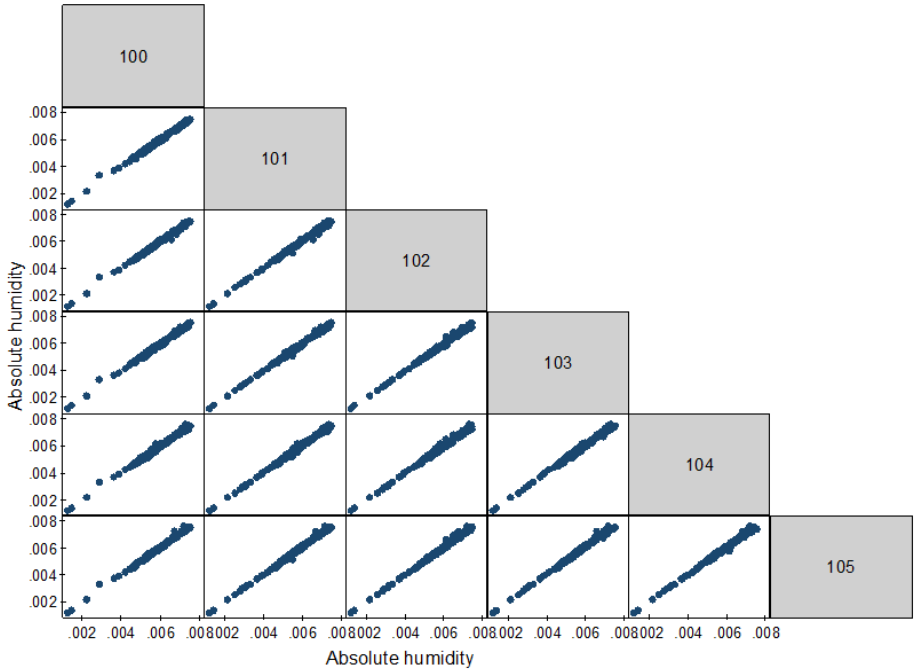

Figure 77. Correlation matrix for daily average absolute humidity across lower level nurse station and patient rooms.

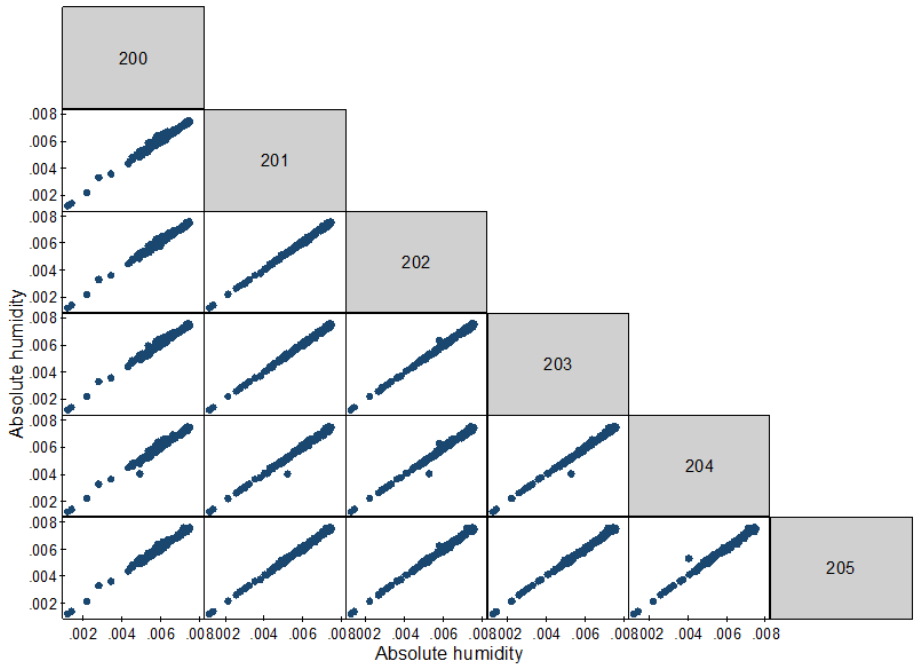

Figure 78. Correlation matrix for daily average absolute humidity across upper level nurse station and patient rooms.

Table 15 confirms the high correlations viewed in the previous two figures, with highest correlations between rooms on each floor. The nurse station and rooms on the lower floor all have correlation factors greater than 0.995. Rooms on the upper floor have factors greater than 0.992, with factors as low as 0.986 between the upper floor nurse station and rooms. Between floors, there was less correlation, apparent in Figure 79. Factors were as low and 0.899 and as high as 0.921 between patient rooms, 0.943 between nurse stations and rooms of each floor, and 0.947 between the two nurse stations on each floor.

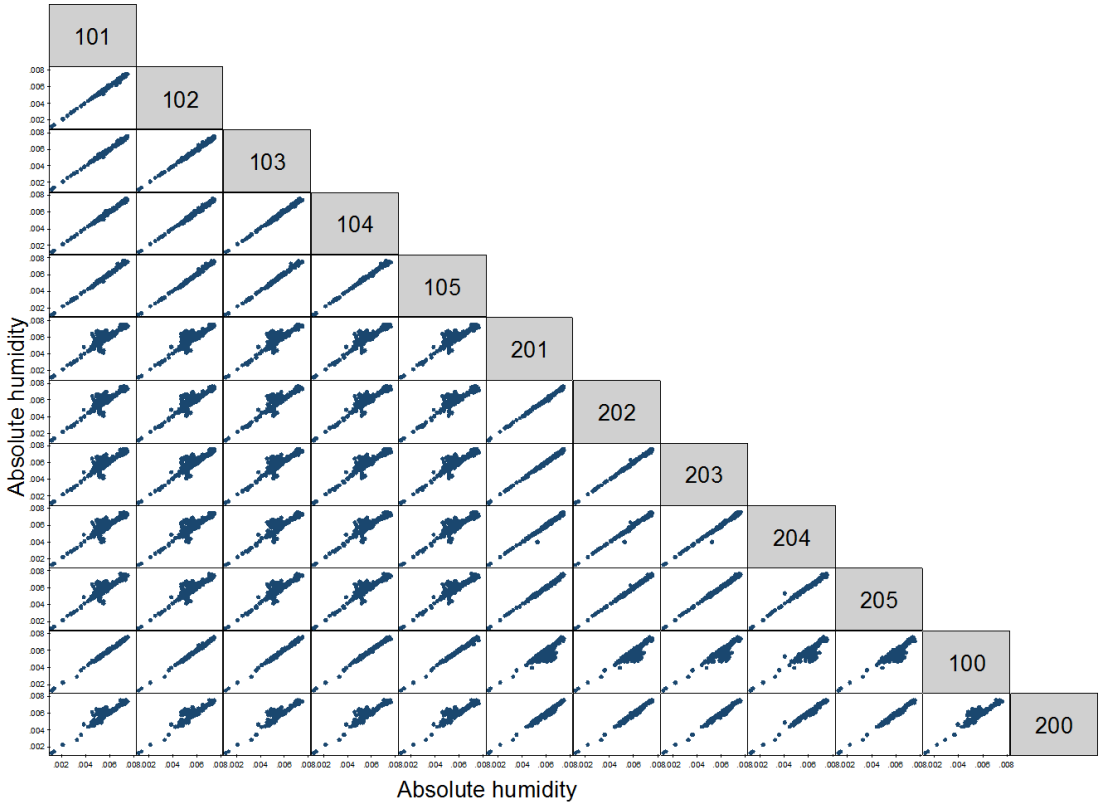

Figure 79. Correlation matrix for daily average absolute humidity across all nurse stations and patient rooms.

Table 15. Correlation matrix for daily average absolute humidity across all patient room and nurse stations.

	101	102	103	104	105	201	202	203	204	205	100	200
101	1											
102	0.998 ***	1										
103	0.997 ***	0.997 ***	1									
104	0.997 ***	0.997 ***	0.996 ***	1								
105	0.998 ***	0.997 ***	0.997 ***	0.997 ***	1							
201	0.909 ***	0.908 ***	0.908 ***	0.903 ***	0.906 ***	1						
202	0.917 ***	0.916 ***	0.915 ***	0.910 ***	0.915 ***	0.998 ***	1					
203	0.914 ***	0.913 ***	0.913 ***	0.908 ***	0.912 ***	0.998 ***	0.998 ***	1				
204	0.905 ***	0.904 ***	0.904 ***	0.899 ***	0.903 ***	0.994 ***	0.994 ***	0.994 ***	1			
205	0.921 ***	0.920 ***	0.920 ***	0.915 ***	0.919 ***	0.997 ***	0.997 ***	0.997 ***	0.993 ***	1		
100	0.998 ***	0.998 ***	0.997 ***	0.997 ***	0.998 ***	0.911 ***	0.919 ***	0.916 ***	0.907 ***	0.923 ***	1	
200	0.943 ***	0.942 ***	0.942 ***	0.938 ***	0.942 ***	0.987 ***	0.990 ***	0.989 ***	0.986 ***	0.992 ***	0.947 ***	1

p<0.05 * p<0.01 ** p<0.001 ***

Table 16 shows the fraction of those measured absolute humidity differences in the correlations above that fell within the range of propagated instrument uncertainty (0.00014 kg_w/kg_{da}), which was estimated by calculating the impact of uncertainty from both the individual temperature and RH sensors on absolute humidity (0.0001 kg_w/kg_{da}), and adding that value in quadrature. About 63.4% of all measured absolute humidity differences were found to be within the range of propagated instrument uncertainty, with individual room comparisons ranging from 24.4% to 98.1%. Within patient rooms and nurse stations on the same floor, about 85% of the daily average measurements fall within the range of uncertainty. As with relative humidity, this supports the strong

correlations, showing that the observed differences between daily average room measurements were small and generally within the range of propagated uncertainty.

Table 16. Fraction of measured absolute humidity differences between rooms that were within the range of propagated uncertainty

	101	102	103	104	105	201	202	203	204	205	100
101											
102	0.947										
103	0.894	0.829									
104	0.945	0.896	0.841								
105	0.897	0.959	0.643	0.858							
201	0.504	0.481	0.382	0.435	0.504						
202	0.401	0.462	0.276	0.361	0.476	0.970					
203	0.419	0.464	0.309	0.356	0.507	0.973	0.975				
204	0.462	0.467	0.377	0.438	0.476	0.960	0.890	0.925			
205	0.340	0.431	0.244	0.326	0.476	0.897	0.946	0.948	0.801		
100	0.940	0.981	0.714	0.932	0.976	0.526	0.443	0.488	0.503	0.421	
200	0.568	0.603	0.390	0.477	0.613	0.673	0.631	0.639	0.682	0.609	0.643

4.5.4 Light intensity. Daily average light intensity between rooms on the same floor appeared to show some correlation, particularly at lower light intensity levels. No correlation is apparent between nurse stations and rooms on the same floor, with nurse station light levels remaining relatively low compared to rooms.

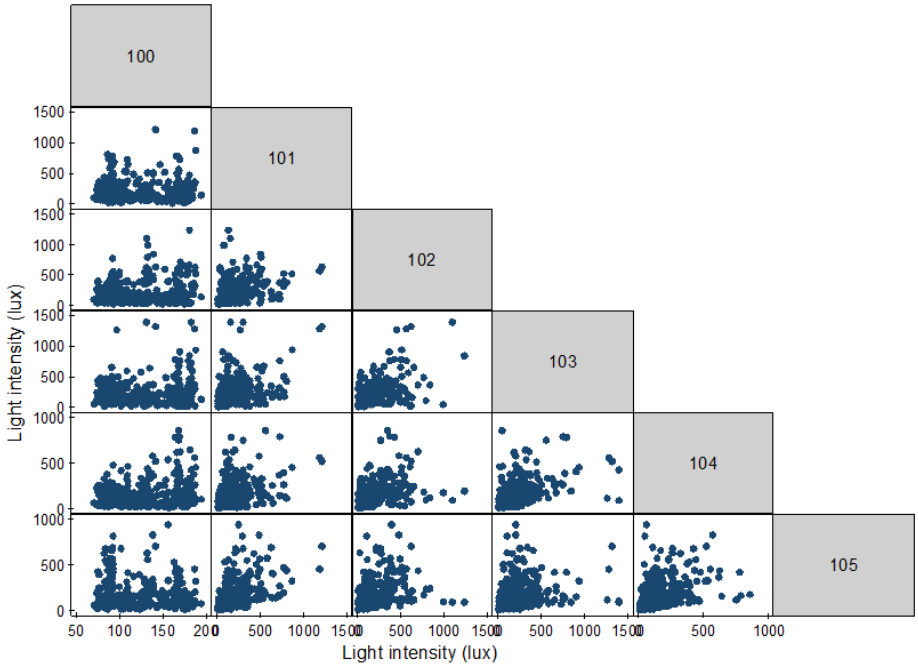

Figure 80. Correlation matrix for daily average light intensity across lower level nurse station and patient rooms.

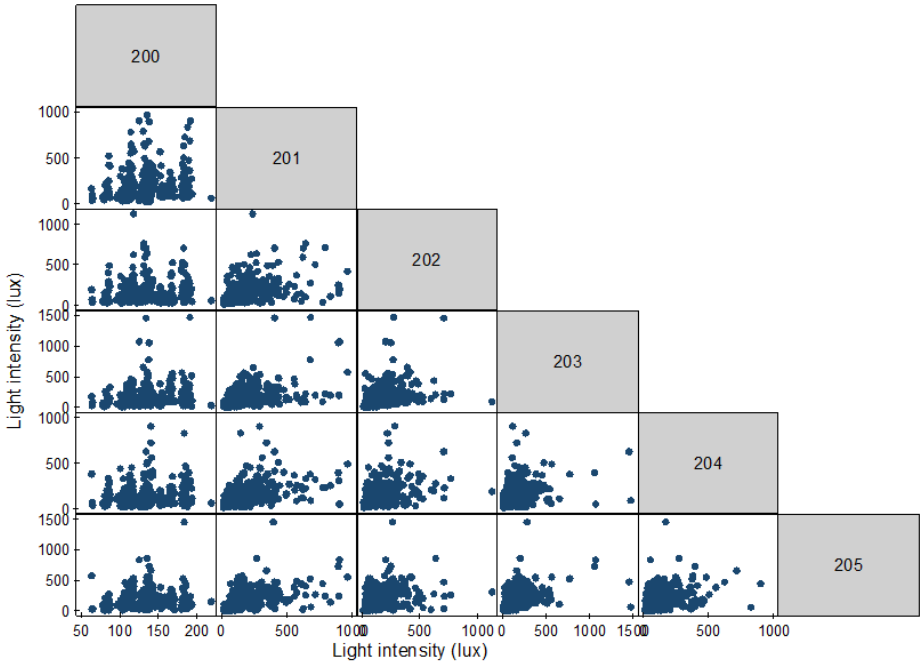

Figure 81. Correlation matrix for daily average light intensity across upper level nurse station and patient rooms.

Correlation coefficients across all patient rooms and nurse stations shown in Figure 79 and listed in Table 17 show a wide variation, both within floors and between floors. Between rooms of the lower floor, correlation coefficients are as low as 0.214 and has high as 0.534. Between rooms on the upper floor, factors are as low as 0.270 and as high as 0.478. Nurse stations on both floors correlate poorly, both with other rooms and the opposite nurse station. Interestingly, the highest correlations between nurse stations and others are between the upper level nurse station and a couple of rooms on the lower floor, with a factor of 0.238 between nurse station 200 and room 105. This is unexpected given the differences in light exposure in those two spaces. Uncertainty in light measurements was not explored because the manufacturer did not report sensor accuracy.

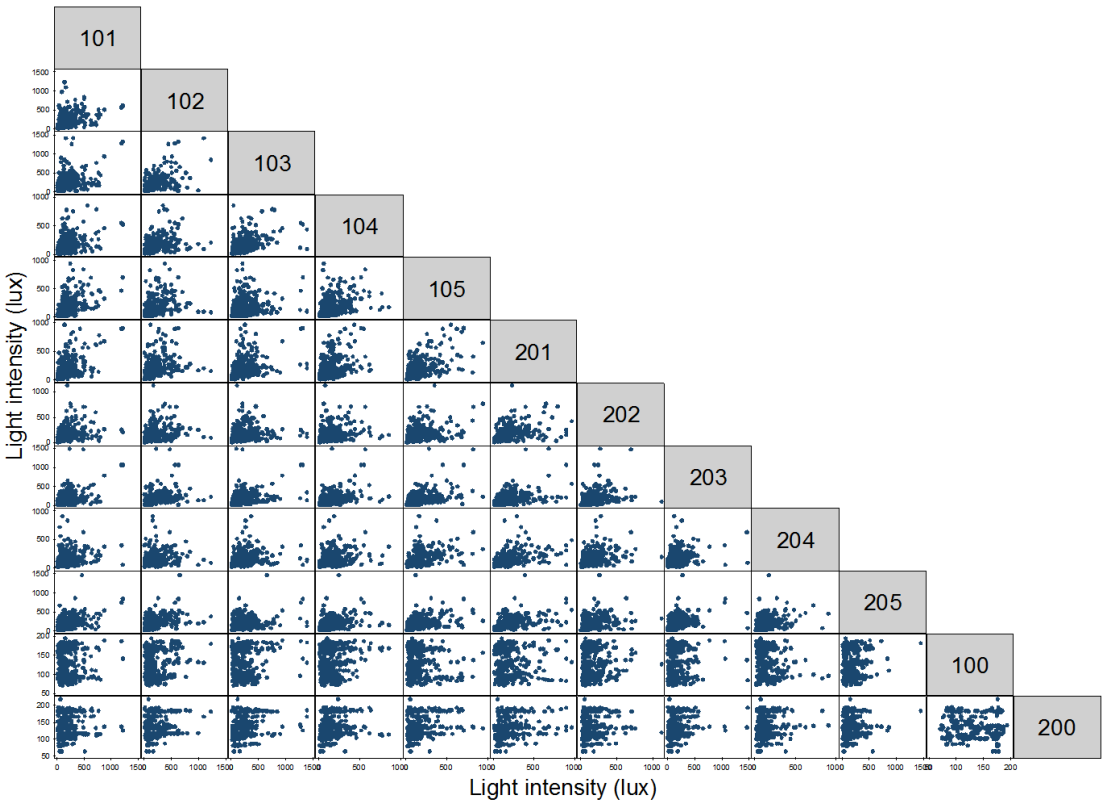

Figure 82. Correlation matrix for daily average light intensity across all patient rooms and nurse stations.

Table 17. Correlation matrix for daily average light intensity across all patient rooms and nurse stations.

	101	102	103	104	105	201	202	203	204	205	100	200
101	1											
102	0.403 ***	1										
103	0.450 ***	0.505 ***	1									
104	0.386 ***	0.349 ***	0.443 ***	1								
105	0.534 ***	0.287 ***	0.214 ***	0.462 ***	1							
201	0.527 ***	0.305 ***	0.370 ***	0.419 ***	0.515 ***	1						
202	0.236 ***	0.227 ***	0.138 *	0.249 ***	0.303 ***	0.359 ***	1					
203	0.390 ***	0.310 ***	0.388 ***	0.476 ***	0.474 ***	0.478 ***	0.309 ***	1				
204	0.255 ***	0.156 *	0.252 ***	0.302 ***	0.417 ***	0.386 ***	0.329 ***	0.297 ***	1			
205	0.443 ***	0.427 ***	0.343 ***	0.368 ***	0.406 ***	0.443 ***	0.270 ***	0.359 ***	0.339 ***	1		
100	-0.109	0.0467	0.0175	0.111	-0.136 *	-0.0745	-0.0220	-0.0329	-0.123 *	0.0690	1	
200	0.151 *	0.231 ***	0.209 ***	0.132 *	0.238 ***	0.157 *	0.0912	0.189 **	0.157 *	0.0462	-0.106	1
p<0.05 *	p<0.01 **	p<0.001 ***										

4.5.5 IR beam-break at patient room doorways. The correlation matrices for daily total IR beam-break in Figure 83 and Figure 84 show little correlation between rooms on the same floor.

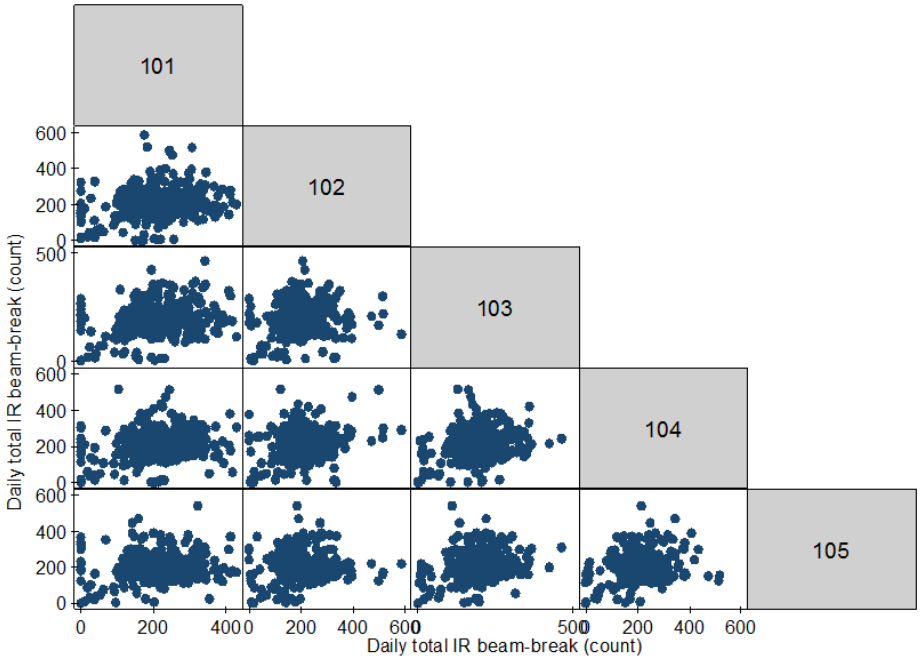

Figure 83. Correlation matrix for daily total IR beam-break across lower level patient rooms.

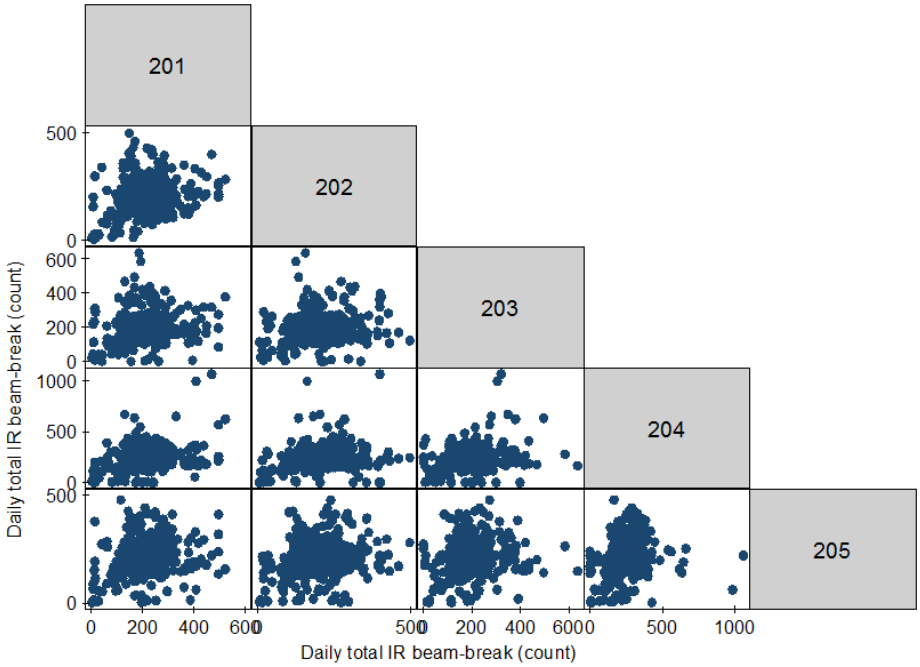

Figure 84. Correlation matrix for daily total IR beam-break across upper level patient rooms.

Figure 85 and Table 17 show that there is indeed little correlation between daily total IR beam breaks among individual rooms, albeit slightly more so within floors than between floors. On the first floor, correlation coefficients range from as low as 0.096 to as high as 0.275. On the second floor, the correlation coefficients range from 0.173 to 0.344. Between floors, correlation coefficients vary more widely, between 0.0195 to 0.242. Uncertainty in IR beam break measurements was not explored because the nature of the measurement did not allow for direct comparisons.

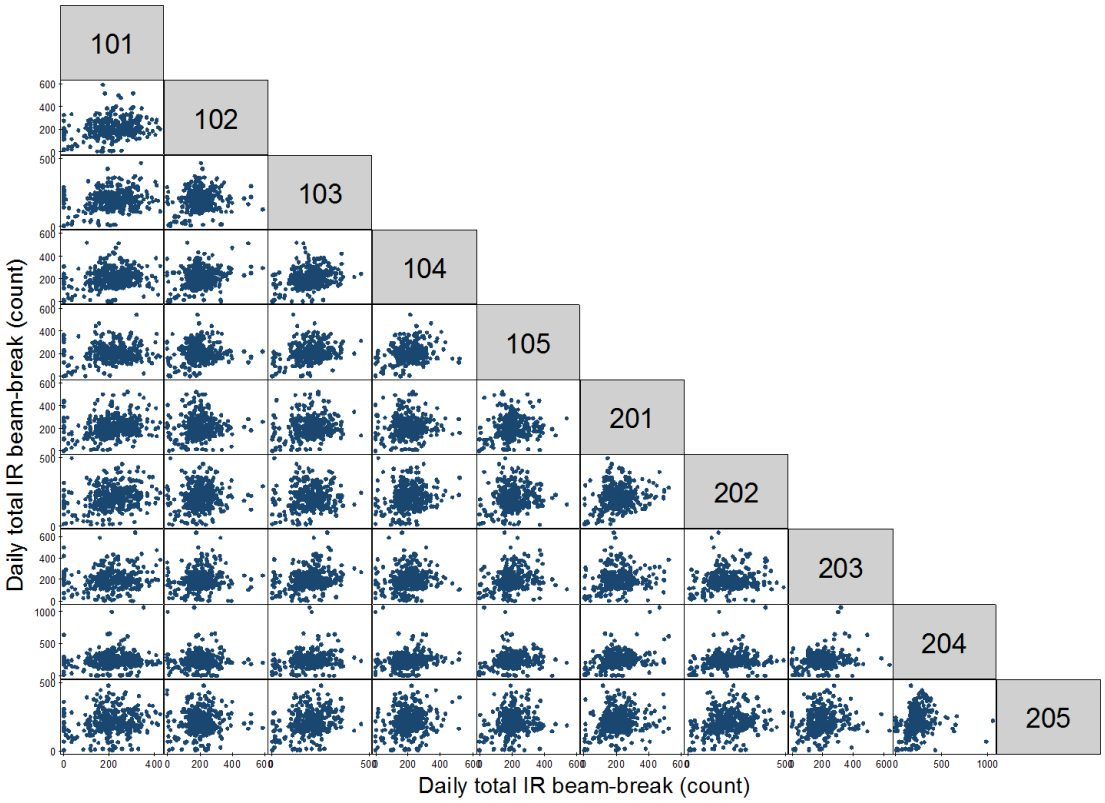

Figure 85. Correlation matrix for daily total IR beam-break across all patient rooms and nurse stations.

Table 18. Correlation matrix for daily total IR beam-break across all patient rooms and nurse stations.

	101	102	103	104	105	201	202	203	204	205
101	1									
102	0.229 ***	1								
103	0.216 ***	0.144 **	1							
104	0.184 ***	0.264 ***	0.289 ***	1						
105	0.113 *	0.0965	0.257 ***	0.275 ***	1					
201	0.162 **	0.0448	0.153 **	0.0195	0.0958	1				
202	0.223 ***	0.129 *	0.0997	0.166 **	0.114 *	0.243 ***	1			
203	0.123 *	0.116 *	0.242 ***	0.0669	0.175 **	0.173 **	0.166 **	1		
204	0.104	0.0239	0.168 **	0.0904	0.0738	0.344 ***	0.194 ***	0.229 ***	1	
205	0.123 *	0.0855	0.239 ***	0.203 ***	0.147 **	0.192 ***	0.237 ***	0.174 **	0.213 ***	1
p<0.05 *	p<0.01 **	p<0.001 ***								

Overall, there is very weak correlation between daily total IR beam-breaks in individual rooms, suggesting that the patient rooms were highly variable in terms of human occupancy and activity.

4.5.6 CO_2 concentrations in patient rooms. Figure 86 and Figure 87 show correlations of CO_2 between patient rooms on each floor, accounting for total CO_2 measured in each patient room. This includes sources from both the HVAC system and within-room sources. The figures show moderate correlation between rooms and Figure 88 shows this same correlation in rooms between floors.

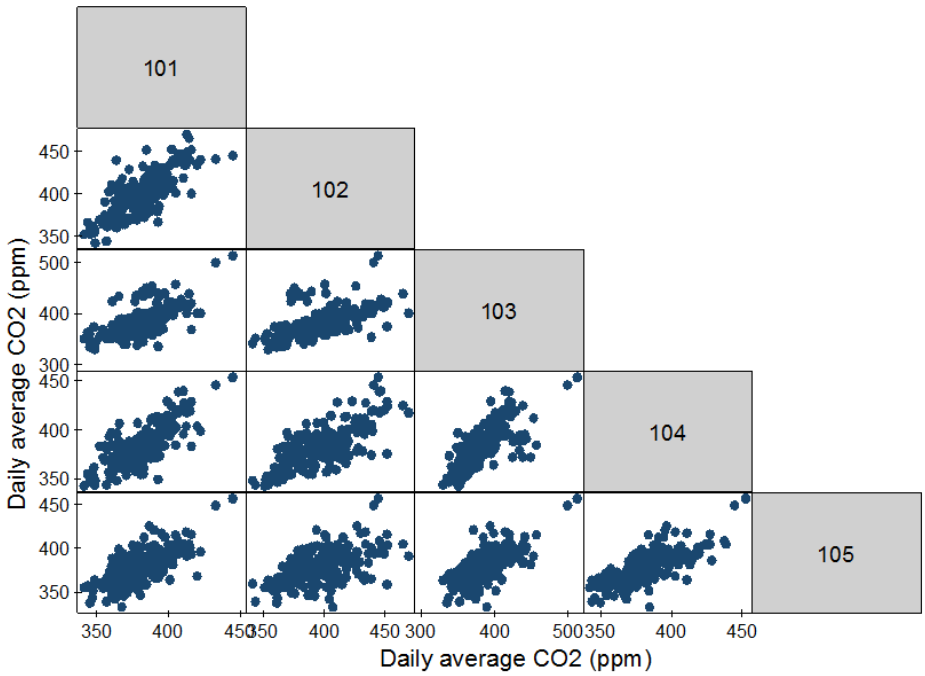

Figure 86. Correlation matrix for daily average CO_2 across lower level patient rooms.

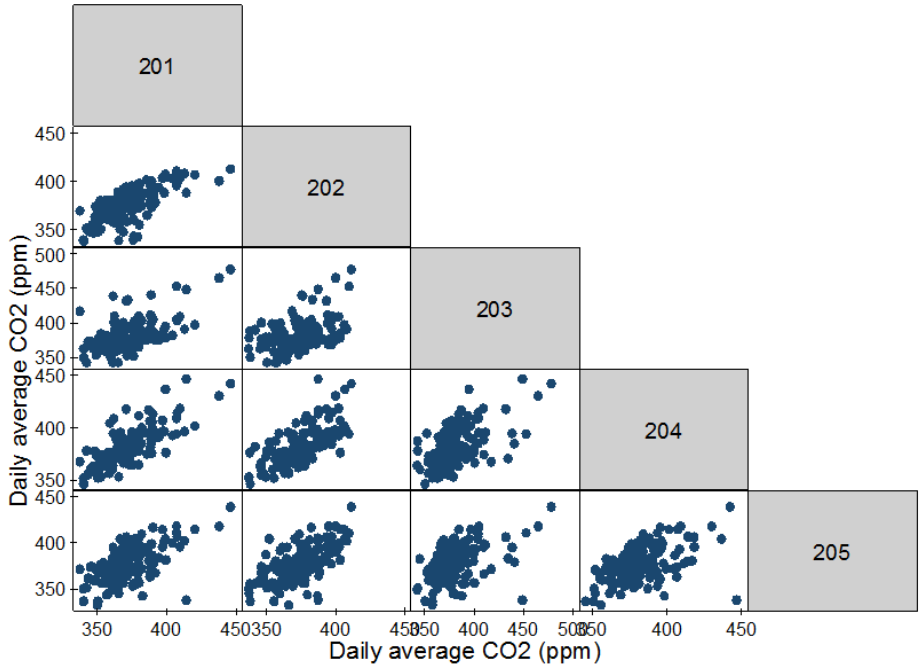

Figure 87. Correlation matrix for daily average CO_2 across upper level patient rooms

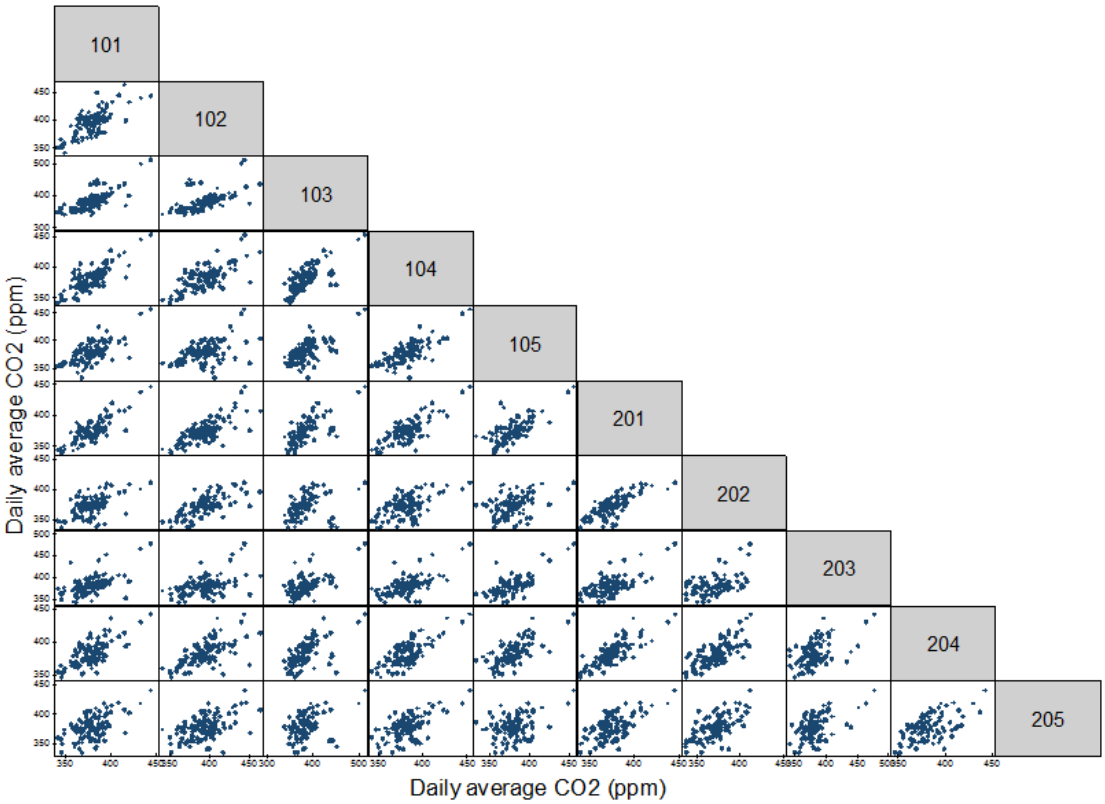

Figure 88. Correlation matrix for daily average CO_2 across all patient rooms

Table 19 confirms a moderate correlation between rooms, with similar correlations between floors as well as within floors. Although each floor is served by a separate AHU, the two AHUs perform similarly and correlate strongly, explaining the similar correlations between floors. The highest correlation exists between rooms 101 and 201 with a correlation coefficient of 0.805 and the lowest correlation coefficient is 0.331 between rooms 103 and 202. These capture combined impacts of ventilation system operation and human occupancy.

Table 19. Correlation matrix for daily average CO2 across all patient rooms and nurse stations.

	101	102	103	104	105	201	202	203	204	205
101	1									
102	0.727***	1								
103	0.726***	0.570***	1							
104	0.766***	0.680***	0.710***	1						
105	0.650***	0.473***	0.649***	0.739***	1					
201	0.805***	0.754***	0.701***	0.783***	0.695***	1				
202	0.549***	0.725***	0.331***	0.562***	0.408***	0.768***	1			
203	0.593***	0.480***	0.603***	0.612***	0.704***	0.657***	0.457***	1		
204	0.683***	0.634***	0.602***	0.764***	0.701***	0.814***	0.721***	0.520***	1	
205	0.558***	0.531***	0.337***	0.591***	0.388***	0.625***	0.636***	0.544***	0.527***	1
p<0.05	p<0.01	p<0.001								
*	**	***								

Table 20 shows the fraction of those measured CO_2 differences in the correlations above that fell within the range of uncertainty, considering sensor uncertainty reported by the manufacturer (20 ppm) and data logger uncertainty (2 mV ± 2.5% absolute reading). By considering the higher range of raw CO_2 values, approximately 700 ppm, a maximum data logger uncertainty value of 20 ppm was estimated and the combined uncertainty was calculated taking the two values in quadrature (± 28.28 ppm). The final range of uncertainty, 40 ppm, was calculated by taking the combined value in quadrature (for two sensors). About 93% of all measured CO_2 differences were found to be within this range of propagated uncertainty, with individual room comparisons ranging from 75.9% to 99.6%. This suggests that correlations may be considered higher than those stated above because of high uncertainty in the CO_2 measurements.

Table 20. Fraction of measured differences in daily mean CO2 concentrations between rooms that were within the range of propagated uncertainty

	101	102	103	104	105	201	202	203	204	205
101										
102	0.940									
103	0.919	0.869								
104	0.993	0.943	0.933							
105	0.988	0.759	0.916	0.925						
201	0.996	0.911	0.941	0.977	0.913					
202	0.974	0.891	0.918	0.962	0.910	0.984				
203	0.940	0.849	0.911	0.896	0.850	0.903	0.904			
204	0.983	0.953	0.904	0.955	0.879	0.944	0.972	0.946		
205	0.988	0.858	0.896	0.970	0.941	0.996	0.991	0.900	0.979	

In order to explore within-room sources of CO_2 (i.e., people), the supply air CO_2 concentration from each floor's AHU was subtracted from the CO_2 concentration measured within each patient room. Figure 89 and Figure 90 show very little correlation in this parameter between rooms on each floor.

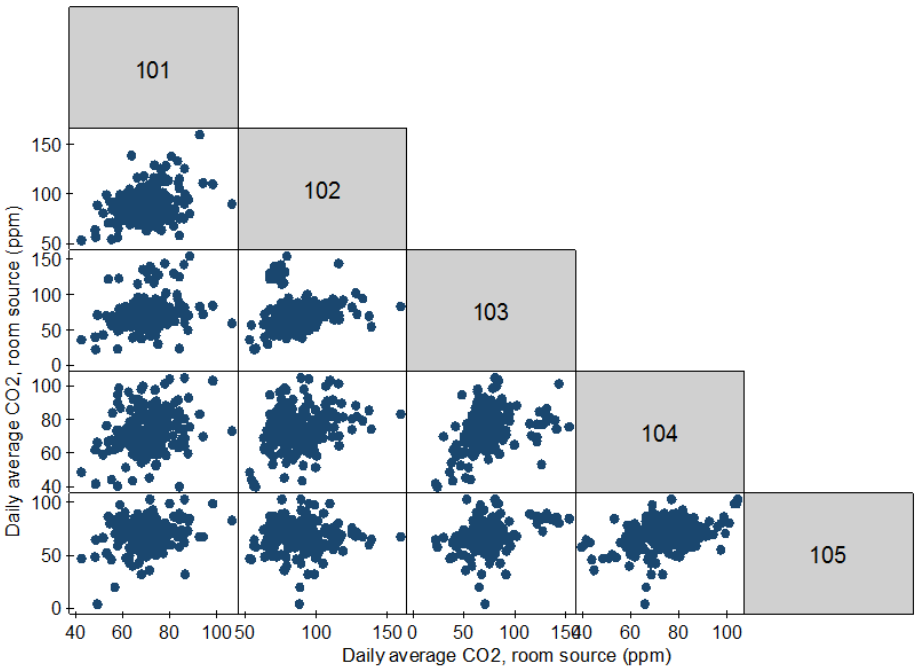

Figure 89. Correlation matrix for daily average CO_2 minus supply air CO_2 (limited to occupant-generated CO_2) across lower level patient rooms

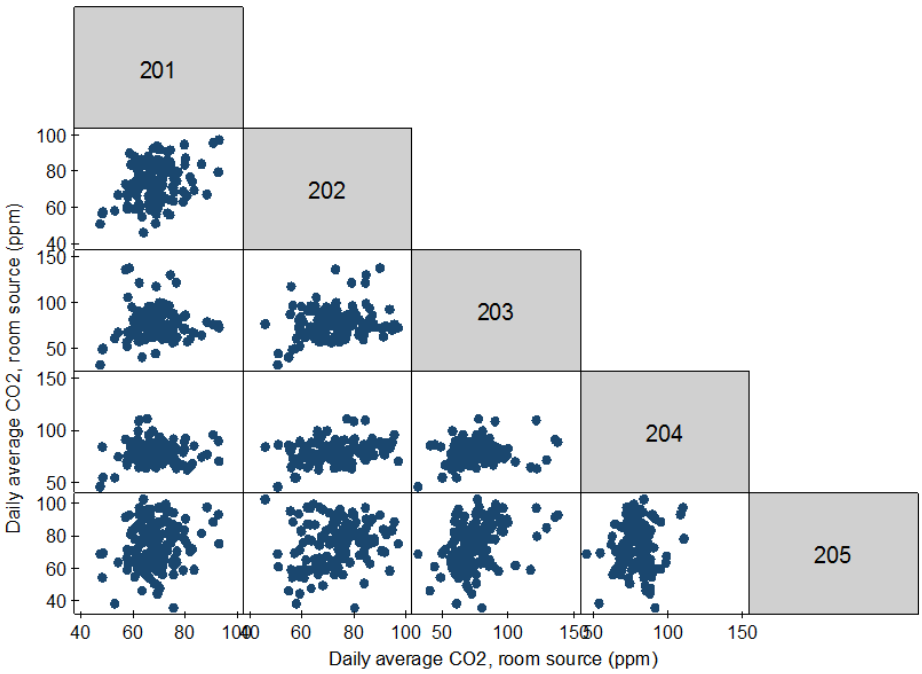

Figure 90. Correlation matrix for daily average CO_2 minus supply air CO_2 (limited to occupant-generated CO_2) across upper level patient rooms

Figure 91 continues to show a lack of correlation between all rooms and Table 21 largely confirms this. However, several rooms show moderate correlation as high as 0.524 between rooms 202 and 202 and 0.480 between rooms 105 and 204. Unfortunately these are not the same rooms with high correlation coefficients for daily IR beam breaks, suggesting that the difference may not be attributed to occupancy alone but perhaps uncertainty in the CO_2 measurements themselves.

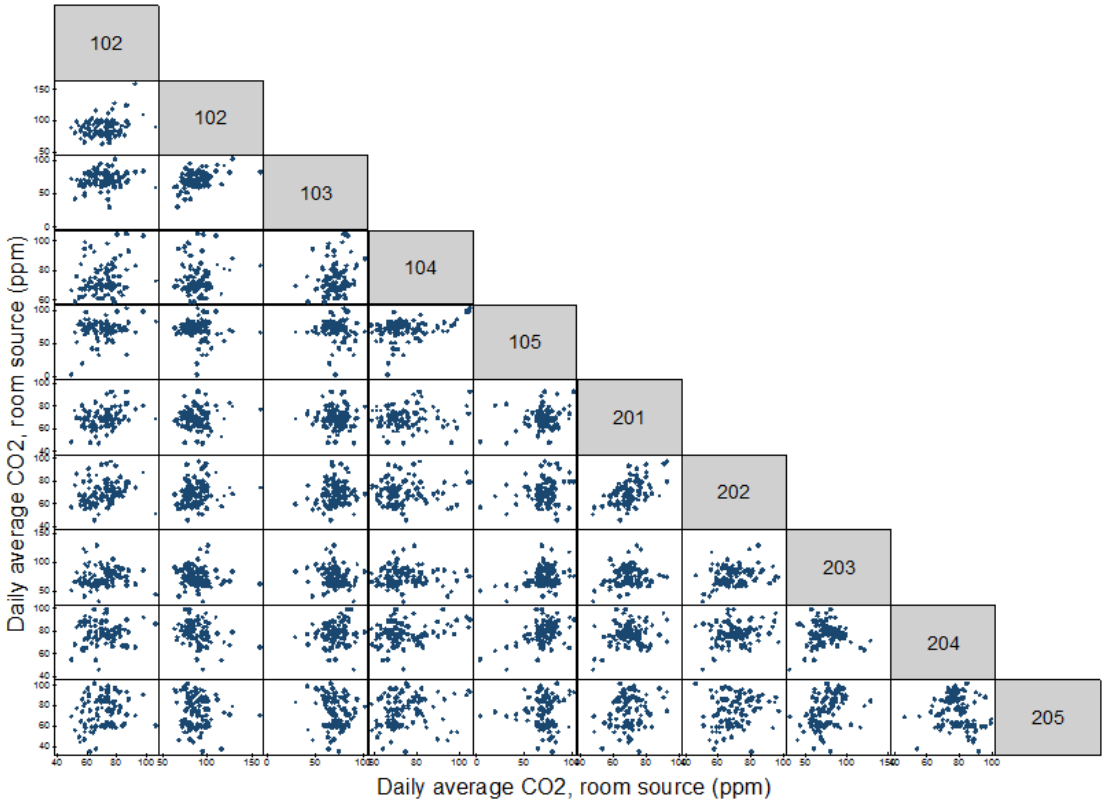

Figure 91. Correlation matrix for daily average CO_2 minus supply air CO_2 (limited to occupant-generated CO_2) across all patient rooms

Table 21. Correlation matrix for daily average CO_2 minus supply air CO_2 (limited to occupant-generated CO_2) across all patient rooms and nurse stations

	101	102	103	104	105	201	202	203	204	205
101	1									
102	0.279**	1								
103	0.115	0.242*	1							
104	0.231*	0.0968	0.103	1						
105	0.183	-0.125	-0.0632	0.335***	1					
201	0.280**	0.103	0.0358	0.0948	0.254*	1				
202	0.234*	0.180	0.237*	0.0633	0.169	0.524***	1			
203	0.0436	-0.138	-0.122	0.0217	0.379***	0.218*	0.212*	1		
204	0.0788	-0.289**	0.116	0.241*	0.480***	0.225*	0.215*	-0.00875	1	
205	0.232*	-0.128	-0.0713	0.187	0.0663	0.209*	0.200*	0.391***	-0.0913	1
p<0.05	p<0.01	p<0.001								
*	**	***								

Table 22 shows the fraction of those measured room-source CO_2 differences in the correlations above that fell within the range of propagated uncertainty, as described previously. An average of 89.4% of all measured differences in daily average room source CO_2 between rooms were found to be within the range of propagated uncertainty, with individual room comparisons ranging from 75.9% to 99.6%. Between rooms on the same floor, 95% of measured differences were within the range of uncertainty. This again suggests actual correlations may be much higher than those stated above due to high instrument uncertainty.

Table 22. Fraction of measured differences in daily mean CO2 concentrations (room source) between rooms that were within the range of propagated instrument uncertainty

	101	102	103	104	105	201	202	203	204	205
101										
102	0.940									
103	0.915	0.865								
104	0.993	0.943	0.929							
105	0.984	0.755	0.907	0.921						
201	0.967	0.801	0.933	0.878	0.848					
202	0.929	0.850	0.905	0.935	0.897	0.988				
203	0.898	0.747	0.837	0.799	0.786	0.903	0.900			
204	0.904	0.815	0.838	0.814	0.786	0.940	0.972	0.946		
205	0.930	0.810	0.877	0.906	0.900	0.996	0.987	0.900	0.979	

4.6 Variations between floors

To further our analysis we compared measurements between floors for all parameters (Figure 92). Air temperature was slightly higher on the upper floor, with both

a higher range of temperatures and a higher median. Absolute humidity had a higher range on the lower floor and a slightly lower median value compared to the upper floor. The difference is intuitive given the effect from the HVAC systems and the fact that the two floors are served by different AHUs that have already been shown to operate at different OA fractions during some outdoor climate conditions. Light intensity between floors was found to be very similar, with the lower floor showing a slightly higher range. Differences are expected to be minimal given that the rooms are all facing the same direction (west-facing) and have similar elevations. Hourly IR beam-break and CO_2 concentrations were very similar between floors, indicating occupancy and activity between floors to be very similar (although within-room differences have already been shown to be large). Lastly, OA fraction on the lower floor, served by AHU 11, covered a much wider range and a slightly lower median than the upper floor, which is served by AHU 6. These values are expected given the difference in minimum OA fractions between the two AHUs, 61.25% and 75%, for AHU 11 and AHU 6 respectively.

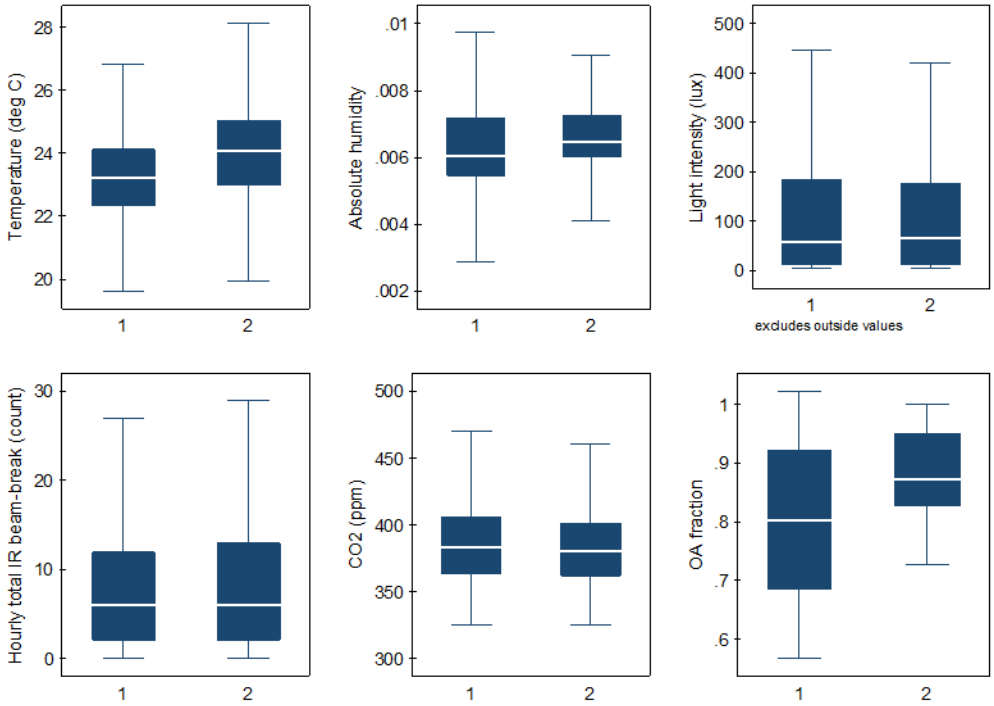

Figure 92. Variations between floors for temperature, RH, absolute humidity, light intensity, CO_2 and OA fraction; lower floor is denoted by 1, upper floor by 2.

4.7 Within day differences (i.e. night and day)

A similar analysis was done comparing measurements across all rooms between night and day, with night defined as 7:00pm to 6:59am and day defined as 7:00am to 6:59pm. Figure 93 shows the variation between floors for temperature, absolute humidity, light intensity, IR beam-break counts, CO_2 concentrations and OA fractions. Temperature and absolute humidity did not differ between night and day. As expected, light intensity had a much higher range and median during the day compared to night. Hourly total IR beam-break and CO_2 concentrations were both higher during the day, compared to night, suggesting intuitively that human occupancy patterns were much more pronounced during the day. Finally, OA fractions covered the same range between

night and day, but median OA fractions during the night were slightly higher than those during the day. This is expected as our analysis showed that warmer temperatures, as occur during the day, result in lower OA fractions, while moderate temperatures, as occur during the night, result in higher OA fractions.

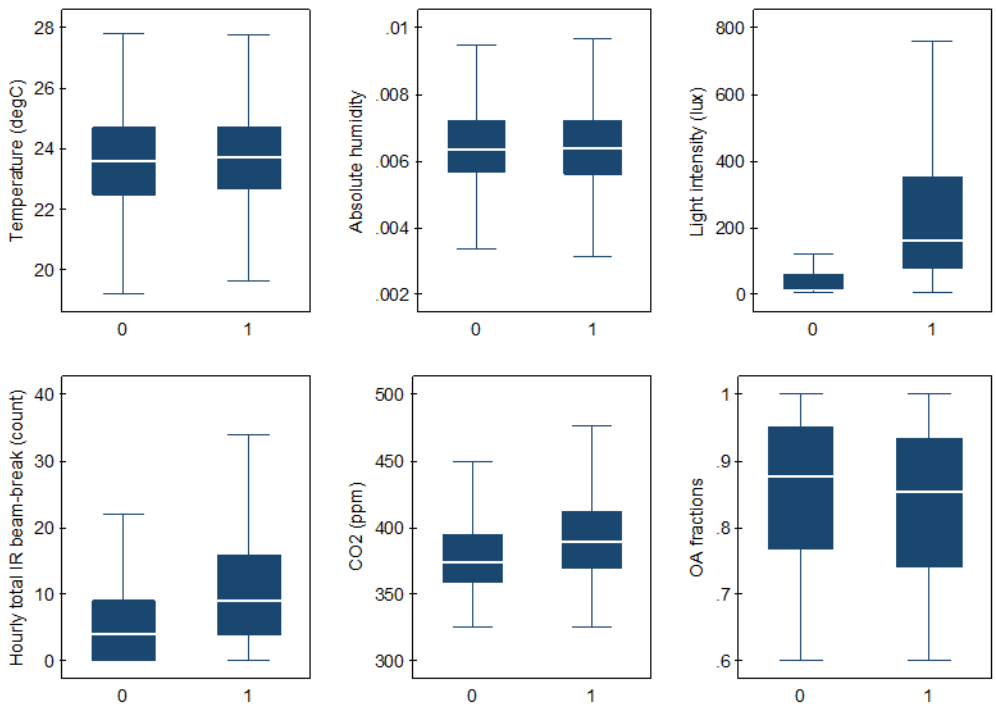

Figure 93. Variations between night and day for temperature, absolute humidity, light intensity, IR beam-break, CO2 and OA fractions; night is denoted by 0 and daytime is denoted by 1.

4.8 Monthly and seasonal variations within and between rooms

Finally, we analyzed monthly and seasonal variations in rooms and nurse stations to characterize changes over time as well as differences between rooms and nurse stations. Seasons were defined as the periods January – March, April – June, July –

September and October – December. Months were defined from the 1st to the last day of each month.

4.8.1 Temperature. As seen previously, little variation exists in temperature between rooms and between floors overall. Figure 94 shows variation between rooms and nurse stations over the four seasons. Here we see that the first season has much more variability, which we expect to see after viewing the wider range of temperatures seen prior to the hospital opening, attributed to system testing within the hospital. For the remaining seasons, we see slightly higher temperatures in upper floor rooms compared to lower floors, a difference of approximately 1°C in median temperatures. Additionally, nurse stations denoted by 100 and 200 consistently have a lower range of temperatures, with the upper floor nurse station consistently at slightly higher temperature than the lower floor.

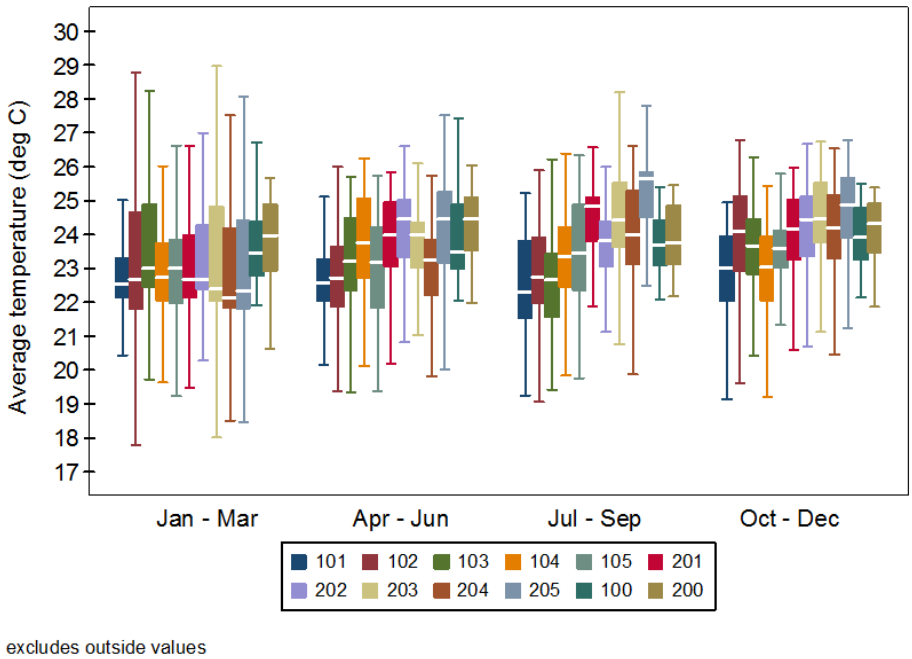

Figure 94. Seasonal average temperatures over all rooms and nurse stations.

4.8.2 Relative humidity. Indoor relative humidity changed distinctly over seasons. In the first season, RH covers a wider range and has a higher median in upper floor rooms than lower floor, with nurse station RH similar to the rooms on the same floor. In the remaining seasons, the floors become more similar, covering a wider range in the second season, and with smaller ranges and higher medians in the summer months. The final season shows a similar range to those values in the first season, but more similarity across floors.

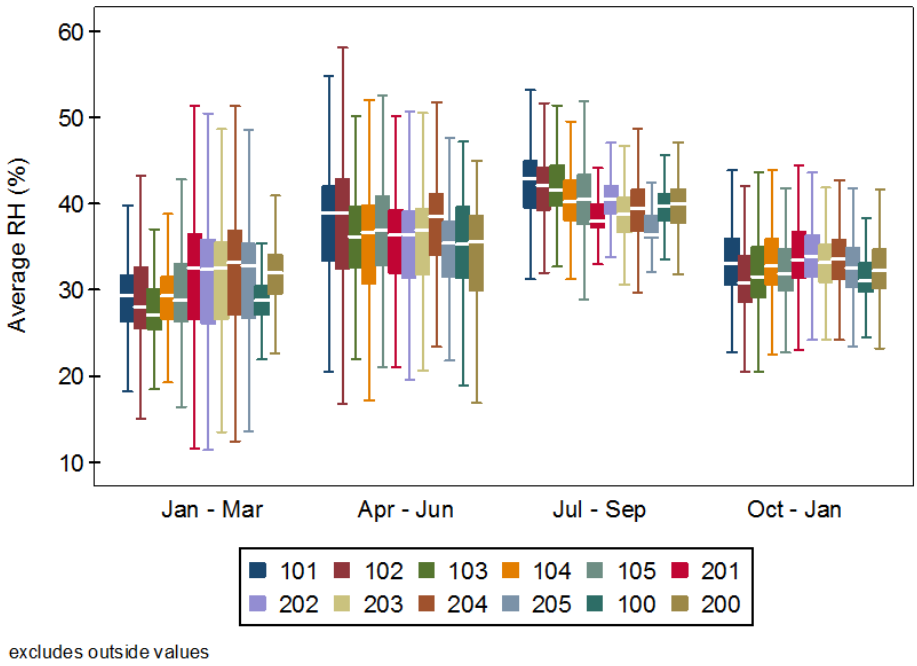

Figure 95. Seasonal average RH over all rooms and nurse stations.

4.8.3 Absolute humidity. Seasonal absolute humidity shows more distinct patterns across seasons and between floors. In the first season (Jan – Mar), rooms on the upper floor cover a much larger range as compared to those on the lower floor. Rooms and nurse stations on the same floor have cover similar ranges and have similar medians. In the second season (Apr – Jun), differences between floors are less distinct, but rooms across the same floors continue to be very similar, all covering a wide range. During the summer months of July through September, absolute humidity covers a much tighter range around 0.007 kg_w/kg_{da}, indicating high control during these summer months. In the last season, absolute humidity covers a wider range, with strong similarities between rooms on each floor, and slightly higher values on the upper floor. To take a closer look at these patterns, monthly averages were also plotted for all rooms and nurse stations (Figure 97).

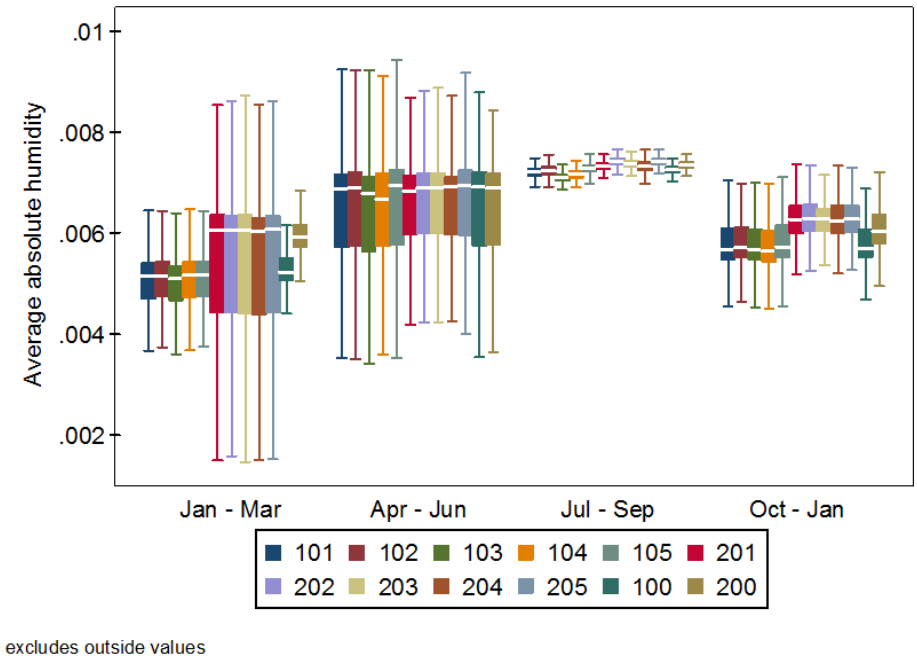

Figure 96. Seasonal averages absolute humidity over all rooms and nurse stations.

Distinct differences exist over monthly averages, with the tightest control during summer months (June – September) and winter months (November – January) where values have little variation. In contrast, the months of May and October cover a wider range, indicating less central humidity control. February also covers a large range, with values lower than other months, but this is likely explained by the large fluctuations in temperature and RH prior to the hospital's opening in late February.

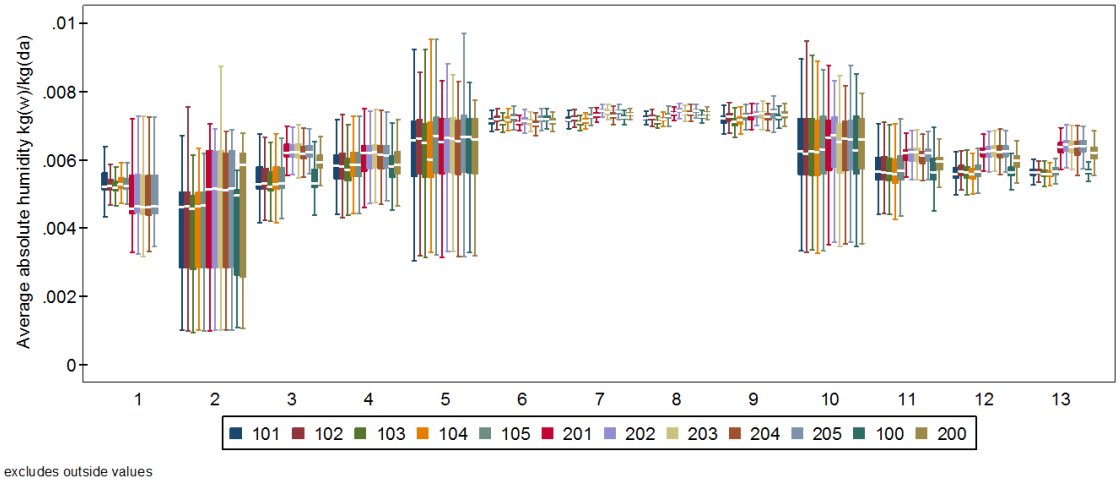

Figure 97. Monthly average absolute humidity over all rooms and nurse stations; each consecutive number denotes consecutive months beginning January 2013.

4.8.4 Light intensity. Light intensity levels also exhibit seasonal differences, with highest values during summer months and lowest during winter months. Monthly averages (Figure 99) show distinct differences between spring/summer months and fall/winter months, with much higher ranges during spring/summer months.

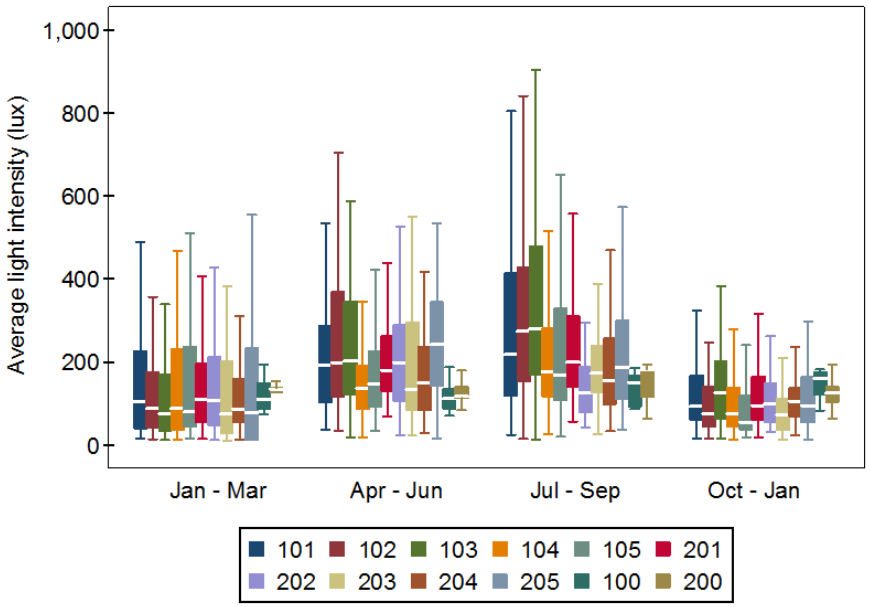

Figure 98. Seasonal average light intensity over all rooms and nurse stations.

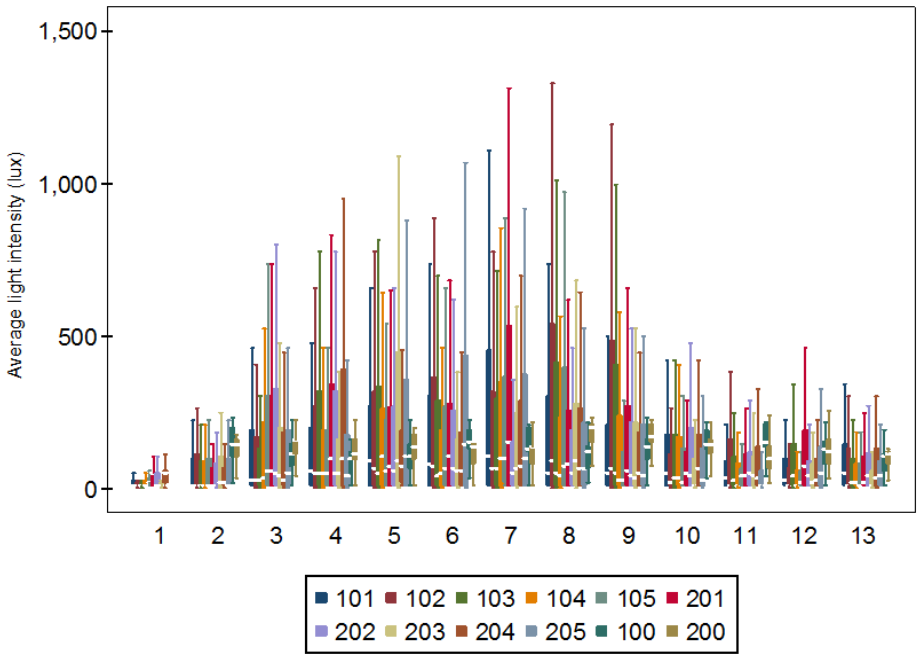

Figure 99. Monthly average light intensity over all rooms and nurse stations; each consecutive number denotes consecutive months beginning January 2013.

4.8.5 IR beam-break. Figure 100 shows seasonal averages over all rooms. No significant differences in IR beam-break frequency were found over seasons as well as between rooms.

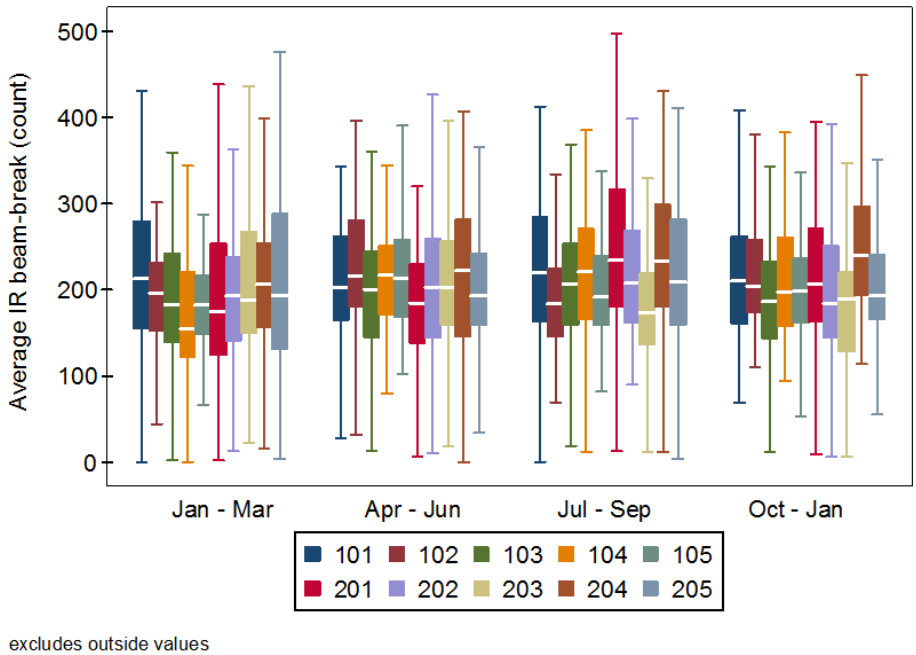

Figure 100. Seasonal average daily IR beam-break over all rooms.

4.8.6 CO_2 concentrations. We compared seasonal average CO_2 concentrations, beginning with April 2013. Due to sensor issues in the first month of sampling, data in the first season is incomplete. Seasonal average CO_2 concentration in patient rooms (Figure 101) also showed no distinct differences between seasons.

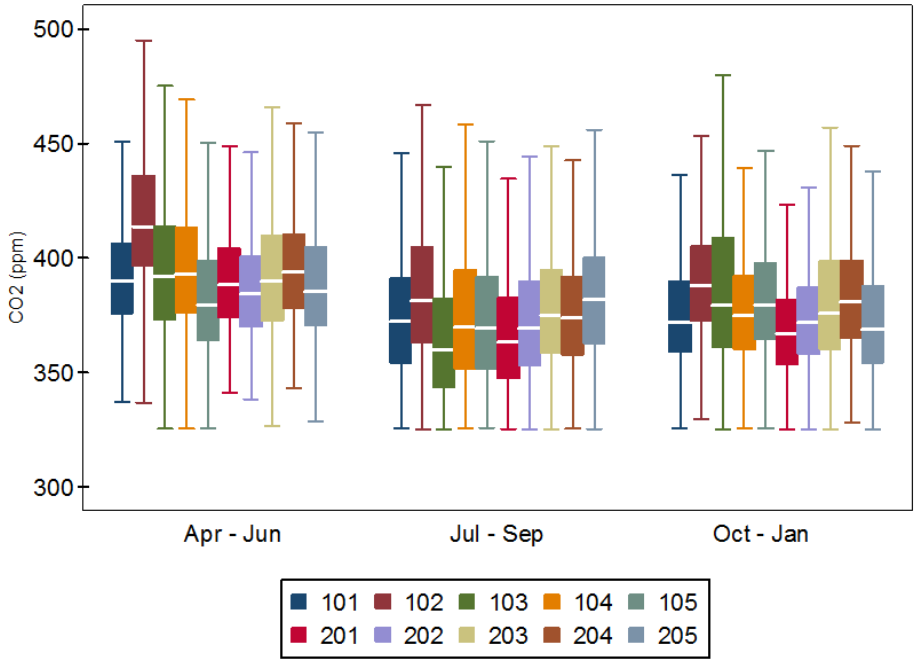

Figure 101. Seasonal average CO_2 concentrations over all rooms.

CHAPTER 5

DISCUSSION

5.1 Interpretation of results

Overall, we were successful in the collection of more than 8 million data points covering a range of building environmental and operational parameters that may have had some effect on the growth, survival, or progression of microbes within the hospital. Within-room, between-room, and seasonal variations in individual parameters revealed interesting patterns throughout the project. For example, patient room and nurse station air temperatures varied more than expected for such a typically tightly controlled environment. Although temperature settings within rooms are surely kept within a specific range of comfort, effects from occupant control likely contributed to the range and variation within patient rooms. RH and absolute humidity were highly correlated between patient rooms, indicating a strong effect from the HVAC system and little effect from occupants. The time-series data indicate that humidity is tightly controlled during summer and winter months when the weather is most extreme in Chicago. Between those seasons, humidity varies widely, indicating a lack of central control during transition months.

Light intensity levels were not found to be different between rooms and floors, which was expected given that all rooms are facing the same direction (west-facing) and received similar solar exposure. While occupants have control of artificial light within patient rooms, these levels are low compared to natural light levels. Occupant control over window shades is more likely to have a greater effect on measured light levels, as this limits the amount of natural light within patient rooms.

To measure occupancy, we used IR beam-break people counters alongside CO_2 concentrations. It could be reasonably assumed that two beam-break counts were the result of one person entering and exiting the room, but this alone gave us little information on the length of occupancy or the number of occupants within the room at any given time. CO_2 concentrations measured within each patient room supplemented data from people counters, as an additional indicator of occupancy. CO_2 was found to correlate well with IR beam-break counts at times, but not consistently.

OA fractions were successfully calculated using CO_2 concentrations measured in the outdoor air intake, recirculation air, and supply air of the HVAC systems serving the sample rooms. The data were subject to substantial noise due primarily to very low changes in CO_2 concentrations in each airstream because of the very large volumes of air being handled relative to the number of occupants throughout the hospital. However, averages taken over specified temperature groups revealed a clearer pattern in OA fractions and correlations with temperature that were also confirmed by periodic collection of data from the building automation system controlled by hospital facilities.

Many of these parameters are expected to influence microbial community results stemming from weekly sampling in all rooms and daily sampling in two rooms. Human occupancy, environmental conditions (including T/RH, absolute humidity, and light intensity), and HVAC characteristics (particularly OA fractions) can all influence microbial community survival and growth as described in the literature review. These built environment metadata will be supplied to the microbiology team to compare daily, weekly, monthly, and seasonal differences in absolute values of the parameters measured herein, as well as differences between rooms and floors.

5.2 Meaning for other building science characterization studies

While there have been many methods for characterizing building science factors that may affect microbial growth in other indoor microbial community explorations, there is currently no robust, standardized set of methodologies or time scales with which to measure built environment metadata. This work attempted to explore a systematic way to gather potentially valuable building environmental data with minimal costs, but at very high temporal and spatial resolution within the hospital. Using a suite of off-the-shelf sensors, we were able to measure multiple parameters continuously at 5-minute intervals over the span of a year, providing millions of built environment data points for future comparison. In doing so, we can provide a detailed context for the study of microbial growth within the hospital and inform future studies characterizing building science parameters.

5.3 Practical cost and reliability constraints

The use of off-the-shelf sensors to measure temperature, RH, and light with built-in data logging capabilities allowed for lost cost and low maintenance throughout the project. The people counters, by using uni-directional rather than bi-directional functionality, allowed for lower costs but gave a less accurate measure of occupancy. CO_2 sensors were useful in supplementing the people counters to measure occupancy, but had much higher costs and higher maintenance due to additional components such as an absorber column and sampling lines. These often required maintenance every several weeks to ensure proper functioning of the sensor. Additionally, their relatively high power requirements meant we were limited to sampling where electrical power was

available. Finally, differential pressure sensors used were relatively low cost (although more than the T/RH/light sensors), but also required an external data logging device and large battery packs and external sampling lines. Overall, while this suite of measurements and methods provided a large robust dataset, additional development of lower cost sensors using common data collection platforms and remote uploading to the internet should be prioritized in future investigations.

5.4 Data exclusions

The amount of data that had to be excluded varied by sensor. For temperature, RH, and light, very few data points were dropped, including data points collected 15 minutes before and 15 minutes after collecting data and relaunching. This involved removing the data logger from its sampling location, so any data collected during that time was ignored. These sensors proved to be robust and accurate with long battery lives and large data storage capacity.

The same 15-minute before and after data exclusion process was performed for the IR beam-break people counters, CO_2 sensors, and differential pressure sensors, as these also involved interference with the sensors and data loggers during data collection. In addition to excluding data recorded during data collection, data was also excluded for a number of sensor displacement or malfunctions. IR beam-break sensors and differential pressure sensors were in a particularly vulnerable position at patient room doorways and sensors were found displaced on several occasions. Measures were taken to change adhesives holding IR beam-break sensors to doorframes to make them more secure, but prior to this, several periods of data were ignored due to displacement.

CO_2 sensors were located in a more secure location, under a cabinet space, but were still accessible to occupants. Occasionally, sensors and accompanying absorber column and tubes were found displaced, and data collected during those periods were ignored. Additionally, the first month of data collection proved to be somewhat of a testing period with issues arising concerning absorber columns and electrical connections resulting in data quality issues. Therefore, a large portion of the data from both patient rooms and mechanical rooms in the first month of sampling was excluded.

5.5 What would we have done differently?

The original design for data collection involved the installation of sensors with minimal visibility and accessibility to patient room occupants. This included the placement of sensors in the plenum spaces above ceilings at supply diffusers and return grilles, with electrical connections and tubing all located above ceiling. Issues arose with obtaining approval from the state public health department and such approval was not received in time for scheduled sampling to begin. While the initial plan would have allowed more secure placement of the sensors, the new design, with all sensors located within the rooms, allowed more accessibility, which proved to be valuable throughout the project.

Due to the project timeline and slow communication between parties, installation of sensors was done with very little time to conduct testing and calibration before the hospital's opening. Much of the first month of sampling occurred after the hospital opened, and much of that time was spent becoming familiarized with the sensors and

associated software. Consequently, much of the data at the beginning of the sampling period was suspect.

Other improvements would have included using directional beam break counters or other methods for assessing human occupancy, the installation of pressure taps to measure any changes in supply and return airflow rates over time, measurements of water activity on sample surfaces, and measurements of human proximity near sample surfaces.

CHAPTER 6

CONCLUSIONS

To conclude, this study reviewed the literature regarding important building environmental and operational parameters that may affect microbial abundance and diversity in indoor environments (e.g., temperature, relative humidity, light intensity, occupancy, outdoor air fraction, among others). We developed a study design to systematically collect robust data on these parameters with high temporal and spatial resolution within the hospital, providing more than 8 million data points for future comparison. The results of our analysis are summarized here:

- ***Variations within individual rooms.*** Air temperatures were found to vary widely over the course of the project, normally ranging from 19°C to 26°C, with occasional hourly averages as low as 17°C and as high as 31°C. Despite this variation, median values across all rooms and nurse stations were similar, between 23°C and 24°C. Relative and absolute humidity were similar across rooms and nurse stations, with RH ranging from 5% to 55% with a median around 35% and absolute humidity ratios ranging from 0.001 to 0.008 kg_w/kg_{da} with medians around 0.006 kg_w/kg_{da} in lower floor rooms and slightly higher in upper floor rooms. Daily average light intensity had a wide range between 0 and 500 lux consistently across patient rooms, and between 100 and 200 lux for nurse stations; medians across all rooms and nurse stations were approximately 150 lux. Total IR beam breaks varied highly within individual rooms from day to day.
- ***Variations between individual rooms.*** Interestingly, air temperatures showed little to no correlation between rooms and nurse stations. In contrast, relative and

absolute humidity were highly correlated between rooms and nurse stations. Light intensity was moderately correlated between rooms and nurse stations while IR beam break and CO_2 concentrations (room source) showed little correlation.

- ***Variations between floors.*** Temperature was found to be slightly higher on the upper floor compared to the lower floor. Relative and absolute humidity covered a wider range on the lower floor, with a slightly lower median value than the upper floor. There were very little differences in light intensity, IR beam-break and CO_2 between floors. OA fractions had wider range in the lower floor with a lower minimum value close to 60% compared to the upper floor's minimum of 75%, resulting in a slightly lower median value compared to the upper floor.
- ***Within day differences.*** There were no noticeable differences between night and day for temperature and relative or absolute humidity. In contrast, light intensity differed widely with significantly higher values during the day. IR beam-break and CO_2 were noticeably higher during the day, while OA fractions were slightly higher at night.
- ***Monthly and seasonal variations.*** Very small differences in temperature were observed between seasons. Relative and absolute humidity showed large seasonal differences, with very tight ranges in winter and summer months and slightly higher levels during summer months. Light intensity also showed a seasonal effect, with noticeably higher ranges in the months between March and September. Finally, IR beam-break and CO_2 concentrations showed no substantial differences between seasons.

Taken together, the measurements and results herein represent one of the largest field measurement campaigns to assess long-term built environment metadata in an investigation of the microbiology of an indoor environment, let alone a unique hospital environment. These results will be compared alongside results from microbial community analyses to explore how the built environment may have affected microbial abundance and diversity in this hospital.

BIBLIOGRAPHY

Adams, R. I., Miletto, M., Taylor, J. W., & Bruns, T. D. (2013). Dispersal in microbes: fungi in indoor air are dominated by outdoor air and show dispersal limitation at short distances. *The ISME Journal*, *7*(7), 1262–1273. doi:10.1038/ismej.2013.28

Amend, A. S., Seifert, K. A., Samson, R., & Bruns, T. D. (2010). Indoor fungal composition is geographically patterned and more diverse in temperate zones than in the tropics. *Proceedings of the National Academy of Sciences*, *107*(31), 13748–13753. doi:10.1073/pnas.1000454107

Anderson, R. N., & Smith, B. L. (2005). Deaths: leading causes for 2002. *National Vital Statistics Reports: From the Centers for Disease Control and Prevention, National Center for Health Statistics, National Vital Statistics System*, *53*(17), 1–89.

ASHRAE. (2013a). ASHRAE Handbook of Fundamentals: Chapter 1: Psychrometrics. American Society of Heating, Refrigerating and Air-Conditioning Engineers.

ASHRAE. (2013b). ASHRAE Handbook of Fundamentals: Chapter 36: Measurement and Instruments. American Society of Heating, Refrigerating and Air-Conditioning Engineers.

ASHRAE. (2013c). Standard 55: Thermal Environmental Conditions for Human Occupancy. American Society of Heating, Refrigerating and Air-Conditioning Engineers.

ASTM E 741. (2006). Standard Test Method for Determining Air Change in a Single Zone by Means of a Tracer Gas Dilution.

Aydogdu, H., Asan, A., & Tatman Otkun, M. (2009). Indoor and outdoor airborne bacteria in child day-care centers in Edirne City (Turkey), seasonal distribution and influence of meteorological factors. *Environmental Monitoring and Assessment*, *164*(1-4), 53–66. doi:10.1007/s10661-009-0874-0

Bartlett, K. H., Martinez, M., & Bert, J. (2004). Modeling of Occupant-Generated CO_2 Dynamics in Naturally Ventilated Classrooms. *Journal of Occupational and Environmental Hygiene*, *1*(3), 139–148. doi:10.1080/15459620490424393

Baughman, A. V., & Arens, E. A. (1996). Indoor humidity and human health - Part 1: Literature review of health effects of humidity-influenced indoor pollutants. *ASHRAE Transactions*, *102*(1), 193–211.

Blachere, F. M., Lindsley, W. G., Pearce, T. A., Anderson, S. E., Fisher, M., Khakoo, R., … Beezhold, D. H. (2009). Measurement of Airborne Influenza Virus in a Hospital Emergency Department. *Clinical Infectious Diseases*, *48*(4), 438–440. doi:10.1086/596478

Bluyssen, P. M., Cox, C., Seppänen, O., Oliveira Fernandes, E. de, Clausen, G., Müller, B., & Roulet, C.-A. (2003). Why, when and how do HVAC-systems pollute the indoor environment and what to do about it? the European AIRLESS project. *Building and Environment*, *38*(2), 209–225. doi:10.1016/S0360-1323(02)00058-6

Bruno, R., & Delmastro, F. (2003). Design and Analysis of a Bluetooth-Based Indoor Localization System. In M. Conti, S. Giordano, E. Gregori, & S. Olariu (Eds.), *Personal Wireless Communications* (Vol. 2775, pp. 711–725). Berlin, Heidelberg: Springer Berlin Heidelberg. Retrieved from http://www.springerlink.com/index/10.1007/978-3-540-39867-7_66

Cai, G.-H., Mälarstig, B., Kumlin, A., Johansson, I., Janson, C., & Norbäck, D. (2011). Fungal DNA and pet allergen levels in Swedish day care centers and associations with building characteristics. *Journal of Environmental Monitoring*, *13*(7), 2018. doi:10.1039/c0em00553c

Chen, T., Chen, T., & Chen, Z. (2006). An Intelligent People-Flow Counting Method for Passing Through a Gate (pp. 1–6). Presented at the IEEE Conference on Robotics, Automation and Mechatronics, IEEE. doi:10.1109/RAMECH.2006.252623

Cornaro, C., Paravicini, A., & Cimini, A. (2011). Monitoring Indoor Carbon Dioxide Concentration and Effectiveness of Natural Trickle Ventilation in a Middle School in Rome. *Indoor and Built Environment*, *22*(2), 445–455. doi:10.1177/1420326X11430099

Corsi, R. L., Kinney, K. A., & Levin, H. (2012). Microbiomes of built environments: 2011 symposium highlights and workgroup recommendations. *Indoor Air*, *22*(3), 171–172. doi:10.1111/j.1600-0668.2012.00782.x

Dodier, R. H., Henze, G. P., Tiller, D. K., & Guo, X. (2006). Building occupancy detection through sensor belief networks. *Energy and Buildings*, *38*(9), 1033–1043. doi:10.1016/j.enbuild.2005.12.001

Dong, B., & Andrews, B. (2009). Sensor-based occupancy behavioral pattern recognition for energy and comfort management in intelligent buildings (pp. 1444–1451). Presented at the Building Simuilation 2009. 11th International IBPSA Conference, Glasgow, Scotland.

Dunn, R. R., Fierer, N., Henley, J. B., Leff, J. W., & Menninger, H. L. (2013). Home Life: Factors Structuring the Bacterial Diversity Found within and between Homes. *PLoS ONE*, *8*(5), e64133. doi:10.1371/journal.pone.0064133

Eames, I., Tang, J. W., Li, Y., & Wilson, P. (2009). Airborne transmission of disease in hospitals. *Journal of The Royal Society Interface*, *6*(Suppl_6), S697–S702. doi:10.1098/rsif.2009.0407.focus

Erickson, V. L., Lin, Y., Kamthe, A., Brahme, R., Surana, A., Cerpa, A. E., … Narayanan, S. (2009). Energy efficient building environment control strategies using real-time occupancy measurements (pp. 19–24). Presented at the BuildSys 2009. The First ACM Workshop on Embedded Sensing Systems for Energy-Efficiency in Buildings, ACM Press. doi:10.1145/1810279.1810284

Fierer, N., Hamady, M., Lauber, C. L., & Knight, R. (2008). The influence of sex, handedness, and washing on the diversity of hand surface bacteria. *Proceedings of the National Academy of Sciences*, *105*(46), 17994–17999. doi:10.1073/pnas.0807920105

Flores, G. E., Bates, S. T., Caporaso, J. G., Lauber, C. L., Leff, J. W., Knight, R., & Fierer, N. (2013). Diversity, distribution and sources of bacteria in residential kitchens. *Environmental Microbiology*, *15*(2), 588–596. doi:10.1111/1462-2920.12036

Francisco, P. W., & Palmiter, L. (2003). Field Evaluation of a New Device to Measure Air Handler Flow. *ASHRAE Transactions*, *109*(2), 403–412.

Frankel, M., Beko, G., Timm, M., Gustavsen, S., Hansen, E. W., & Madsen, A. M. (2012). Seasonal Variations of Indoor Microbial Exposures and Their Relation to Temperature, Relative Humidity, and Air Exchange Rate. *Applied and Environmental Microbiology*, *78*(23), 8289–8297. doi:10.1128/AEM.02069-12

Gammaitoni, L., & Nucci, M. C. (1997). Using a mathematical model to evaluate the efficacy of TB control measures. *Emerging Infectious Diseases*, *3*(3), 335–342. doi:10.3201/eid0303.970310

Gaüzère, C., Moletta-Denat, M., Blanquart, H., Ferreira, S., Moularat, S., Godon, J.-J., & Robine, E. (2013). Stability of airborne microbes in the Louvre Museum over time. *Indoor Air*, n/a–n/a. doi:10.1111/ina.12053

Gillott, M., Holland, R., Riffat, S., & Fitchett, J. A. (2006). Post-Occupancy Evaluation of Space Use in a Dwelling Using RFID Tracking. *Architectural Engineering and Design Management*, *2*(4), 273–288.

Glass, E. M., Dribinsky, Y., Yilmaz, P., Levin, H., Van Pelt, R., Wendel, D., … Schriml, L. M. (2013). MIxS-BE: a MIxS extension defining a minimum information standard for sequence data from the built environment. *The ISME Journal*. doi:10.1038/ismej.2013.176

He, C., Morawska, L., & Gilbert, D. (2005). Particle deposition rates in residential houses. *Atmospheric Environment*, *39*(21), 3891–3899. doi:doi: 10.1016/j.atmosenv.2005.03.016

Hewitt, K. M., Gerba, C. P., Maxwell, S. L., & Kelley, S. T. (2012). Office Space Bacterial Abundance and Diversity in Three Metropolitan Areas. *PLoS ONE*, *7*(5), e37849. doi:10.1371/journal.pone.0037849

Hewitt, K. M., Mannino, F. L., Gonzalez, A., Chase, J. H., Caporaso, J. G., Knight, R., & Kelley, S. T. (2013). Bacterial Diversity in Two Neonatal Intensive Care Units (NICUs). *PLoS ONE*, *8*(1), e54703. doi:10.1371/journal.pone.0054703

Hobday, R. A., & Dancer, S. J. (2013). Roles of sunlight and natural ventilation for controlling infection: historical and current perspectives. *Journal of Hospital Infection*. doi:10.1016/j.jhin.2013.04.011

Hoisington, A., Maestre, J. P., Siegel, J. A., & Kinney, K. A. (2014). Exploring the microbiome of the built environment: A primer on four biological methods available to building professionals. *HVAC&R Research*, *20*(1), 167–175. doi:10.1080/10789669.2013.840524

Hospodsky, D., Qian, J., Nazaroff, W. W., Yamamoto, N., Bibby, K., Rismani-Yazdi, H., & Peccia, J. (2012). Human occupancy as a source of indoor airborne bacteria. *PLoS ONE*, *7*(4), e34867. doi:10.1371/journal.pone.0034867

Humphries, C. (2012). Indoor Ecosystems. *Science*, *335*(6069), 648–650. doi:10.1126/science.335.6069.648

Hutchins, J., Ihler, A., & Smyth, P. (2007). Modeling Count Data from Multiple Sensors: A Building Occupancy Model (pp. 241–244). Presented at the 2nd IEEE International Workshop on Computational Advances in Multi-Sensor Adaptive Processing, IEEE. doi:10.1109/CAMSAP.2007.4498010

Ihler, A., Hutchins, J., & Smyth, P. (2006). Adaptive event detection with time-varying poisson processes (pp. 207–216). Presented at the 12th International Conference on Knowledge Discovery and Data Mining, Philadelphia, PA: ACM Press. doi:10.1145/1150402.1150428

Jennings, J. D., Rubinstein, F. M., DiBartolomeo, D., & Blanc, S. L. (1999). Comparison of control options in private offices in an advanced lighting controls testbed (pp. 275–298). Presented at the Illuminating Engineering Society.

Jeon, Y.-S., Chun, J., & Kim, B.-S. (2013). Identification of Household Bacterial Community and Analysis of Species Shared with Human Microbiome. *Current Microbiology*. doi:10.1007/s00284-013-0401-y

Kelley, S. T., & Gilbert, J. A. (2013). Studying the microbiology of the indoor environment. *Genome Biology*, *14*(2), 202. doi:10.1186/gb-2013-14-2-202

Kelley, S. T., Theisen, U., Angenent, L. T., St. Amand, A., & Pace, N. R. (2004). Molecular Analysis of Shower Curtain Biofilm Microbes. *Applied and Environmental Microbiology*, *70*(7), 4187–4192. doi:10.1128/AEM.70.7.4187-4192.2004

Kembel, S. W., Jones, E., Kline, J., Northcutt, D., Stenson, J., Womack, A. M., … Green, J. L. (2012). Architectural design influences the diversity and structure of the built environment microbiome. *The ISME Journal*, *6*(8), 1469–1479. doi:10.1038/ismej.2011.211

King, M.-F., Noakes, C. J., Sleigh, P. A., & Camargo-Valero, M. A. (2013). Bioaerosol deposition in single and two-bed hospital rooms: A numerical and experimental study. *Building and Environment*, *59*, 436–447. doi:10.1016/j.buildenv.2012.09.011

Kjærgaard, M. B., Treu, G., Ruppel, P., & Küpper, A. (2008). Efficient Indoor Proximity and Separation Detection for Location Fingerprinting. Presented at the MOBILWARE ’08 Proceedings of the 1st international conference on MOBILe Wireless MiddleWARE, Operating Systems, and Applications, Brussels, Belgium.

Klepeis, N. E., Nelson, W. C., Ott, W. R., Robinson, J. P., Tsang, A. M., Switzer, P., … Engelmann, W. H. (2001). The National Human Activity Pattern Survey (NHAPS): a resource for assessing exposure to environmental pollutants. *Journal of Exposure Analysis and Environmental Epidemiology*, *11*(3), 231–252. doi:10.1038/sj.jea.7500165

Klevens, R. M., Edwards, J. R., Richards, C. L., Jr, Horan, T. C., Gaynes, R. P., Pollock, D. A., & Cardo, D. M. (2007). Estimating health care-associated infections and deaths in U.S. hospitals, 2002. *Public Health Reports (Washington, D.C.: 1974)*, *122*(2), 160–166.

Knibbs, L. D., Morawska, L., Bell, S. C., & Grzybowski, P. (2011). Room ventilation and the risk of airborne infection transmission in 3 health care settings within a large teaching hospital. *American Journal of Infection Control*, *39*(10), 866–872. doi:10.1016/j.ajic.2011.02.014

Korves, T. M., Piceno, Y. M., Tom, L. M., DeSantis, T. Z., Jones, B. W., Andersen, G. L., & Hwang, G. M. (2013). Bacterial communities in commercial aircraft high-efficiency particulate air (HEPA) filters assessed by PhyloChip analysis. *Indoor Air*, *23*(1), 50–61. doi:10.1111/j.1600-0668.2012.00787.x

Kramer, A., Schwebke, I., & Kampf, G. (2006). How long do nosocomial pathogens persist on inanimate surfaces? A systematic review. *BMC Infectious Diseases*, *6*(1), 130. doi:10.1186/1471-2334-6-130

Lai, A. C. K. (2002). Particle deposition indoors: a review. *Indoor Air*, *12*(4), 211–214. doi:10.1046/j.0905-6947.2002.1r159a.x

Lam, K. P., Höynck, M., Dong, B., Andrews, B., Chiou, Y.-S., Zhang, R., … Choi, J. (2009). Occupancy detection through an extensive environmental sensor network in an open-plan office building (pp. 1452–1459). Presented at the Building Simulation 2009. 11th International IBPSA Conference, Glasgow, Scotland.

Lawrence, T. M., & Braun, J. E. (2007). A methodology for estimating occupant CO2 source generation rates from measurements in small commercial buildings. *Building and Environment*, *42*(2), 623–639. doi:10.1016/j.buildenv.2004.10.021

Lee, L., Tin, S., & Kelley, S. T. (2007). Culture-independent analysis of bacterial diversity in a child-care facility. *BMC Microbiology*, *7*(1), 27. doi:10.1186/1471-2180-7-27

Li, A., Liu, Z., Zhu, X., Liu, Y., & Wang, Q. (2010). The effect of air-conditioning parameters and deposition dust on microbial growth in supply air ducts. *Energy and Buildings*, *42*(4), 449–454. doi:10.1016/j.enbuild.2009.10.013

Li, N., & Becerik-Gerber, B. (2011). Performance-based evaluation of RFID-based indoor location sensing solutions for the built environment. *Advanced Engineering Informatics*, *25*(3), 535–546. doi:10.1016/j.aei.2011.02.004

Li, N., Calis, G., & Becerik-Gerber, B. (2012). Measuring and monitoring occupancy with an RFID based system for demand-driven HVAC operations. *Automation in Construction*, *24*, 89–99. doi:10.1016/j.autcon.2012.02.013

Liu, D., Guan, X., Du, Y., & Zhao, Q. (2013). Measuring indoor occupancy in intelligent buildings using the fusion of vision sensors. *Measurement Science and Technology*, *24*(7), 074023. doi:10.1088/0957-0233/24/7/074023

Lunden, M., Faulkner, D., Heredia, E., Cohn, S., Dickerhoff, D., Noris, F., … Sherman, M. H. (2012). *Experiments to Evaluate and Implement Passive Tracer Gas Methods to Measure Ventilation Rates in Homes* (No. LBNL-5984E). Berkeley, CA: Lawrence Berkeley National Laboratory.

McDevitt, J., Rudnick, S., First, M., & Spengler, J. (2010). Role of Absolute Humidity in the Inactivation of Influenza Viruses on Stainless Steel Surfaces at Elevated Temperatures. *Applied and Environmental Microbiology*, *76*(12), 3943–3947. doi:10.1128/AEM.02674-09

Meadow, J. F., Altrichter, A. E., Kembel, S. W., Kline, J., Mhuireach, G., Moriyama, M., … Bohannan, B. J. M. (2013). Indoor airborne bacterial communities are influenced by ventilation, occupancy, and outdoor air source. *Indoor Air*, n/a–n/a. doi:10.1111/ina.12047

Medrano-Félix, A., Martínez, C., Castro-del Campo, N., León-Félix, J., Peraza-Garay, F., Gerba, C. P., & Chaidez, C. (2011). Impact of prescribed cleaning and disinfectant use on microbial contamination in the home. *Journal of Applied Microbiology*, *110*(2), 463–471. doi:10.1111/j.1365-2672.2010.04901.x

Meyn, S., Surana, A., Lin, Y., Oggianu, S. M., Narayanan, S., & Frewen, T. A. (2009). A sensor-utility-network method for estimation of occupancy in buildings (pp. 1494–1500). Presented at the Joint 48th IEEE Conference on Decision and Control and 28th Chinese Control Conference, Shanghai, China.

Miller, S. L., Leiserson, K., & Nazaroff, W. W. (1997). Nonlinear Least-Squares Minimization Applied to Tracer Gas Decay for Determining Airflow Rates in a Two-Zone Building. *Indoor Air*, *7*(1), 64–75. doi:10.1111/j.1600-0668.1997.t01-1-00008.x

Naya, F., Noma, H., Ren Ohmura, & Kogure, K. (2005). Bluetooth-based Indoor Proximity Sensing for Nursing Context Awareness (pp. 212–213). Presented at the Ninth IEEE International Symposium on Wearable Computers, IEEE. doi:10.1109/ISWC.2005.13

Nazaroff, W. W. (2004). Indoor particle dynamics. *Indoor Air*, *14*(s7), 175–183. doi:10.1111/j.1600-0668.2004.00286.x

Nielsen, K. F., Holm, G., Uttrup, L. P., & Nielsen, P. A. (2004). Mould growth on building materials under low water activities. Influence of humidity and

temperature on fungal growth and secondary metabolism. *International Biodeterioration & Biodegradation*, *54*(4), 325–336. doi:10.1016/j.ibiod.2004.05.002

Noris, F., Siegel, J. A., & Kinney, K. A. (2011). Evaluation of HVAC filters as a sampling mechanism for indoor microbial communities. *Atmospheric Environment*, *45*(2), 338–346. doi:10.1016/j.atmosenv.2010.10.017

Oberauner, L., Zachow, C., Lackner, S., Högenauer, C., Smolle, K.-H., & Berg, G. (2013). The ignored diversity: complex bacterial communities in intensive care units revealed by 16S pyrosequencing. *Scientific Reports*, *3*. doi:10.1038/srep01413

Page, J., Robinson, D., Morel, N., & Scartezzini, J.-L. (2008). A generalised stochastic model for the simulation of occupant presence. *Energy and Buildings*, *40*(2), 83–98. doi:10.1016/j.enbuild.2007.01.018

Park, J. H., Spiegelman, D. L., Burge, H. A., Gold, D. R., Chew, G. L., & Milton, D. K. (2000). Longitudinal study of dust and airborne endotoxin in the home. *Environmental Health Perspectives*, *108*(11), 1023–1028.

Persily, A. (1997). Evaluating building IAQ and Ventilation with Indoor Carbon Dioxide. *ASHRAE*.

Persily, A. K. (1997). Evaluating building IAQ and ventilation with indoor carbon dioxide. *ASHRAE Transactions*, *103*(2), 1–12.

Poza, M., Gayoso, C., Gómez, M. J., Rumbo-Feal, S., Tomás, M., Aranda, J., … Bou, G. (2012). Exploring Bacterial Diversity in Hospital Environments by GS-FLX Titanium Pyrosequencing. *PLoS ONE*, *7*(8), e44105. doi:10.1371/journal.pone.0044105

Qian, H., Li, Y., Nielsen, P. V., & Huang, X. (2009). Spatial distribution of infection risk of SARS transmission in a hospital ward. *Building and Environment*, *44*(8), 1651–1658. doi:10.1016/j.buildenv.2008.11.002

Qian, J., Hospodsky, D., Yamamoto, N., Nazaroff, W. W., & Peccia, J. (2012). Size-resolved emission rates of airborne bacteria and fungi in an occupied classroom. *Indoor Air*, *22*(4), 339–351. doi:10.1111/j.1600-0668.2012.00769.x

Riley, E. C., Murphy, G., & Riley, R. L. (1978). Airborne Spread of Measles in a Suburban Elementary School. *American Journal of Epidemiology*, *107*(5), 421–432.

Rintala, H., Pitkaranta, M., Toivola, M., Paulin, L., & Nevalainen, A. (2008). Diversity and seasonal dynamics of bacterial community in indoor environment. *BMC Microbiology*, *8*(1), 56. doi:10.1186/1471-2180-8-56

Robertson, C. E., Baumgartner, L. K., Harris, J. K., Peterson, K. L., Stevens, M. J., Frank, D. N., & Pace, N. R. (2013). Culture-Independent Analysis of Aerosol Microbiology in a Metropolitan Subway System. *Applied and Environmental Microbiology*, *79*(11), 3485–3493. doi:10.1128/AEM.00331-13

Rubinstein, F. M., Colak, N., Jennings, J., & Niels, D. (2003). Analyzing Occupancy Profiles from a Lighting Controls Field Study. Presented at the CIE Conference, San Diego, CA.

Salonen, H., Duchaine, C., Létourneau, V., Mazaheri, M., Clifford, S., & Morawska, L. (2013). Endotoxins in Indoor Air and Settled Dust in Primary Schools in a Subtropical Climate. *Environmental Science & Technology*, *47*(17), 9882–9890. doi:10.1021/es4023706

Shaman, J., & Kohn, M. (2009). Absolute humidity modulates influenza survival, transmission, and seasonality. *Proceedings of the National Academy of Sciences*, *106*(9), 3243–3248. doi:10.1073/pnas.0806852106

Shaman, J., Pitzer, V. E., Viboud, C., Grenfell, B. T., & Lipsitch, M. (2010). Absolute Humidity and the Seasonal Onset of Influenza in the Continental United States. *PLoS Biology*, *8*(2), e1000316. doi:10.1371/journal.pbio.1000316

Sharpe, P. A., & Schmidt, M. G. (2011). Control and Mitigation of Healthcare-Acquired Infections: Designing Clinical Trials To Evaluate New Materials and Technologies. *HERD : Health Environments Research & Design Journal*, *5*(1), 94–115.

Sherman, M. H. (1989). On the estimation of multizone ventilation rates from tracer gas measurements. *Building and Environment*, *24*(4), 355–362. doi:10.1016/0360-1323(89)90030-9

Sherman, M. H. (1990). Tracer-gas techniques for measuring ventilation in a single zone. *Building and Environment*, *25*(4), 365–374. doi:10.1016/0360-1323(90)90010-O

Sippola, M., & Nazaroff, W. (2004). Experiments Measuring Particle Deposition from Fully Developed Turbulent Flow in Ventilation Ducts. *Aerosol Science and Technology*, *38*(9), 914–925. doi:10.1080/027868290507213

Stephens, B., Novoselac, A., & Siegel, J. A. (2010). The effects of filtration on pressure drop and energy consumption in residential HVAC systems. *HVAC&R Research*, *16*(3), 273–294.

Stephens, B., & Siegel, J. A. (2012). Comparison of test methods for determining the particle removal efficiency of filters in residential and light-commercial central HVAC systems. *Aerosol Science and Technology*, *46*(5), 504–513. doi:10.1080/02786826.2011.642825

Stephens, B., Siegel, J. A., & Novoselac, A. (2010). Energy implications of filtration in residential and light-commercial buildings (RP-1299). *ASHRAE Transactions*, *116*(1), 346–357.

Stiefel, U., Cadnum, J. L., Eckstein, B. C., Guerrero, D. M., Tima, M. A., & Donskey, C. J. (2011). Contamination of hands with methicillin-resistant Staphylococcus aureus after contact with environmental surfaces and after contact with the skin of colonized patients. *Infection Control and Hospital Epidemiology: The Official Journal of the Society of Hospital Epidemiologists of America*, *32*(2), 185–187. doi:10.1086/657944

Terada, K., Yoshida, D., Oe, S., & Yamaguchi, J. (1999). A method of counting the passing people by using the stereo images (Vol. 2, pp. 338–342). Presented at the IEEE International Conference on Image Processing, IEEE. doi:10.1109/ICIP.1999.822913

The Energy Conservatory. (2006). TrueFlow Air Handler Flow Meter Operation Manual. The Energy Conservatory, Minneapolis, MN.

The Energy Conservatory. (2007). Minneapolis Duct Blaster Operation Manual. The Energy Conservatory, Minneapolis, MN.

Tringe, S. G., Zhang, T., Liu, X., Yu, Y., Lee, W. H., Yap, J., … Ruan, Y. (2008). The Airborne Metagenome in an Indoor Urban Environment. *PLoS ONE*, *3*(4), e1862. doi:10.1371/journal.pone.0001862

Viitanen, H., Vinha, J., Salminen, K., Ojanen, T., Peuhkuri, R., Paajanen, L., & Lahdesmaki, K. (2010). Moisture and Bio-deterioration Risk of Building Materials and Structures. *Journal of Building Physics*, *33*(3), 201–224. doi:10.1177/1744259109343511

Walker, I. S., Dickerhoff, D. J., Faulkner, D., & Turner, W. J. N. (2012). *Energy Implications of In--Line Filtration in California* (No. LBNL--6143E). Berkeley, CA: Lawrence Berkeley National Laboratory.

Wallace, L. A., Emmerich, S. J., & Howard-Reed, C. (2002). Continuous measurements of air change rates in an occupied house for 1 year: the effect of temperature, wind, fans, and windows. *Journal of Exposure Analysis and Environmental Epidemiology*, *12*(4), 296–306. doi:10.1038/sj.jea.7500229

Wang, S., Burnett, J., & Chong, H. (1999). Experimental Validation of CO2-Based Occupancy Detection for Demand-Controlled Ventilation. *Indoor and Built Environment*, *8*(6), 377–391. doi:10.1177/1420326X9900800605

Waring, M. S., & Siegel, J. A. (2008). Particle loading rates for HVAC filters, heat exchangers, and ducts. *Indoor Air*, *18*(3), 209–224. doi:10.1111/j.1600-0668.2008.00518.x

Wooley, J. C., Godzik, A., & Friedberg, I. (2010). A Primer on Metagenomics. *PLoS Comput Biol*, *6*(2), e1000667. doi:10.1371/journal.pcbi.1000667